

**A Multi-Faceted Approach to Advancing Materials Science: Investigations in Materials Research
and Education**

by

Brandon A. Carter

A dissertation submitted in partial fulfillment
of the requirements for the degree of
Doctor of Philosophy
(Materials Science and Engineering)
in the University of Michigan
2023

Doctoral Committee:

Professor Joanna. M. Millunchick, Chair
Associate Professor John T. Heron
Assistant Professor Robert Hovden
Professor Chris Pearson
Assistant Professor Shalaunda Reeves, University of Tennessee

Brandon A. Carter

bacart@umich.edu

ORCID iD: [0000-0002-7028-7970](https://orcid.org/0000-0002-7028-7970)

© Brandon A. Carter 2023

Dedication

This work is dedicated to my wife, Carolyn Hernandez. Without her support, patience and encouragement, this work would not have been possible.

Acknowledgements

First and foremost, I would like to acknowledge my Ph.D. advisor, Joanna Millunchick. Without ‘senior’ lab mates as mentors for most of my Ph.D., Joanna always made herself available to help troubleshoot the seemingly constantly broken lab equipment, and more generally for advice. She always remained calm even when equipment failure threatened my original research plans and helped me in develop alternative paths forward for research. Without her support and guidance, both in the lab as a researcher, and as a person I would not have reached this final hurdle of my Ph.D.

I would also like to acknowledge my lab mate Ryan Tait, although he graduated a few short months after I started my Ph.D., he taught me almost everything I know about the operation and maintenance of our MBE chamber.

I would also like to thank my lab mate Veronica Caro for her help with the research presented in this dissertation. She assisted greatly in XRD and SEM data collection and was instrumental in assisting in maintenance of the MBE chamber.

Lastly, I would like to thank Chris Pearson for his assistance with my endeavors in STM. Although untimely equipment failure prevented inclusion of an originally planned STM study in this dissertation, his guidance and knowledge taught me a lot about the characterization technique which I hope I can utilize in the future. Furthermore, his willingness to listen to my scientific issues helped me overcome difficult times in my research.

Table of Contents

| | |
|--|-------------|
| Dedication | ii |
| Acknowledgements | iii |
| List of Tables | viii |
| List of Figures..... | ix |
| List of Appendices..... | xiii |
| Abstract..... | xiv |
| Chapter 1 Investigations in Materials Science Research and Education | 1 |
| 1.1 Part 1 Motivation: Maximizing Bi Incorporation in III-V Semiconductors | 1 |
| 1.2 Part 2 Motivation: Disciplinary Researchers That Perform Educational Research..... | 3 |
| 1.3 Organization:..... | 5 |
| 1.4 References..... | 7 |
| Chapter 2 Experimental Procedures: | 11 |
| 2.1 Molecular Beam Epitaxy | 11 |
| 2.2 System Details | 11 |
| 2.2.1 Effusion Cells and Measuring Material Beam Flux | 13 |
| 2.2.2 Sample Preparation and Growth..... | 15 |
| 2.2.3 RHEED | 15 |
| 2.3 Sample Characterization | 17 |
| 2.3.1 Scanning Electron Microscopy..... | 17 |
| 2.3.2 Atomic Force Microscopy | 17 |
| 2.3.3 Scanning Tunneling Microscopy | 18 |
| 2.3.4 Energy Dispersive Spectroscopy (EDS)..... | 18 |
| 2.3.5 Focused Ion Beams (FIB)..... | 19 |
| 2.3.6 X-Ray Diffraction (XRD)..... | 19 |

| | |
|---|-----------|
| 2.3.7 Scanning Transmission Electron Microscopy (STEM)..... | 20 |
| 2.3.8 Atomic Probe Tomography | 21 |
| 2.4 References..... | 22 |
| Chapter 3 Chapter 1 Systematic Exploration of Material Flux Parameter Space to Maximize Bi Incorporation in GaAsBi | 24 |
| 3.1 Introduction: Challenges with Bi Incorporation | 24 |
| 3.2 Growth Conditions and Parameters | 29 |
| 3.3 Four Morphological Regimes Verified With SEM..... | 30 |
| 3.4 Establishing a New Parameter W_{OOM} to Capture Variations in Lattice Parameter..... | 31 |
| 3.5 Droplet Driven Lattice Variations | 32 |
| 3.6 Morphology Map | 35 |
| 3.7 Compositional Variations Explain Large W_{OOM} Linewidths: | 38 |
| 3.7.1 Bi Droplets:..... | 38 |
| 3.7.2 Bi-Phasic Droplets | 41 |
| 3.8 Conclusions:..... | 42 |
| 3.9 References:..... | 43 |
| Chapter 4 Comparing Bi Incorporation on the (110) and (001) Surfaces | 46 |
| 4.1 Introduction: Orientation Dependent Bi Incorporation..... | 46 |
| 4.2 Background: Growth of (110) III-V Films, and Bi Terminated Surfaces..... | 47 |
| 4.2.1 Applications: Why the (110) Orientation? | 47 |
| 4.2.2 Epitaxial Growth on the (110) Surface | 48 |
| 4.2.3 Bi Interactions in the Crystal Termination Layer | 50 |
| 4.3 Experimental Procedures: | 51 |
| 4.4 XRD Shows Differences in Bi Incorporation Between the (001) and (110) Surfaces | 52 |
| 4.4.1 (001) Oriented Superlattice Bi Incorporation | 53 |
| 4.4.2 (110) Oriented Superlattice Bi incorporation | 55 |
| 4.5 The Effect of Bi on Surface Morphology | 57 |
| 4.5.1 (001) Surface Morphology Evolution..... | 57 |
| 4.5.2 (110) Surface Morphology Evolution..... | 59 |
| 4.5.3 Bi Induced Disorder..... | 62 |

| | |
|---|------------|
| 4.6 Conclusions..... | 63 |
| 4.7 References..... | 64 |
| Chapter 5 Future Work..... | 70 |
| 5.1 Temperature Series Growth Maps | 70 |
| 5.2 Kinetic Bi Incorporation in (110) oriented Bismide films..... | 71 |
| 5.3 STM Study of Bi Incorporation on (110) Surfaces..... | 71 |
| 5.4 Growth of Core-Shell Bismide Nanowires | 72 |
| 5.5 References..... | 72 |
| Chapter 6 Promoting Effective Educational Research in MSE..... | 74 |
| 6.1 Introduction..... | 74 |
| 6.2 Methodology | 77 |
| 6.2.1 Search and. Refinement Criteria..... | 77 |
| 6.2.2 Coding Procedures and Analysis | 80 |
| 6.3 Results..... | 82 |
| 6.3.1 Henderson Framework: Change Targets and Change Outcomes | 82 |
| 6.3.2 Trends in Framework Usage, Author Affiliations and Publication Type..... | 89 |
| 6.3.3 Author Collaboration Journal Types and Framework Usage | 94 |
| 6.4 Discussion:..... | 96 |
| 6.4.1 Areas For Improvemnt: It’s Unclear if the Themes and Approaches Utilized by MSE Authors are Effective at Promoting Change..... | 96 |
| 6.4.2 Areas For Improvement: MSE Educational Research Needs To Be Situated in Theory | 98 |
| 6.5 Conclusions..... | 99 |
| 6.6 References..... | 100 |
| Chapter 7 Reflecting on Using VR to Teach Crystal Structures..... | 108 |
| 7.1 Introduction: Motivation for Studying VR to Teach Crystal Structure | 109 |
| 7.2 Background: Crystal Structure Visualization in Educational Literature | 110 |
| 7.3 Design and Implementation of VR Learning Activities | 111 |
| 7.3.1 Context and Participants | 111 |
| 7.3.2 Arthea: The XR application..... | 112 |
| 7.3.3 Methods: Development of Learning Activities | 113 |

| | |
|--|------------|
| 7.4 Analysis Procedures..... | 118 |
| 7.5 Results..... | 119 |
| 7.6 Discussion:..... | 123 |
| 7.7 Critique: | 124 |
| 7.7.1 The Positive: Incorporating a Variety of Representation Types | 124 |
| 7.7.2 The Room for Improvement: Supporting Different Learner Roles | 127 |
| 7.7.3 The Bad: Not Likely to Encourage the Use of VR..... | 129 |
| 7.8 Suggestions for Future Work | 130 |
| 7.9 Conclusions..... | 132 |
| 7.10 References..... | 132 |
| Appendix A Crystal Structure Concept Inventory Pretest/Posttest | 136 |
| Appendix B Crystal Structure Individual Activity..... | 137 |
| Appendix C Crystal Structure Paired Activity Iteration 1 | 140 |
| Appendix D Crystal Structure Paired Activity Iteration 2..... | 142 |

List of Tables

| | |
|--|-----|
| Table 3.1 Growth conditions for a representative sample with each surface morphology/droplet type. Film composition and parameters derived from XRD are also reported here | 30 |
| Table 4.1: Growth Conditions for Superlattice Growths | 52 |
| Table 6.1 Inclusion and exclusion criteria for article refinement procedures..... | 79 |
| Table 6.2 List of paper titles, journal types, collaboration author types, whether a paper utilized a theoretical framework, change targets, and change outcomes..... | 89 |
| Table 7.1 Demographic data for each iteration cohort | 110 |
| Table 7.2 Summary of the elements included in each iteration of the study..... | 113 |
| Table 7.3 Questions asked to students in the pilot iteration | 114 |
| Table 7.4 Percent scores for the correct answers to each question when answered individually on paper, in pairs on paper, and in pairs in XR for the first iteration of the crystal structure activity | 120 |
| Table 7.5 Percent scores for the correct answers to each question for two separate treatment groups of the crystal structure activity in iteration 2. | 121 |
| Table 7.6 Pre and Posttest results for the second iteration of the crystal structure learning activity | 122 |
| Table 7.7 Analysis of learner roles supported in the activities in this study | 128 |

List of Figures

| | |
|---|----|
| Figure 1.1 Diagram showing the bandgap of several III-V alloys vs lattice parameter, including the Bismides InAsBi and GaAsBi ⁶ | 2 |
| Figure 2.1 Schematic diagram of the experimental equipment used in this dissertation ⁶ | 12 |
| Figure 2.2 Photograph of the MBE chamber used for the experimental growths in this dissertation ⁵ | 13 |
| Figure 2.3 Schematic diagram of the MBE chamber. We excluded the doping effusion cells for Si and Be in this representation as they were not used in the growth presented in this dissertation | 14 |
| Figure 2.4 Schematic showing how growth rate is measures as the sample temporally roughens ⁷ | 16 |
| Figure 2.5 A schematic diagram of the Cameca LEAP 5000XR atom probe showing the sample tip, local electrode, reflectron and detector ⁵ | 21 |
| Figure 3.1 a) Phase diagram of GaBi binary material system ¹ b) Phase diagram of InBi binary material system ² | 24 |
| Figure 3.2 a) Temperature series of Bi incorporation as a function of Bi/As flux ratio ³ . b) Temperature series of Bi incorporation as a function of As ₂ /Ga. ⁴ | 25 |
| Figure 3.3 Kinetic Monte Carlo simulations showing the dependence of Bi Incorporation on material flux ratio and droplet formation ⁹ | 26 |
| Figure 3.4 a) HAADF TEM showing inhomogeneous distribution of Bi. The dotted line shows an outline for Ga on the surface. b) APT of the same sample with Bi atoms mapped in blue, with a cross sectional region of interest shown. c) Average Bi composition of the identified cross section. d) illustration of the Ga wicking effect of the droplet which creates a region of elevated incorporation near the droplets, that is not observed further away from the droplet leading to the variations in composition ¹⁰ | 27 |
| Figure 3.5 SEM micrographs of samples with each surface morphology. a) droplet free, b) Bi droplets, c) Ga droplets, d) biphasic droplets ²⁴ | 31 |
| Figure 3.6 XRD ω -2 θ (004) scans taken from samples a-d. The upper x-axis represents atomic % Bi calculated via Vegard's law. Graphical examples of how the maximum Bi incorporation (x_{max}), the median Bi incorporation (x_{med}), and the line scan width one order of magnitude | |

| | |
|--|----|
| below the highest-intensity peak (W_{OOM}) of each sample are determined are superimposed on the scans ²⁴ | 33 |
| Figure 3.7 Morphological map of the 25 samples growth at 325 °C and annealed for 5 min at various flux ratios. The qualitative boundaries between each regime is given by dashed lines. Specific samples are labeled according the Table 1. The color of the data point represents the median composition, and the size of the data points represents breadth of the peak ²⁴ | 36 |
| Figure 3.8 a)HAADF STEM of sample b grown under conditions that yield Bi droplets on the surface. Atomic number contrast shows compositional inhomogeneities in Bi incorporation. b) SEM micrograph showing how Bi droplets travel across the surface during growth, coalescing surface Bi in their path ²⁴ | 39 |
| Figure 3.9 a) Bi concentration cross section of sample b with Bi droplets on the surface collected with APT. b) Average Bi concentration throughout the length of the atom probe tip ²⁴ | 40 |
| Figure 3.10 a)HAADF STEM showing streaky composition inhomogeneities in sample d with biphasic droplets. b) model for the cause of the compositional inhomogeneities showing the droplet wicking Ga and traveling across the surface ²⁴ | 41 |
| Figure 4.1a) Phase diagram of the Bi-terminated GaAs(001) surface reconstructions as a function of Bi and As chemical potentials. Thick solid lines separate the different reconstructions from one another, while dashed lines separate the individual configurations within each reconstruction. The thicker dotted line in the $c(4 \times 4)$ reconstruction region separates the $c(4 \times 4)\alpha$ reconstruction on the left of the line from the $c(4 \times 4)\beta$ configurations on the right. The entropy curves presented in Fig. 5 are plotted along the dotted line, with the open circles indicating where Monte Carlo cooling runs were performed. The letters in brackets correspond to the configurations of the region on the phase diagram. Stable configurations include the (b) $\beta(4 \times 3)$ -2, (c) $\beta(4 \times 3)$ -5, (d) $\beta(4 \times 3)$ -6, (e) $h0(4 \times 3)$ -10, (f) $c(4 \times 4)$, (g) $c(4 \times 4)$ -6/2, (h) $c(4 \times 4)$ -6, (i) (2×1) -2, and (j) $\alpha2(2 \times 4)$ -4. The order of Bi occupation in the $\beta(4 \times 3)$ reconstruction is given in (b); sites with the same number are symmetrically degenerate. ³⁹ | 49 |
| Figure 4.2 (a) Top view of the (110) plane of the (1x2) missing row structure (b) Perspective view of the (1x2) missing-row structure. ³⁸ (c) STM of the (1x2) missing row reconstruction showing the rows of Bi incorporation along the [1-10]..... | 50 |
| Figure 4.3 XRD line-scans showing the leftward shift corresponding to the increase in Bi incorporation for the samples grown in this study. The vertical dotted line shows the substrate peak, and the canted line tracks the leftward shift. Each curve is labeled with the Bi deposition time and corresponding incorporation calculated using Vegards law. (a) (004) ω -2 θ scans on the (001) surface show that Bi incorporation stalls at 1.7% Bi at Bi deposition times equal to or greater than 30 sec. (b) (220) ω -2 θ scans on the (110) surface show that the incorporation increases monotonically as the Bi deposition time increases, up to 2.3% Bi for the growth conditions used in this study. ⁵⁸ | 53 |
| Figure 4.4 AFM micrographs and directional texture analysis maps of the (001) InAs superlattices with (a-c) 15 s of Bi deposition. (d-f) 30 s of Bi deposition and (g-i) 45s of Bi deposition..... | 55 |

| | |
|--|-----|
| Figure 4.5. AFM micrographs and directional texture analysis maps of the (110) InAs superlattices with (a-c) 0 s of Bi deposition. (d-f) 15 s of Bi deposition and (g-i) 30 s of Bi deposition and (j-l) 45 s of Bi deposition..... | 56 |
| Figure 4.6 a) HAADF STEM of sample b(t=15s) on the InAs(110) surface.(b-d) Heat maps of strain in the HAAD STEM.(e)FFT of (a) showing the reference vectors used for strain calculations. | 57 |
| Figure 4.7. Shows the reduction in height and lateral dimensions of the prisms as more Bi is deposited on the surface, as well as the increase in island density. | 59 |
| Figure 4.8 AFM micrographs show the transition of the step edges from straight to meandering as a result of Bi induced disorder in surface. (a) 0 sec Bi deposition (b) 15s Bi deposition, (c) 30 sec Bi deposition, (d) 45 s Bi deposition. (e) line profiles showing the reduction in step bunching. ⁵⁸ | 62 |
| Figure.6.1: Quadrant based classification of papers based on the change target and change outcome adapted from ⁹ . Within each quadrant a brief description of the types of papers that fall within it are included. | 76 |
| Figure 6.2 Flow Chart of the refinement procedures used in this review..... | 78 |
| Figure 6.3 Bar graph showing the number of papers that fall into each quadrant of the Henderson Framework and the themes of the papers | 83 |
| Figure 6.4 Frequency of an article being published in a type of journal versus the types of authors that published it. The size of the data points is proportional to the number of papers and the pie charts show the fraction of papers that utilize a theoretical framework | 94 |
| Figure 7.1 Reduced sphere representations of commonly taught crystal structures in introductory level MSE classes; Body Centered Cubic (BCC) and Face Centered Cubic (FCC) with different crystal planes superimposed | 108 |
| Figure 7.2 Screenshot of the Arthea web interface (left) and the virtual environment user interface (right)for importing 3D tiles | 111 |
| Figure 7.3 Arthea user interface and virtual environment with an FCC crystal structure unit cell loaded. This scene shows the annotation capacity of Arthea with an octahedral interstitial site drawn in red. | 112 |
| Figure 7.4 Example of a student response to question 2 in the pilot study. The densest packed plane is identified by the green triangle towards the bottom right of the image. The unit cell is also identified in blue towards the top left of the crystal structure | 115 |
| Figure 7.5 The different types of representations described by Lesh, the arrows indicate that students must be able to understand how these representations relate to one another and the information provided by each ¹⁸ | 126 |

Figure 7.6: Example of a question asking students to draw the planes of atoms and rank their planar density 129

List of Appendices

| | |
|---|-----|
| Appendix A Crystal Structure Concept Inventory Pretest/Posttest | 136 |
| Appendix B Crystal Structure Individual Activity | 137 |
| Appendix C Crystal Structure Paired Activity Iteration 1 | 140 |
| Appendix D Crystal Structure Paired Activity Iteration 2..... | 142 |

Abstract

This dissertation presents a unique approach for conducting doctoral research in Materials Science and Engineering(MSE). Traditionally, MSE research consists of novel material synthesis, characterization, and analysis. However, advancements in MSE are also driven by improvements in education. As such, this dissertation is split into two sections. The first section presents experiments on the synthesis and characterization of highly mismatched III-V alloys, and the second section discusses the state of teaching innovations in MSE.

Bismuth containing III-V alloys are of interest for spintronics and devices operating in the far-infrared due to large spin-orbit splitting and a large bandgap reduction per percent Bi. However, low miscibility of Bi in III-Vs has made identifying growth conditions that support appreciable Bi incorporation challenging and often leads to phase segregation and droplet formation. To address this challenge, a series GaAsBi(001) molecular beam epitaxy growths were performed to understand the relation between material flux, droplet formation, film microstructure, and Bi composition. It was observed that Bi composition reached a peak value 18.3% when Bi-rich droplets formed on the surface. However, these droplets are also associated with inhomogeneous Bi concentration. Droplet-free films minimize these inhomogeneities but exhibit lower Bi concentration up to 13.6%. We also investigated the effect of surface orientation on Bi incorporation in (110) and (001) InAs. Experimental growths, and subsequent characterization showed that InAs(110) supports higher levels of Bi incorporation compared to InAs (001). It is also observed that Bi causes large changes to the surface morphology on each

crystalline orientation which is attributed to modified diffusion and adatom attachment mechanisms.

Large expenditures on developing student centered teaching methodologies, have not been met with a corresponding shift in the teaching practices of STEM, and more specifically MSE faculty. We conducted a systematic review of educational research conducted by MSE faculty over the past decade to understand why. We find that this research most often discusses the development of pedagogical practices, learning activities, and teaching tools. However, it does not usually discuss the efficacy of these tools with respect to student learning, or report on their implementation in educational settings and adoption by instructors. As such, it is unclear if these instruments are being utilized and suggests a need for a paradigm shift in how education research is conducted by MSE faculty. Furthermore, we find evidence that MSE researchers are unfamiliar with educational literature, which may explain our findings. The findings of this review were used to analyze three studies that we conducted to encourage the use of virtual reality in engineering education. The positives and negatives of the experimental design are discussed; however, we acknowledged that our approach of disseminating virtual reality learning activities is unlikely to encourage uptake of VR by instructors. As such, directions for future research are suggested.

Chapter 1 Investigations in Materials Science Research and Education

To me, the pursuit of scientific research and scientific education are inextricably linked; to promote high quality research, we must first properly educate future scientists and engineers. Therefore, when I started my PhD in Materials Science and Engineering (MSE) I wanted to split my research between traditional materials research and educational research. As a result, this dissertation is presented in two parts. The first part focusses on the epitaxial growth of highly mismatched III-V semiconductor alloys, and the second part focuses on the state of educational research performed by materials science faculty. The purpose of this chapter is to introduce the research that is presented in each of these sections.

1.1 Part 1 Motivation: Maximizing Bi Incorporation in III-V Semiconductors

Over the last two decades there has been a surge of publications investigating the alloying properties of Bi containing III-V semiconductor alloys, due to their interesting electronic properties. Commonly referred to as Bismides, these alloys exhibit massive bandgap bowing,¹⁻³ a large spin-orbit splitting due to the heavy Bi nucleus,³ and a strong upward shift of the valence band maximum with increasing Bi concentration.⁴ As a result, the bandgap is reduced by as much as 88 meV/Bi%⁴ in GaAs and 55 meV/ Bi%.⁵ in InAs. Figure 1.1 shows that this effect enables the bandgap of III-Vs to be tuned throughout the infrared regime (1.59 - 0.001 eV) while introducing only small amounts of strain into the crystalline lattice⁶. Looking to take advantage of these properties, researchers have used Bismides to fabricate devices spanning the infrared regime, including solar cells,^{7,8} and long wavelength optoelectronic lasers.^{9,10}

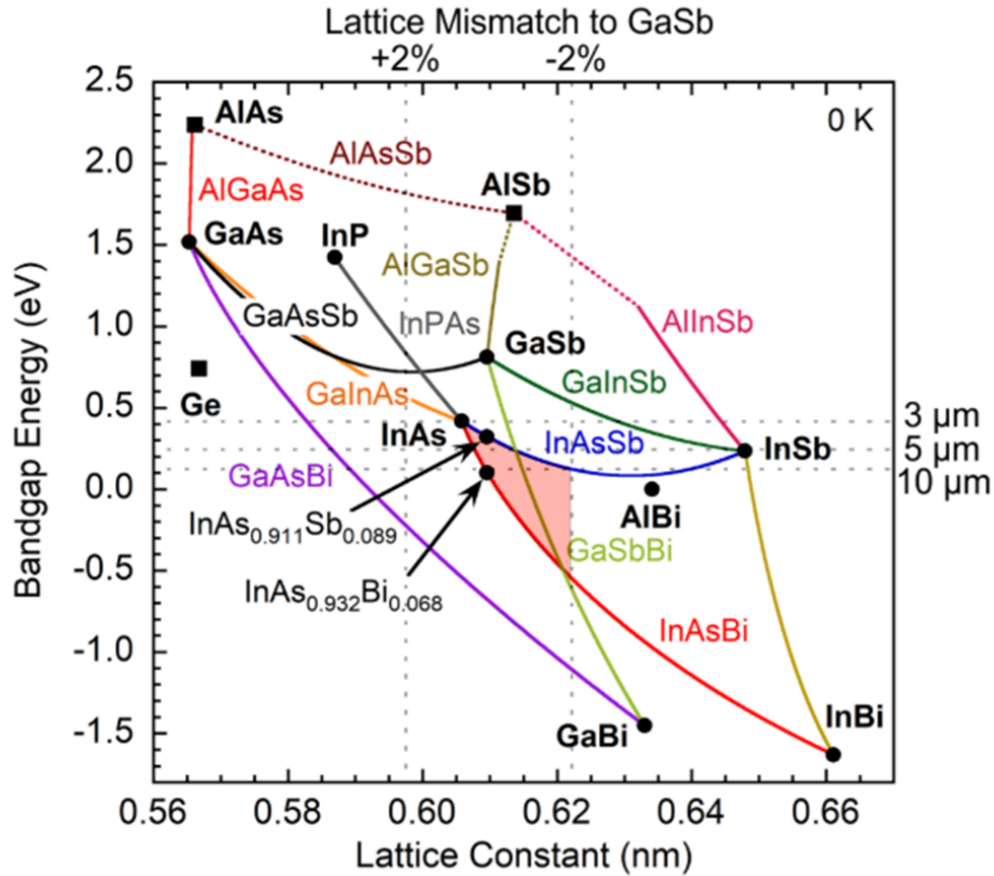


Figure 1.1 Diagram showing the bandgap of several III-V alloys vs lattice parameter, including the Bismides InAsBi and GaAsBi⁶

Bismides also exhibit several other properties that offer distinct advantages over the current state of the art HgCdTe infrared semiconductors. First, HgCdTe is limited by intrinsic thermal Auger generation and recombination which increases the turn-on voltage of diodes and limits their efficiency.¹¹ In Bismides, conduction-hole spin-hole Auger recombination is suppressed when the spin-orbit splitting is larger than the bandgap. This crossover occurs at about 9% Bi in GaAs.¹² However, a corresponding effect is not observed in InAsBi because the energy splitting is larger than the bandgap for all Bi mole fractions.¹³ Second, the bandgap of HgCdTe exhibits a strong temperature dependence that necessitates the use of Peltier cooling in extreme environments.^{11,14} On the other hand, the temperature coefficient of the bandgap in

Bismides is reduced compared to pure III-V's.¹⁵⁻¹⁷ For example, Oe et al showed that the temperature coefficient of GaAsBi (x=2.6 at. % Bi) is 1/3 of its value for pure GaAs.¹⁵

However, experimentally realizing and optimizing the properties discussed above is contingent on the ability to grow highly crystalline, and uniformly alloyed films with large mole fractions of Bi. This has proved challenging due to low miscibility of Bi in III-Vs^{18,19} which leads to a small range of growth conditions that yield elevated Bi incorporation.³³ Furthermore, the low miscibility of Bi leads to a chemical driving force for it to phase segregate, which causes a litany of compositional effects including droplet formation,^{20,21} lateral composition modulation,^{22,23} Bi clustering,²⁴⁻²⁹ and compositional ordering.³⁰⁻³² As such, the main purpose of part 1 of this dissertation is to address this challenge by asking the research question; what growth conditions maximize Bi incorporation in III-Vs. An emphasis is placed on investigating the effects of crystalline orientation and beam flux ratio on Bi incorporation.

1.2 Part 2 Motivation: Disciplinary Researchers That Perform Educational Research

While brainstorming possible educational studies, our experience told us that students in MSE struggle learning crystal structures. A brief literature review revealed corroborating findings, showing that students often demonstrate misconceptions related to the atomic arrangement of atoms and atomic packing.³⁴⁻³⁶ Because having a complete understanding of crystal structures is vital to learning mechanical and electrical properties in later coursework, we viewed this as a foundational issue in materials science education worthy of further investigation.

Misconceptions related to atomic arrangement and atomic packing suggested that students have an incorrect mental model of crystal structures. We hypothesized these errors in mental models arise from using simplified 2-D representations to teach crystal structures, such as those presented in textbooks. Because crystal structure is an inherently 3-D subject matter, we

wanted to investigate if using VR, an inherently 3-D media platform, could help improve students' mental models of crystal structures and alleviate misconceptions. We attempted to engineer a solution to this problem by designing learning activities to compare the efficacy of using 2-D representations on paper to 3-D representations in VR to teach crystal structure. Specifically, we ask the research question: how do virtual reality (VR) learning tools enhance student learning of multidimensional concepts, specifically crystal structures? As you will see in Chapter 6, our findings didn't show strong evidence regarding of the effectiveness of using VR to teach crystal structures.

We consulted with STEM education researchers and STEM educational literature to understand why our study showed inconclusive results. We performed a systematic analysis of literature on educational studies conducted by MSE faculty over the past decade to understand what good experimental design looks like in this space. We discovered common trends and approaches to educational research conducted by STEM faculty. Our analysis of the literature shows that most MSE faculty write about the development and implementation of pedagogies, learning activities, labs, and teaching tools. While these studies provide useful information, Henderson et al.³⁷ showed that they are unlikely to convince instructors to change their teaching practices, suggesting that new approaches to educational research are needed. Furthermore, we found evidence to suggest that MSE faculty are largely unfamiliar with established educational theory to help them conduct high-quality educational research. We use our experiences to make suggestions to improve the state of educational research in MSE. We also suggest a path for future research that investigates the efficacy of using VR in the engineering classroom with these findings in mind.

1.3 Organization:

The remainder of this dissertation is organized into two parts. Part 1 is comprised of chapters 2-5 and focuses on identifying growth conditions that maximize Bi incorporation in highly mismatched III-V alloys.

Chapter 2 contains an overview of the experimental methods used throughout this dissertation. It discusses Molecular Beam Epitaxy (MBE) and the related techniques used to control and monitor crystal growth with a high degree of precision. It also discusses the broad array of techniques used to characterize surface morphology and film microstructure, including scanning electron microscopy (SEM), atomic force microscopy (AFM), electron dispersion spectroscopy (EDS), X-Ray diffraction (XRD), focused ion beam (FIB), scanning transmission electron microscopy (STEM), scanning tunneling microscopy (STM) and atomic probe tomography (APT).

Chapter 3 presents a study to identify the material beam flux ratios that maximize Bi incorporation in GaAsBi. To accomplish this, a series of GaAsBi (001) growths were conducted at 325°C over a large range of As₂/Ga and Bi/As₂ beam flux ratios. The results are used to establish a relationship between surface morphology, Bi incorporation, and microstructure. Notably, it was found that while films with Bi droplets support the highest levels of Bi incorporation, they also cause large compositional inhomogeneities. We use this finding to present a model that discusses the driving mechanism behind the phase segregation effects in films with Bi droplets.

Chapter 4 presents a study that investigates the influence of crystalline orientation on maximum Bi incorporation. We performed InAs:Bi superlattice growths on the (110) and (001) crystal surfaces to identify differences in incorporation. We found the (001) surface saturates

quicker than the (110) surface, and that higher incorporation can be achieved on the (110). Bi flux is also shown to induce a drastic reduction in RMS roughness of InAs (110) films, suppressing 3D growth and island formation.

Chapter 5 contains recommendations for future Bismides research, particularly as it applies to high index surfaces and nanostructure growth.

Part 2 is comprised of chapters 6-7 and discusses educational research in MSE. In chapter 6 we present a systematic review of educational literature conducted by materials science faculty. We analyze the approaches that MSE researchers take when they conduct educational research to determine their effectiveness at promoting changes in the teaching practices of instructors. We also analyze the effect of interdisciplinary collaboration on the research approaches of MSE faculty and the types of journals they publish in. We use our findings to discuss ways to promote more effective educational research in MSE.

Chapter 7 presents a study conducted to determine if using virtual reality (VR) to teach crystal structures is more effective than traditional paper-based methods. We designed a series of activities and studied their use in classroom settings. This approach led to inconclusive evidence regarding the effectiveness of using VR to teach crystal structures. We discuss the pros and cons of the experimental design of our study and suggest directions for future work.

1.4 References

1. Tiedje, T., Young, E. C. & Mascarenhas, A. Growth and properties of the dilute bismide semiconductor GaAs_{1-x}Bi_x a complementary alloy to the dilute nitrides. *Int J Nanotechnol* 5, 963–983 (2008).
2. Madouri, D., Boukra, A., Zaoui, A. & Ferhat, M. Bismuth alloying in GaAs : a first-principles study. *Comput Mater Sci* 43, 818–822 (2008).
3. Fluegel, B. et al. Giant spin-orbit bowing in GaAs_{1-x}Bi_x. *Phys Rev Lett* 97, 11–14 (2006).
4. Francoeur, S. et al. Band gap of GaAs_{1-x}Bi_x, 0<x< 3.6%. *Appl Phys Lett* 82, 3874–3876 (2003).
5. Ma, K. Y. et al. Organometallic vapor phase epitaxial growth and characterization of InAsBi and InAsSbBi. *Appl Phys Lett* 55, 26–29 (1989).
6. Schaefer, S. T., Kosireddy, R. R., Webster, P. T. & Johnson, S. R. Molecular beam epitaxy growth and optical properties of InAsSbBi. *J Appl Phys* 126, (2019).
7. Khanom, S. et al. Simulation Study of MultiJunction Solar Cell Incorporating GaAsBi. 2017 IEEE Region 10 Humanitarian Technology Conference 21–23 (2017).
8. Thomas, T. et al. Requirements for a GaAsBi 1 eV sub-cell in a GaAs-based multi-junction solar cell. *Semicond Sci Technol* 30, (2015).
9. Broderick, C. A., Harnedy, P. E. & O'Reilly, E. P. Theory of the Electronic and Optical Properties of Dilute Bismide Quantum Well Lasers. *IEEE Journal of Selected Topics in Quantum Electronics* 21, 287–299 (2015).
10. Marko, I. P. et al. Properties of hybrid MOVPE/MBE grown GaAsBi/GaAs based near-infrared emitting quantum well lasers. *Semicond Sci Technol* 30, (2015).
11. Velicu, S. et al. MWIR and LWIR HgCdTe infrared detectors operated with reduced cooling requirements. in *Journal of Electronic Materials* vol. 39 873–881 (2010).

12. Hild, K. et al. Auger recombination suppression and band alignment in GaAsBi/GaAs heterostructures. in AIP Conference Proceedings vol. 1566 488–489 (American Institute of Physics Inc., 2013).
13. Hader, J. et al. Auger losses in dilute InAsBi. *Appl Phys Lett* 112, (2018).
14. Krishnamurthy, S., Chen, A.-B., Sher, A. & van Schilfgaarde, M. Temperature Dependence of Band Gaps in HgCdTe and Other Semiconductors. *Journal of Electronic Materials* vol. 24 (1995).
15. Yoshida, J., Kita, T., Wada, O. & Oe, K. Temperature dependence of GaAs_{1-x}Bi_x band gap studied by photoreflectance spectroscopy. *Japanese Journal of Applied Physics, Part 1: Regular Papers and Short Notes and Review Papers* 42, 371–374 (2003).
16. Mohmad, A. R., Bastiman, F., Ng, J. S., Sweeney, S. J. & David, J. P. R. Room temperature photoluminescence intensity enhancement in GaAs_{1-x}Bi_x alloys. *Physica Status Solidi (C) Current Topics in Solid State Physics* 9, 259–261 (2012).
17. Fitouri, H., Essouda, Y., Zaied, I., Rebey, A. & el Jani, B. Photoreflectance and photoluminescence study of localization effects in GaAsBi alloys. *Opt Mater (Amst)* 42, 67–71 (2015).
18. Elayech, N., Fitouri, H., Boussaha, R., Rebey, A. & Jani, B. el. Calculation of InAsBi ternary phase diagram. *Vacuum* 131, 147–155 (2016).
19. Elayech, N., Fitouri, H., Essouda, Y., Rebey, A. & el Jani, B. Thermodynamic study of the ternary system gallium-arsenic-bismuth. *Physica Status Solidi (C) Current Topics in Solid State Physics* 12, 138–141 (2015).
20. Tait, C. R., Yan, L. & Millunchick, J. M. Droplet induced compositional inhomogeneities in GaAsBi. *Appl Phys Lett* 111, 1–5 (2017).
21. Wood, A. W., Collar, K., Li, J., Brown, A. S. & Babcock, S. E. Droplet-mediated formation of embedded GaAs nanowires in MBE GaAs_{1-x}Bi_x films. *Nanotechnology* 27, (2016).
22. Tait, C. R., Yan, L. & Millunchick, J. M. Spontaneous nanostructure formation in GaAsBi alloys. *J Cryst Growth* 493, 20–24 (2018).

23. Darowski, N., Pietsch, U., Zeimer, U., Smirnitzki, V. & Bugge, F. X-ray study of lateral strain and composition modulation in an AlGaAs overlayer induced by a GaAs lateral surface grating. *J Appl Phys* 84, 1366–1370 (1998).
24. Puustinen, J. et al. Variation of lattice constant and cluster formation in GaAsBi. *J Appl Phys* 114, (2013).
25. Dominguez, L. et al. Formation of tetragonal InBi clusters in InAsBi/InAs(100) heterostructures grown by molecular beam epitaxy. *Applied Physics Express* 6, (2013).
26. Likhachev, I. A. et al. Microstructure of QD-like clusters in GaAs/In(As,Bi) heterosystems. *J Mater Res* 33, 2342–2349 (2018).
27. Imhof, S. et al. Clustering effects in Ga(AsBi). *Appl Phys Lett* 96, 3–6 (2010).
28. Ciatto, G. et al. Spatial correlation between Bi atoms in dilute GaAs_{1-x}Bi_x: From random distribution to Bi pairing and clustering. *Phys Rev B Condens Matter Mater Phys* 78, 1–5 (2008).
29. Wu, M., Luna, E., Puustinen, J., Guina, M. & Trampert, A. Formation and phase transformation of Bi-containing QD-like clusters in annealed GaAsBi. *Nanotechnology* 25, (2014).
30. Wu, M., Luna, E., Puustinen, J., Guina, M. & Trampert, A. Observation of atomic ordering of triple-period-A and -B type in GaAsBi. *Appl Phys Lett* 105, (2014).
31. Reyes, D. F. et al. Bismuth incorporation and the role of ordering in GaAsBi/GaAs structures. *Nanoscale Res Lett* 9, 1–8 (2014).
32. Norman, A. G., France, R. & Ptak, A. J. Atomic ordering and phase separation in MBE GaAs_{1-x}Bi_x. *Journal of Vacuum Science & Technology B, Nanotechnology and Microelectronics: Materials, Processing, Measurement, and Phenomena* 29, 03C121 (2011).
33. Rodriguez, G. v. & Millunchick, J. M. Predictive modeling of low solubility semiconductor alloys. *J Appl Phys* 120, (2016).

34. Krause, S. & Waters, C. Uncovering and repairing crystal structure misconceptions in an introductory materials engineering class. Proceedings - Frontiers in Education Conference, FIE (2012) doi:10.1109/FIE.2012.6462296.
35. Krause, S., Kelly, J., Baker, D. & Kurpius-Robinson, S. Effect of pedagogy on conceptual change in repairing misconceptions of differing origins in an introductory materials course. ASEE Annual Conference and Exposition, Conference Proceedings (2010).
36. Gentry, S. P. & Faltens, T. A computer-based interactive activity for visualizing crystal structures in introductory materials science courses. ASEE Annual Conference and Exposition, Conference Proceedings 2017-June, (2017).
37. Henderson, C., Beach, A. & Finkelstein, N. Facilitating change in undergraduate STEM instructional practices: An analytic review of the literature. *J Res Sci Teach* 48, 952–984 (2011).

Chapter 2 Experimental Procedures:

The purpose of this chapter is to discuss the experimental procedures used throughout part one of this dissertation.

2.1 Molecular Beam Epitaxy

The Bismide alloys studied in this dissertation are grown using molecular beam epitaxy (MBE). MBE is a physical vapor deposition technique that was developed by Alfred Cho and John Arthur in 1968.¹ In MBE pure elemental source materials are evaporated or sublimated in ultra-high vacuum to produce a ‘vapor beam’ directed at a single crystal substrate. The incident ‘beam’ of material incorporates following the atomic ordering of the substrate allowing for the growth of high-quality single crystal films. Furthermore, the ultra-high vacuum (UHV) minimizes unwanted reactions with atmospheric contaminants and keeps the growth surface clean allowing for film growth with a very low level of defects. MBE also gives precise control over growth conditions including substrate temperature and material flux. For example, the temperature of the source material can be changed to increase or decrease material flux which influences the growth rate of the crystal. The temperature of the substrate can also be increased or decreased to change the kinetics of surface adatoms influencing their adsorption, diffusion, and incorporation into the crystal.

2.2 System Details

An EPI 930 solid source MBE system was used for the growths presented in this dissertation. The schematic diagram shown in Fig 2.1 shows the MBE chamber is connected in

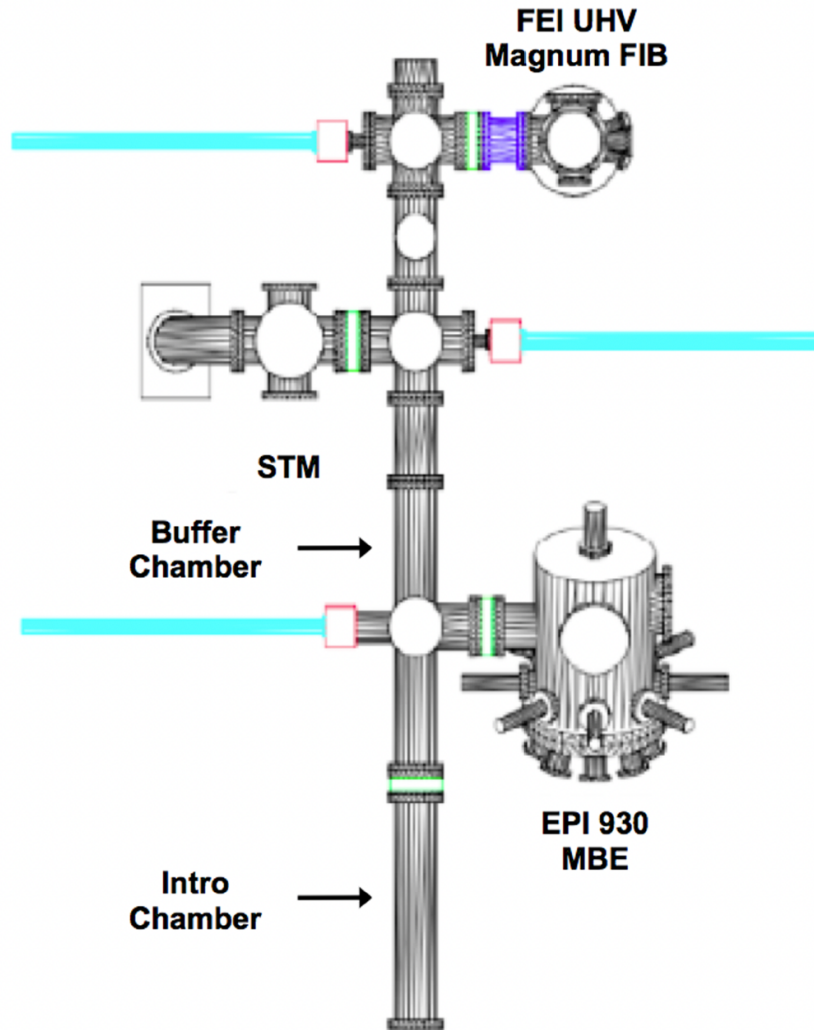


Figure 2.1 Schematic diagram of the experimental equipment used in this dissertation ⁶

series via gate valves with a buffer chamber, sample loading chamber (intro), and an in-vacuo RHK STM-100 scanning tunneling microscope (STM).

The intro chamber was vented to the atmosphere to load and unload samples. The buffer chamber is an intermediate UHV chamber between the MBE and intro chambers to preserve the vacuum integrity in the MBE chamber and maintain clean sample surfaces. Vacuum for the MBE chamber was supplied by an ion-pump and cryogenic pump which achieved vacuums in the low 10^{-8} torr range. This pressure could be dropped at least one order of magnitude by

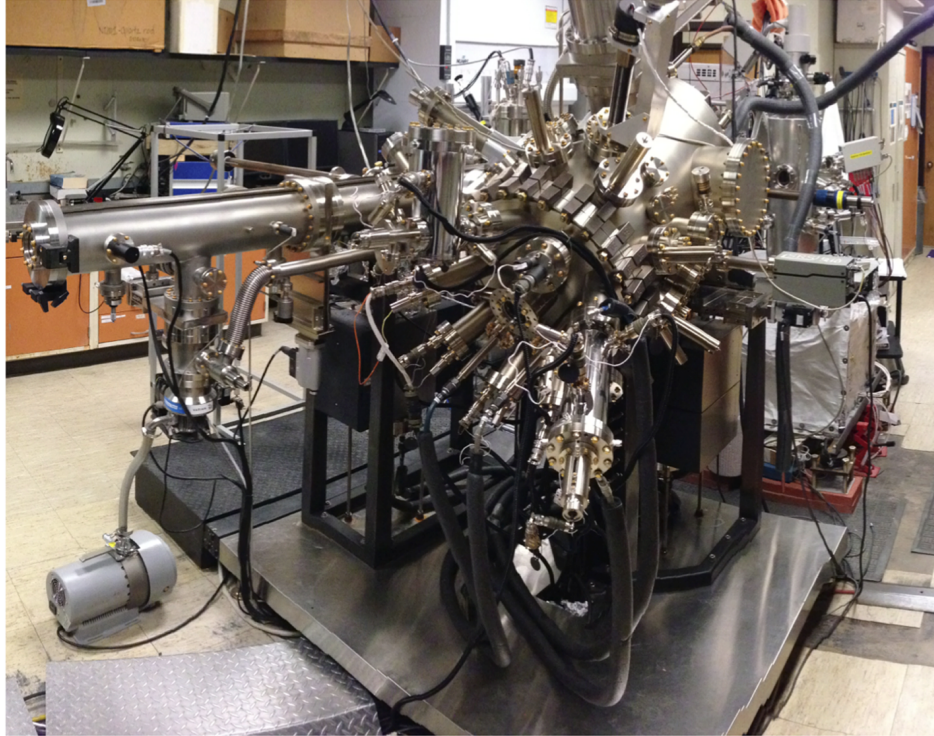


Figure 2.2 Photograph of the MBE chamber used for the experimental growths in this dissertation⁵

cooling the chamber with liquid nitrogen to minimize outgassing of residual material buildup on the interior walls of the MBE chamber.

2.2.1 Effusion Cells and Measuring Material Beam Flux

A photograph and schematic of the MBE chamber are given in Figs 2.2 and 2.3 respectively. Both figures show the Knudson effusion cells, which heat source materials to produce the desired material flux. The group V materials, As and Sb, had valved cracking sources with dual heating zones. In these sources, the bulk zone holds and heats the source material, and the cracking zone controls the atomic species. For example, the cracking zone of the As source can ‘*crack*’ As_4 into As_2 if the temperature is high enough. The As and Sb sources also contain valves which can be actuated to provide fine-tuned control over material flux,

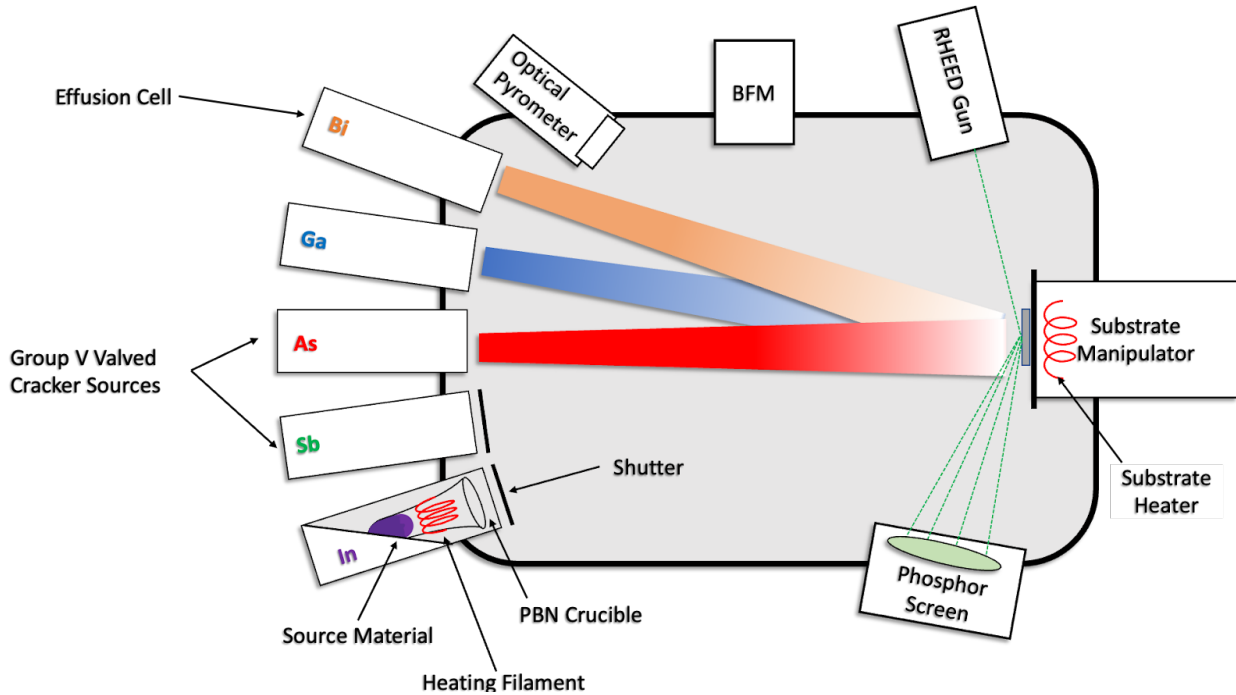


Figure 2.3 Schematic diagram of the MBE chamber. We excluded the doping effusion cells for Si and Be in this representation as they were not used in the growth presented in this dissertation

allowing the targeting of specific V/III ratios. It should also be noted that the effusion cells are thermally isolated from each other via a water-cooling jacket that continuously circulates chilled water.

Material flux was measured with a Bayard-Alpert style ion gauge, also referred to as a beam flux measurement (BFM) gauge, that is lowered directly in front of the sample manipulator and intercepts the ‘beam’ of material. This measurement of material flux is referred to as the beam equivalent pressure (BEP) of the material sources. Furthermore, the chamber is equipped with pneumatic shutters that allow us to quickly actuate the materials sources on and off by physically blocking the material flux.

Figure 2.3 shows that the MBE chamber was equipped with several other instruments for fine-tuned control of growth conditions. The chamber is equipped with a reflection high energy electron diffraction (RHEED) gun and accompanying phosphor screen that are used to determine growth rate, oxide desorption temperature, and surface reconstruction. Substrate temperature was

carefully monitored using an optical pyrometer with an operating range between 250 and 1400°C.

2.2.2 Sample Preparation and Growth

All substrates were single-side polished epi-ready grade. These substrates were cleaved into smaller pieces (~1cm²) and mounted onto molybdenum pucks using indium as a wetting agent. These samples were then placed into the intro chamber to outgas at 150°C for 4 hours to remove any adsorbed atmospheric gases or water vapor. After this stage, samples were transferred into the buffer chamber until growth.

Once in the growth chamber, the samples were heated with the substrate manipulator under an As overpressure to desorb the native oxide. Oxide desorption occurred at ~600°C for GaAs and ~500°C for InAs. Next, film growth was commenced by ramping the substrate to the desired growth temperature and exposing the surface to material flux. After all growth steps were completed, the samples were quenched to 200°C and promptly removed from the growth chamber. Finally, the samples were unmounted from the molybdenum pucks with a hotplate to melt the In wetting layer.

2.2.3 RHEED

The information that can be derived from RHEED patterns is vital and plays an important role in the research presented in this dissertation. The MBE chamber is equipped with a Staib Instruments RHEED gun operated at approximately 15kV and 1.5mA. The RHEED gun was oriented such that collimated electrons strike the sample surface at a shallow angle of only a couple degrees, interacting with only the first few atomic layers of the crystal. Opposite to the RHEED gun there is a phosphor screen where the diffracted and specularly reflected electrons

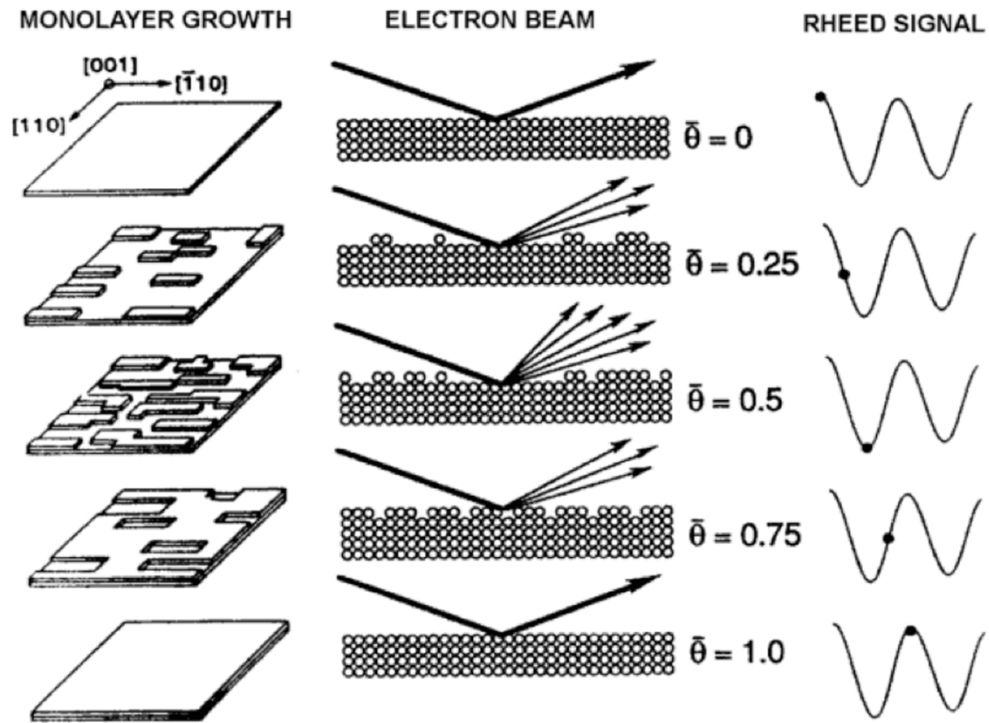


Figure 2.4 Schematic showing how growth rate is measured as the sample temporarily roughens⁷

strike creating a diffraction pattern. This pattern was captured by a K-space Associates KSA 400 RHEED analysis camera and software was used to analyze this pattern.

RHEED is used for several steps during growth. First, it is used to monitor for the oxide desorption. Because oxide layers are amorphous in nature, the electrons are randomly diffracted resulting in a uniform haze on the phosphor screen. However, once the oxide desorbs, the crystalline lattice is exposed and a well-defined diffraction pattern corresponding to the surface reconstruction is observed.

The RHEED pattern also contains other useful information. For example, a streaky diffraction pattern indicates a smooth 2-D surface, and a spotty diffraction pattern indicates a roughened 3-D surface. RHEED is also used to quantify the rate of epitaxial growth, shown in Fig. 2.4. When a new monolayer of growth begins, atomically flat surfaces temporarily roughen as the new layer nucleates. This roughness temporarily reduces the intensity of the specularly

reflected RHEED beam at the phosphor screen. However, as the layer nears completion, the intensity increases again resulting in an oscillation corresponding to one monolayer of growth, allowing for a determination of growth rate.⁷

2.3 Sample Characterization

A large focus in the first section of this dissertation is the characterization of compositional and morphological properties of GaAsBi and InAsBi films. This section presents the techniques used for these characterizations.

2.3.1 Scanning Electron Microscopy

SEM is a valuable technique to image semiconductor materials as it provides high lateral resolution images of the surface. The SEM micrographs presented in this dissertation were taken with the SEMs operating in secondary electron mode. Several SEMs were used to image the samples in this study and were generally used interchangeably depending on the availability and the application. These microscopes included a Thermofisher Scientific Nova 200 Nanolab Dual Beam Microscope, Thermofisher Scientific Helios 650 Nanolab Dual Beam Microscope, and a JEOL IT500 SEM. The imaging conditions used were accelerating voltages of 5 - 10 kV and a beam current of 0.2 - 0.4nA.

2.3.2 Atomic Force Microscopy

While SEM provides good lateral resolution, it provides little quantitative information about the 3D topography of the surface. In contrast, AFM provides a high out-of-plane resolution up to 0.1 nm, small enough to accurately image a single monolayer of material deposition. However, its lateral resolution is limited by the finite probe size. In the studies presented in this dissertation a Digital Instruments NanoScope IIIa AFM was operated in non-contact tapping

mode using Si cantilever probes with a ($<7\text{nm}$) radius of curvature. The scanning parameters were controlled using NanoScope software. The initial scan parameters were a voltage amplitude of $\sim 2\text{V}$, and a scanning frequency of 1Hz , however these parameters were adjusted to ensure an accurate forward and reverse trace of the surface.

2.3.3 Scanning Tunneling Microscopy

An in-vacuo scanning tunneling electron microscopy (STM) was also used to characterize a sample presented in this dissertation. STM can achieve atomic resolution in lateral and vertical directions, while also providing information about the electronic structure of film surfaces. The STM used in this dissertation was an RHK STM 100. The initial scanning parameters for STM was a biasing voltage of approximately 2.0 V , and a tunneling current of 100pA however the biasing voltage was adjusted to achieve an accurate forward and reverse trace of the surface.

2.3.4 Energy Dispersive Spectroscopy (EDS)

All the SEM's and STEMs utilized in this study were equipped with energy dispersive spectroscopy (EDS) detectors which allow for accurate quantification of chemical composition. This technique uses the electron beam of the SEM or STEM to eject core shell electrons. This vacancy left by the ejected electron prompts the decay of a higher energy electron to fill this void. This process emits a characteristic X-ray that is measured by the detector and is specific to atomic species. This experimental technique was valuable to quickly determine the composition of surface droplets during SEM analysis.

2.3.5 Focused Ion Beams (FIB)

Focused Ion Beams (FIBs) were used for the preparation of both atomic probe tomography (APT) tips and STEM cross sectional lift outs. The extensive procedures for preparing APT tips can be found in Dr. Andrew Martin's dissertation entitled "Manipulating Quantum Dot Nanostructures for Photonic and Photovoltaic Applications".⁵

We used multiple FIBs for sample preparation including a Thermofisher Scientific Nova 200 Nanolab Dual Beam Microscope, Thermofisher Scientific Helios 650 Nanolab Dual Beam Microscope and Thermofisher Scientific Helios G4 Plasma FIB UXe. We found that InAs was susceptible to Ga implantation during sample preparation which caused the formation of In droplets on the surface that obscured the microstructure in STEM imaging. We discovered that using the plasma FIB prevented this ion implantation and used it exclusively during the preparation of InAs samples.

2.3.6 X-Ray Diffraction (XRD)

X-ray diffraction is a non-destructive technique that uses monochromatic X-ray radiation to determine the average lattice spacing of crystals. θ - 2θ diffraction curves were measured with a Rigaku Smartlab by sweeping the radiation source and detectors through a range of θ - 2θ , where θ is the angle between the incident X-ray beam and sample, and 2θ is the angle between the diffracted beam and the sample. When the conditions outlined by Bragg's Law (1) are satisfied, the diffraction curve exhibits a sharp peak in intensity. In equation 1, n is the order of the diffraction peak, λ is the wavelength of radiation ($\text{CuK}\alpha = 1.5406 \text{ \AA}$) and d is the lattice spacing between planes.

$$n\lambda = 2d\sin(\theta) \quad (1)$$

Strain induced by Bi incorporation increases the average lattice parameter and shifts the diffraction peak towards lower angles. Vegard's Law (2) is then used to relate the lattice parameter to the Bi composition (x) of ternary alloys.²

$$d_{\text{III-V}(1-x)\text{Bi}(x)} = (1-x)d_{\text{III-V}} + xd_{\text{III-Bi}} \quad (2)$$

The lattice parameter for the GaBi and InBi binary endpoints have been calculated to be 6.33\AA^3 and 6.61\AA^4 respectively.

2.3.7 Scanning Transmission Electron Microscopy (STEM)

The power of scanning transmission electron microscopy (STEM) lies in its ability to achieve atomic resolution. Images were acquired using a high angle annular dark field (HAADF) detector due to its atomic number sensitivity. The large atomic number of Bi ($n=83$) causes electrons to scatter more strongly than the host InAs or GaAs lattice, resulting in a larger signal to noise ratio in regions with enhanced Bi incorporation and atomic number contrast. A few different STEMs were used in this work including a JEOL 2100 AEM Analytic Microscope, JEOL 3100R05 Double Cs Corrected Microscope and a Thermofisher Scientific Talos F200X G2 microscope.

2.3.8 Atomic Probe Tomography

Atom Probe Tomography (APT) is a destructive characterization technique that provides a 3-D reconstruction of samples and chemical composition analysis. It was useful in identifying compositional inhomogeneities within bulk GaAsBi films. It provides 0.1-0.3 nm resolution in depth and 0.3-0.5 nm resolution laterally, but it is limited by the requirement that the sample be milled into a sharp tip resulting in a small area of analysis. The sharp tip geometry is required because APT operates by applying a large electric field to generate a charge concentration at the tip which is then pulsed with an electric field or laser to evaporate ions. A detector measures the time of flight and position data for these ions allowing for chemical analysis and a 3-D reconstruction of atoms.

A Cameca Leap 5000 XR APT was used in voltage pulsing mode to analyze samples in this dissertation. We applied 500 V to the tip and pulsed 100 V with a frequency of 250 Hz. The

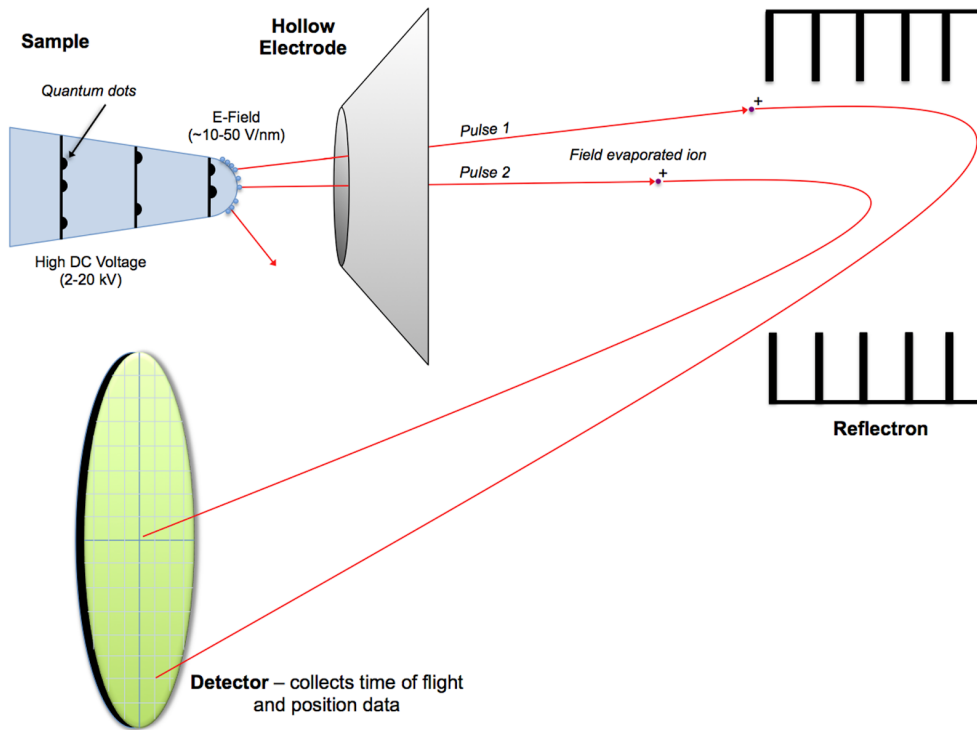


Figure 2.5 A schematic diagram of the Cameca LEAP 5000XR atom probe showing the sample tip, local electrode, reflectron and detector⁵

desired detection rate was set between 0.5% and 1% with the goal of detecting one ion per voltage pulse. This ensured that the mass and time of flight data for each ion could be uniquely interpreted to determine its species and coordinates. To ensure the detection rate was maintained as ions were evaporated and the tip became blunt, the software automatically controlled the voltage, which resulted in a gradual upward creep to maintain the charge concentration. A schematic of the Cameca 5000 XR Leap is given in Fig. 2.5, where the voltages are applied between the hollow electrode and the sample tip.

IVAS analysis software was used to reconstruct and analyze the APT data. This process was adapted from Dr. Andrew Martins dissertation.⁵ First, the reconstruction had to be completed by setting two parameters, the evaporation field, and the image compression factor. These values were adjusted such that the reconstructed data matched the geometry of the APT tip. During this step it is also vital to ensure that known planar features, such as the substrate/film interface, are flattened. After the reconstruction process was complete, the data was analyzed by creating concentration profiles. A voxel size of $0.5 \times 0.5 \times 0.5 \text{ nm}^3$ and delocalization distance of 3 nm were used in this process. We also decomposed the data to ensure that evaporated molecules such as As_4 are counted as 4 As atoms rather than one large ion to yield a more accurate composition profile.

2.4 References

1. Cho, A. Y. & Arthur, J. R. MOLECULAR BEAM EPITAXY. Progress in Solid-State Chemistry vol. 10 (1975).
2. Denton, R. A. & Ashcroft, N. W. Vegard's Law. Phys Rev A (Coll Park) 43, (1991).
3. Tixier, S. et al. Molecular beam epitaxy growth of $\text{GaAs}_{1-x}\text{Bi}_x$. Appl Phys Lett 82, 2245–2247 (2003).

4. Shalindar, A. J., Webster, P. T., Wilkens, B. J., Alford, T. L. & Johnson, S. R. Measurement of InAsBi mole fraction and InBi lattice constant using Rutherford backscattering spectrometry and X-ray diffraction. *J Appl Phys* 120, (2016).
5. Martin, A. *Manipulating Quantum Dot Nanostructures for Photonic and Photovoltaic Applications*. (2013).
6. Ohring, M. *The Materials Science of Thin Films*. (San Diego: Academic Press, 1992).
7. Grossklaus, K. A. *Examination of the Ion Beam Response of III-V Semiconductor Substrates*. (2012).

Chapter 3 Chapter 1 Systematic Exploration of Material Flux Parameter Space to Maximize Bi Incorporation in GaAsBi

The purpose of this chapter is to present experiments designed to answer the research question: what growth conditions maximize Bi incorporation in III-Vs? We discuss the effect of material beam flux ratio on Bi incorporation and identify a small range of growth parameters with elevated Bi incorporation. We show that maximum incorporation occurred in films with Bi rich droplets on the surface. However, microstructural characterization revealed that Bi rich droplets cause compositional inhomogeneities. Finally, we provide a model to explain the mechanisms that drive these compositional inhomogeneities.

3.1 Introduction: Challenges with Bi Incorporation

The experimental realization of III-V films with high mole fractions of Bi is complicated by low solid-state miscibility of Bi in III-Vs.^{1,2} For Bi to incorporate into the crystal lattice it

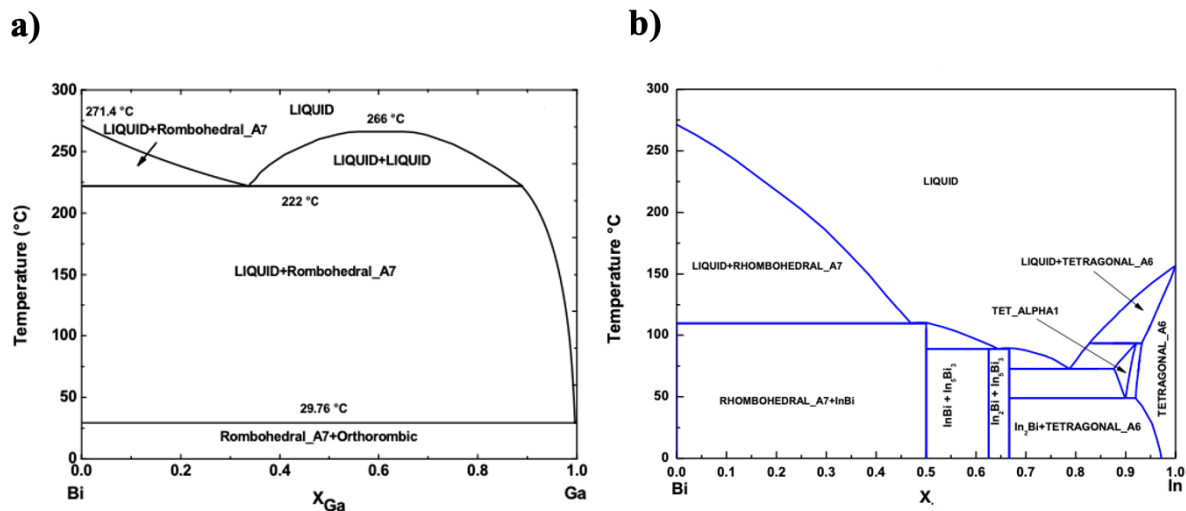


Figure 3.1 a) Phase diagram of GaBi binary material system¹ b) Phase diagram of InBi binary material system²

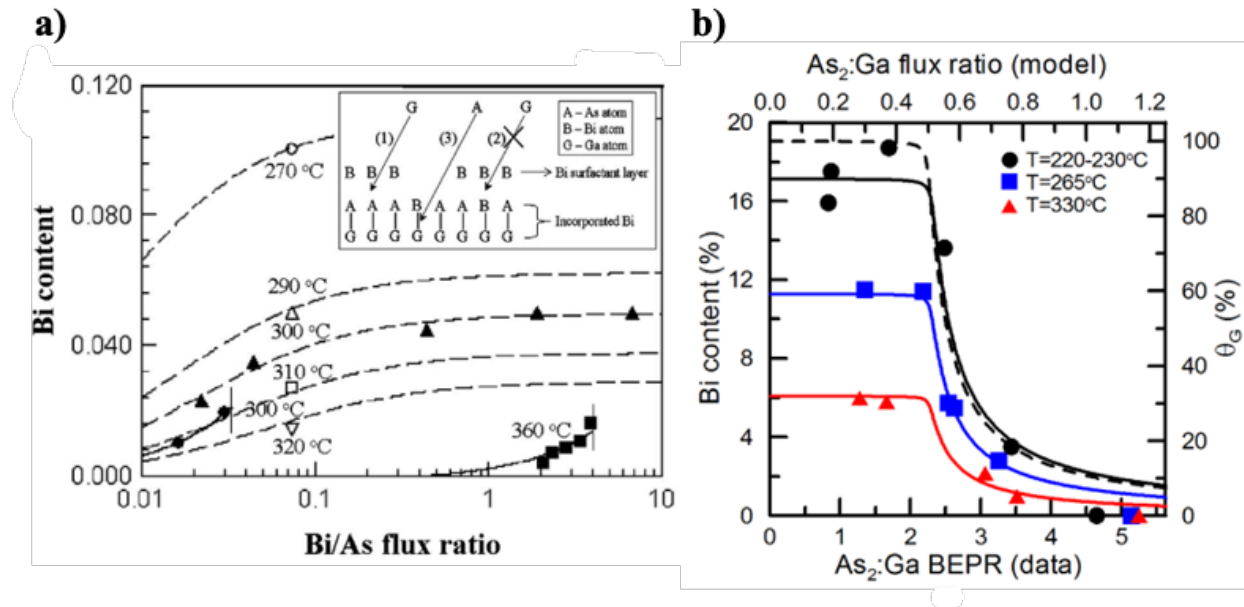


Figure 3.2 a) Temperature series of Bi incorporation as a function of Bi/As flux ratio³. b) Temperature series of Bi incorporation as a function of As₂/Ga.⁴

must form a bond with group III elements. However, the phase diagrams in Fig. 3.1 show that GaBi is an unstable compound, and that Bi only exhibits limited solid state miscibility in In up to 109.5°C. As a result, researchers have explored several tactics to increase Bi incorporation in III-Vs.

MBE provides fine-tuned control over material flux and growth temperature. As such, most strategies for increasing Bi incorporation involve manipulating one of these two parameters. Figures 3.2a and 3.2b show that Bi incorporation is inversely proportional to the growth temperature.^{3,4} As growth temperature increases, the probability that Bi adatoms desorb from the surface, and the probability of Bi desorption from the crystal termination layer both increase, leading to lower levels of Bi incorporation.³⁻⁵ For example, Tait et al. showed that even a modest increase in temperature, from 325 °C to 340 °C, resulted in a 32% decrease in Bi incorporation in GaAsBi films grown with otherwise identical growth conditions.⁶ As a result, GaAsBi films are generally grown with low temperature between 290°C and 330°C. However, it

should be noted that low temperature growth is also associated with an increase in point defects such as Ga vacancies and As antisites.^{7,8}

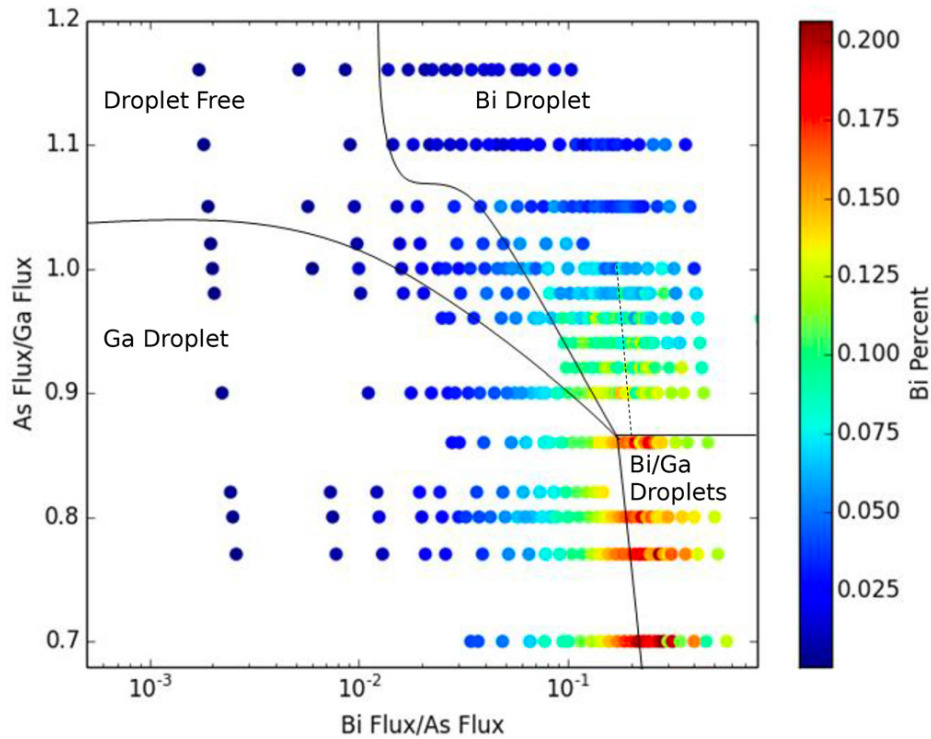


Figure 3.3 Kinetic Monte Carlo simulations showing the dependence of Bi Incorporation on material flux ratio and droplet formation⁹

Figure. 3.2a also shows that increasing the Bi/As flux ratio correspondingly increases Bi incorporation. This is because As and Bi compete for the same group III bonding sites, and a higher Bi flux/lower As flux increases the probability that a Bi adatom will diffuse to an incorporation site before As. Furthermore, a lower As flux minimizes the probability that As will thermally eject and replace previously incorporated Bi in the crystal termination layer.³⁻⁵ Similarly, Fig 3.2b also shows that Bi incorporation can be increased by utilizing low V/III flux ratios close to stoichiometry. This promotes group III terminated surfaces which maximizes the number of bonding sites for Bi. Bi incorporation is observed to plateau once V/III stoichiometry is reached.³⁻⁵

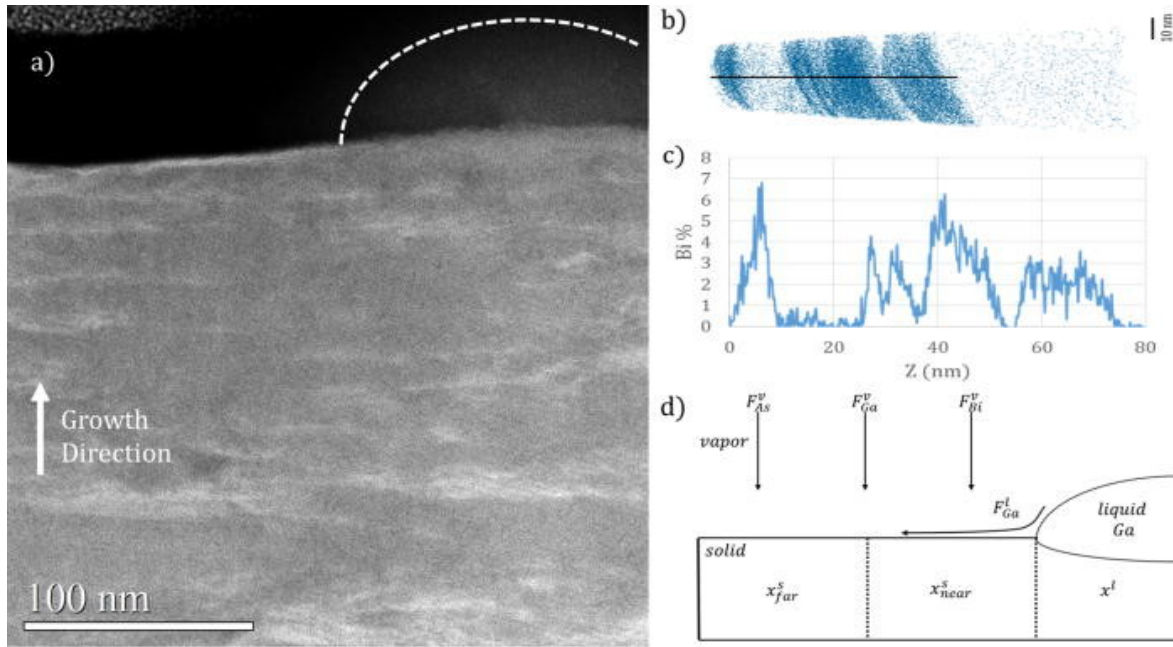


Figure 3.4 a) HAADF TEM showing inhomogeneous distribution of Bi. The dotted line shows an outline for Ga on the surface. b) APT of the same sample with Bi atoms mapped in blue, with a cross sectional region of interest shown. c) Average Bi composition of the identified cross section. d) illustration of the Ga wicking effect of the droplet which creates a region of elevated incorporation near the droplets, that is not observed further away from the droplet leading to the variations in composition¹⁰

However, simulations by Rodriguez et al.⁹ in Fig 3.3 show that using high Bi/As and low As/Ga flux ratios can respectively lead to Bi and Ga droplets if not carefully optimized. This represents a fundamental challenge to the realization of high quality Bismide films because studies have shown that Ga droplets induce compositional inhomogeneities.^{10,11} Specifically, Fig 3.4 shows that Ga droplets wick onto the surface of films and create localized regions of high Ga availability that support elevated Bi incorporation adjacent to the droplet.¹⁰ Similarly, Wood et al. has shown that Ga rich droplets serve as a physical barrier to Bi incorporation and leave a trail of Bi depleted film as the growth front progresses.¹¹ Compositional inhomogeneities, like these, cause detrimental electronic properties, such as carrier localization,^{12–15} which means that growth under conditions that yield Ga droplets should be avoided. However, the compositional effects, if any, induced by Bi-rich droplets are not documented in literature. In this chapter we address this gap and show that Bi droplets also cause large compositional inhomogeneities.

We find it prudent to acknowledge that Bi is also observed to phase segregate in droplet-free films causing several types of compositional inhomogeneities, including; lateral composition modulation,^{6,16} Bi clustering,^{6,17-19} and atomic ordering.^{20,21} Theoretical simulation²² and experimental investigations²³ have indicated that lateral composition modulation is caused by growth instabilities arising from differences in the diffusion length of Bi and As. Tait et al. showed that growth at high temperatures, starting at 325 °C and up, served to mitigate these differences and decrease the degree of compositional inhomogeneities at the expense of Bi incorporation.⁶ Bi clustering is driven by the low miscibility of Bi in III-Vs which creates a chemical driving force for Bi to segregate. This Bi transport is thought to be enabled by the high density of Ga vacancies that occur in low temperature III-V growth.^{7,8} Furthermore, annealing films is shown to enhance clustering and cause a phase transition from zinc-blende clusters to rhombohedral clusters.^{17,18} Finally, research has shown that Bi tends to incorporate into III-V's along preferential planes with a defined order^{20,21}, and is thought to be related to surface reconstruction during growth. Norman et al.²⁰ showed the occurrence of $\{111\}$ B CuPt type ordering in GaAsBi films grown under a (2x1) surface reconstruction. Similarly, Wu et al.²¹ reported two additional ordering variants in GaAsBi: triple-period A-type ordering and triple-period B-type ordering along $\{111\}$ planes. They postulate that the occurrence of triple period-A or triple period-b type ordering is correlated with the multiple stable (nx3) surface reconstructions. All these segregation effects are caused by the intrinsic thermodynamic properties of the GaAsBi material system and therefore likely also occur in films with droplets. As such we place an emphasis on maximizing Bi incorporation in droplet-free films as they likely have the lowest degree of compositional inhomogeneity.

Balancing the goal of high Bi incorporation against compositional uniformity is non-trivial because simulations predict that maximum incorporation occurs when Ga rich droplets form on the surface.⁹ Experiments have borne this prediction out with the maximum reported concentration in GaAsBi, $x = 22\%$ Bi, occurring when Ga droplets form on the surface.⁴ Contrastingly, the maximum reported composition in droplet-free films is 11%, approximately half of the value when droplets form on the surface.⁴

However, the simulations also predict a small window of droplet-free growth with elevated Bi incorporation, near the transition to Bi/Ga biphasic droplets.⁹ In this chapter we present a series of experimental growths dedicated to identifying this window and maximizing Bi incorporation in GaAsBi films, while simultaneously avoiding compositional inhomogeneities caused by droplets. Furthermore, we also characterize the microstructure of films grown with Bi rich droplets to understand origin of their compositional inhomogeneities.

3.2 Growth Conditions and Parameters

A series of 25 GaAsBi (001) growths were performed over a wide range of material flux ratios to identify the growth conditions that yield maximum Bi incorporation, particularly in droplet-free films. Substrates were prepared for growth under almost identical growth conditions. First, a 250 nm GaAs buffer layer was grown at $T = 600^\circ\text{C}$, with a growth rate between 0.8 and 1 ML/s, under a high As_2 backpressure. At the conclusion of the buffer layer growth, RHEED showed streaky (2x4) diffraction indicating high quality 2-D growth. Samples were then cooled to 325°C , and 500nm of GaAsBi was grown with beam flux ratios; $1.62 < \text{As}_2 / \text{Ga} < 3.46$ and $0 < \text{Bi} / \text{As}_2 < 0.37$. The large range of beam flux ratios ensured we obtained samples with four distinct surface morphologies: droplet-free, Ga droplets, Bi droplets and biphasic droplets, qualitatively matching simulation by Rodriguez et al.⁹ To mitigate defects, the samples were

Table 3.1 Growth conditions for a representative sample with each surface morphology/droplet type. Film composition and parameters derived from XRD are also reported here

| Sample | As ₂ :Ga | Bi:As ₂ | T(°C) | R _{Ga} (ML/s) | Anneal | Droplet | X _{max} (%) | X _{med} (%) | W _{OOM} (“) |
|--------|---------------------|--------------------|-------|------------------------|--------|----------|----------------------|----------------------|----------------------|
| a | 2.49 | 0.12 | 325 | 0.90 | Yes | None | 8.1 | 8.5 | 1368 |
| b | 2.76 | 0.33 | 325 | 0.95 | Yes | Bi | 8.0 | 6.5 | 6480 |
| c | 1.78 | 0.05 | 325 | 0.94 | Yes | Ga | 3.0 | 2.8 | 1836 |
| d | 1.62 | 0.37 | 325 | 0.82 | Yes | Biphasic | 3.6 | 8.7 | 5580 |

annealed at 325°C for 5 minutes. Finally, the samples were quenched to 200°C and removed from the growth chamber.

Preliminary characterization with SEM and XRD showed that samples exhibiting the same surface morphology (droplet type) exhibited similar variations in lattice parameter. This suggested, and was later verified, that each surface morphology caused different but internally consistent types of compositional inhomogeneities. As such, one representative sample from each surface morphology was used for further analysis. Table 3.1 gives their respective growth conditions, surface morphology and compositional parameters.

3.3 Four Morphological Regimes Verified With SEM

SEM micrographs of the representative samples a-d from each surface morphology are given in Fig 3.5. Figure 3.5a shows a SEM micrograph of the droplet-free sample a, grown with beam flux ratios of As₂/ Ga=2.5 and Bi/ As₂=0.1. The SEM of sample b given in Fig 3.5b, shows that sufficiently increasing Bi flux (by a factor of ~3) while keeping As₂/ Ga nominally constant, yields Bi droplets. The Bi droplets are irregularly shaped and exhibit a bi-modal size distribution. The larger droplets have diameters between approximately 1 and 3 μm, and smaller droplets have diameters between approximately 100 and 500 nm. The SEM of sample c given in Fig 3.5c, shows that if the As₂/ Ga beam flux ratio is lowered past stoichiometry, the excess Ga forms

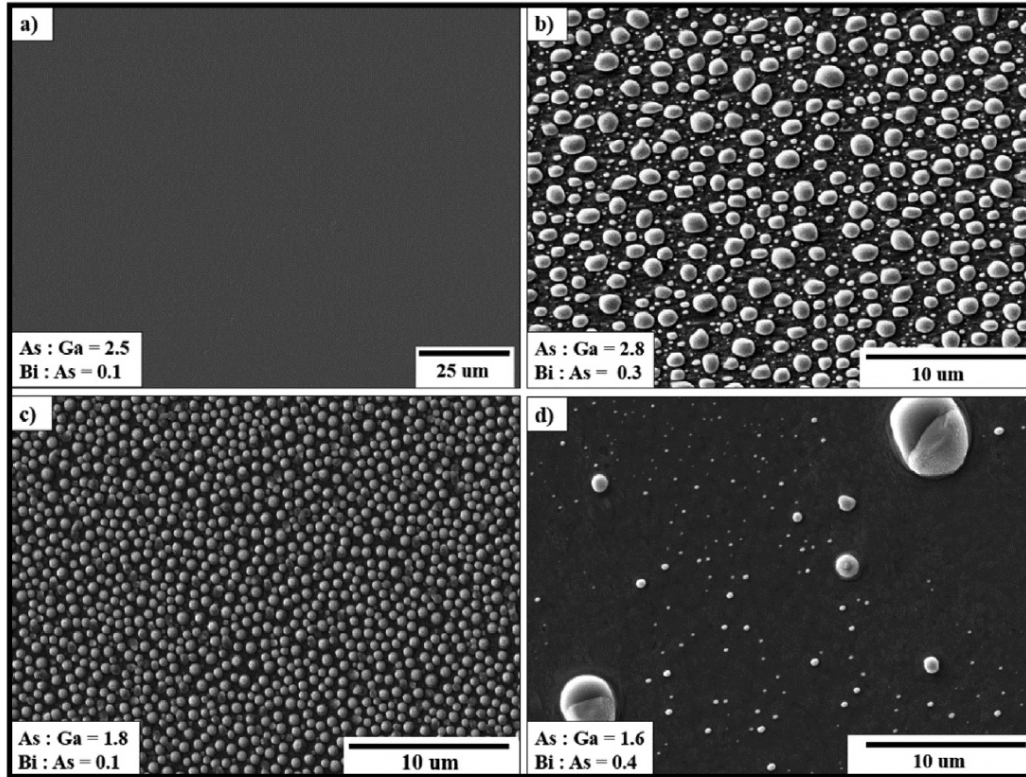


Figure 3.5 SEM micrographs of samples with each surface morphology. a) droplet free, b) Bi droplets, c) Ga droplets, d) biphasic droplets ²⁴

droplets on the surface. The Ga droplets are uniformly sized with diameters between 400 and 600 nm. Finally, the SEM of sample d given in Fig 3.5d, shows that the intersection of these two regimes leads to biphasic droplets composed of both Bi and Ga. Upon cooling these droplets are thought to phase segregate into regions of Bi (bright contrast) and Ga (dark contrast), verified by EDS (not pictured). The biphasic droplets exhibited a huge variation in size ranging between 100 nm and 15 μm .

3.4 Establishing a New Parameter W_{OOM} to Capture Variations in Lattice Parameter

The purpose of this section is to discuss how we used XRD ω -2 θ diffraction curves to define several parameters that quantify Bi incorporation and film quality. The first parameter, full width half maximum (FWHM), is used to indicate the level of crystalline quality. A smaller

FWHM indicates a well-defined lattice parameter and higher quality crystal growth. However, the XRD of the films discussed in this chapter exhibited a high degree of peak broadening, indicative of large variations in lattice parameter, that weren't effectively captured by reporting FWHM alone. Therefore, we defined W_{OOM} as the width of the film peak at one order of magnitude below its maximum value to capture this broadening. Due to the degree of peak broadening, the W_{OOM} sometimes extended into the substrate peak. In these instances, the measurement of W_{OOM} was terminated at the substrate peak to avoid over estimating variation in the lattice parameter. Finally, the composition corresponding to the film peak is reported as x_{max} , and the composition corresponding to the midpoint of W_{OOM} is reported as x_{med} .

3.5 Droplet Driven Lattice Variations

Figure 3.6 shows (004) ω - 2θ diffraction curves of representative samples a-d and demonstrates that each type of droplet has a distinct influence on the lattice parameter of films. Note that although we only report on one sample from each surface morphology, we used XRD to verify that the effect on lattice parameter is consistent within each droplet regime. The diffraction curve corresponding to the droplet-free sample a, exhibits a symmetric and well-defined film-peak corresponding to a composition of $x_{max}=8.1\%$ Bi. However, it has a large FWHM of 764° compared to 125° for the substrate peak. This high degree of broadening is also captured by the W_{OOM} of 1370° and $x_{med}=8.5\%$ Bi. The diffraction curve corresponding to sample b with Bi droplets exhibits a broad shoulder on the low angle side of the substrate peak instead of a distinct film peak. This behavior is also observed in linearly graded films, suggesting that this may be due to a graded variation in Bi incorporation²⁵. The large degree of broadening

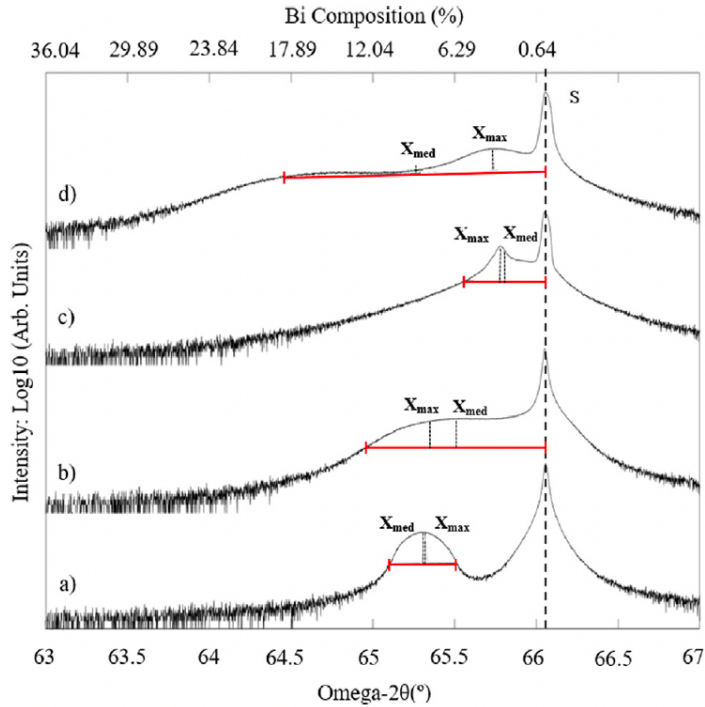


Figure 3.6 XRD ω - 2θ (004) scans taken from samples a-d. The upper x-axis represents atomic % Bi calculated via Vegard's law. Graphical examples of how the maximum Bi incorporation (x_{\max}), the median Bi incorporation (x_{med}), and the line scan width one order of magnitude below the highest-intensity peak (W_{OOM}) of each sample are determined are superimposed on the scans²⁴

was captured by the $W_{\text{OOM}}=3,888''$, approximately 3x larger than what was seen in droplet free films. Assuming this variation is indeed due to a gradient in Bi incorporation, the intersection of the W_{OOM} linewidth with the diffraction curve suggests that Bi incorporation varies between 0 and 13% with $x_{\text{med}}=6.5\%$ Bi. The diffraction curve corresponding to sample c with Ga droplets exhibits a sharp film peak corresponding to $x_{\text{max}}=3.0\%$ Bi with a well-defined FWHM of $295''$. However, this is not indicative of the variation in lattice parameter. Visual inspection reveals a long tail-like feature in the XRD which suggests variations in lattice parameter that are not captured by FWHM. The $W_{\text{OOM}}=1,836''$ and $x_{\text{med}}=2.8\%$ Bi more accurately captures variations in lattice parameter. Finally, XRD of sample d with biphasic droplets exhibits a weak diffraction peak corresponding to $x_{\text{max}}=3.6\%$ Bi superimposed on a low angle shoulder like those observed in films with Bi droplets. The variation in lattice parameter is captured by the $W_{\text{OOM}}=5,880''$ and

$x_{\text{med}} = 8.7\%$ Bi. The intersection of the W_{OOM} linewidth with the diffraction curve suggests that Bi incorporation varies between 0 and 18%.

Some degree of peak broadening can usually be attributed to point defects such as Ga vacancies,^{7,8} and As_{Ga} antisites,²⁶ because of low growth temperature. However, Bi is a known surfactant which serves to increase the diffusion length of adatoms and mitigate point defect formation to a large degree.²⁷ Coupled with previous reports of phase segregation in Bismides, this suggested that variations in lattice parameter were likely a result of compositional inhomogeneities.

Growth strategies such as skipping the annealing step can serve to limit these compositional inhomogeneities and obtain films exhibiting smaller W_{OOM} linewidths. To show this, we re-analyzed two samples from previously published papers in the Millunchick group that were grown without an annealing step.^{6,10} The first sample had a droplet-free surface morphology and a well-defined film peak with a $W_{\text{OOM}} = 144''$ and $x_{\text{med}} = 1.8\%$ Bi.⁶ It should be noted that the W_{OOM} of this sample was approximately 10 times lower than the representative droplet-free sample a. The second sample exhibited Ga droplets and had a $W_{\text{OOM}} = 648''$ and $x_{\text{med}} = 1.6\%$ Bi.¹⁰ Once again, the W_{OOM} was approximately 3 times smaller in the Ga droplet sample without an annealing step compared to the representative Ga droplet sample c. It must be acknowledged that these samples were grown with different growth conditions, which led to differences in observed incorporation that must be taken into consideration when interpreting these results. Nonetheless, the huge reduction of W_{OOM} in samples without annealing steps, coupled with reports that annealing enhances Bi clustering^{17,18}, suggests that skipping annealing may be a viable strategy to obtain films with smaller W_{OOM} linewidths and more uniform incorporation.

Implementing growth interrupts is another strategy that has been shown to minimize compositional inhomogeneities and lead to sharper more well-defined diffraction peaks.¹⁰ It is shown that growth interrupts allow for the excess Ga on the surface, which would normally turn into droplets, to be converted into GaAs.

3.6 Morphology Map

Figure 3.7 gives a map-based summary of the growth conditions, surface morphology, and composition for the 25 films grown in this study. The transitional boundaries between each of the surface morphologies are approximated by a dashed line. The color of the data points represents the median composition (x_{med}), and the size of the data point is directly proportional to the W_{OOM} . The representative samples a-d are also labeled for additional clarity.

In the droplet-free surface morphology regime, Bi incorporation increases as As_2/Ga beam flux ratio decreases and the Bi/As_2 beam flux ratio increases. This trend culminated in a maximum Bi incorporation of $x_{med}=13.6\%$, representing the highest reported Bi incorporation in droplet free GaAsBi (001). This suggested that we successfully homed in on the small window of increased Bi incorporation in droplet free films predicted by Rodriguez et al.⁹ Furthermore, droplet-free films exhibited the smallest W_{OOM} linewidths, ranging between $784''$ and $2105''$, with an average of $1345\pm 344''$. This suggested that droplet free films had the smallest degree of variations in lattice parameter, and likely the smallest degree of compositional inhomogeneities, as originally predicted.

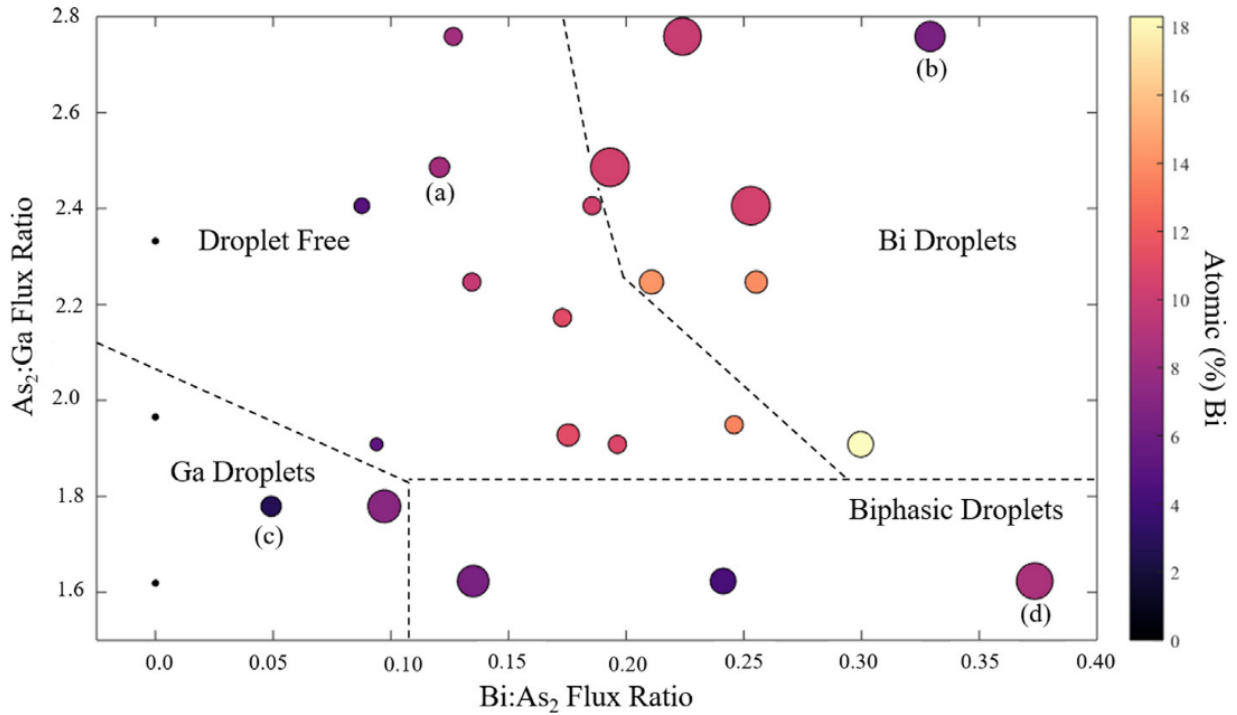


Figure 3.7 Morphological map of the 25 samples growth at 325 °C and annealed for 5 min at various flux ratios. The qualitative boundaries between each regime is given by dashed lines. Specific samples are labeled according to the Table 1. The color of the data point represents the median composition, and the size of the data points represents breadth of the peak²⁴

When Bi droplets form on the surface a different trend was observed. Because Bi incorporation is proportional to Bi adatom coverage,⁵ it was not surprising that Bi incorporation was observed to stall at the onset of Bi droplets after full coverage was reached. Further increasing the Bi/ As₂ beam flux ratio was observed to slightly reduce x_{med} suggesting that increasing droplet coverage may inhibit Bi incorporation. This observation qualitatively agreed with simulations.⁹ However, even after Bi droplets formed on the surface, decreasing the As₂/ Ga beam flux ratio was still seen to increase Bi incorporation, culminating in a maximum value of $x_{med}=18.3\%$ Bi. Samples with Bi droplets exhibited the largest variations in lattice parameter with W_{OOM} 's between 2117'' and 6411'' with an average of $4297\pm 1294''$. This demonstrated that

films with Bi droplets have the highest level of variation in lattice parameter and likely large compositional inhomogeneities.

When Ga droplets form on the surface, incorporation reached a maximum value of $x_{\text{med}}=7.2\%$ Bi. This was lower than the maximum observed compositions in both the droplet-free and Bi droplet regimes and contrasted simulation⁹ which showed that incorporation was highest when Ga rich droplets form on the surface. The transition to Bi-phasic droplets from Ga droplets occurs at a relatively low Bi/ As₂ beam flux ratio. Therefore, the apparently low level of Bi incorporation may be due to a smaller amount of Bi being deposited rather than any fundamental change in the rate at which Bi incorporates. In this regime the W_{OOM} increased from 1834'' to 4611'' as Bi/As₂ beam flux ratio was increased, and exhibited an average value of 3223 ± 1964 ''. This demonstrated a high degree of variation in lattice parameter which is known to be caused by compositional inhomogeneities in films grown with Ga droplets on the surface.¹⁰

Finally, samples that exhibited biphasic droplets also exhibited low Bi incorporation in comparison to the droplet-free and Bi droplet samples, in strong disagreement with simulation.⁹ The maximum incorporation in this regime was $x_{\text{med}}= 8.7\%$ Bi, only slightly higher than what was observed in Ga droplet films despite significantly higher Bi/ As₂ beam flux ratios. Moreover, these films also exhibit large W_{OOM} 's ranging between 2832'' and 5585'' with an average of 4202 ± 1376 '', again showing a high degree of variation in lattice parameter, suggesting that incorporation varies greatly throughout these films.

We found that our experimental growths generally agreed with simulation, however there were a few key differences. First, the experimental growths showed that Bi incorporation was maximized when Bi droplets form on the surface, whereas simulations predicted maximum Bi incorporation at lower As₂/Ga ratios when Ga or biphasic droplets form. Our experimental result

is surprising considering that Ga-rich growth is generally thought to provide a pathway to maximize incorporation and suggested that droplet composition has an undue influence on net Bi incorporation.

Second, the transition from Ga droplets to biphasic droplets is significantly shifted towards lower As_2/Bi beam flux ratios in the experimental map (~ 0.11), compared to the simulations (~ 0.3). We postulate that this shift is due to the Arrhenius nature of Bi desorption at the growth interface.⁵ As a result, growth temperature likely modifies the effective beam flux ratios at the growth surface causing a temperature dependent shift of these boundaries. However, additional growths would be needed to verify this theory.

3.7 Compositional Variations Explain Large WOOM Linewidths:

The variations in lattice parameter shown in the growth map and XRD suggest that each droplet type imparts distinctive microstructural properties and compositional inhomogeneities. Indeed, literature has shown that Ga droplet and droplet-free films both exhibit unique Bi phase segregation effects, that explain the large W_{OOM} linewidths. In this section we focus on characterizing the microstructures of samples with Bi and biphasic droplets to determine the cause of the variations in lattice parameter indicated by the large W_{OOM} linewidths.

3.7.1 Bi Droplets:

Figure 3.8a shows HAADF STEM of a cross-sectional lift out of sample b. It shows regions of bright and dark contrast, respectively indicating regions of high and low Bi incorporation. The regions of increased Bi incorporation are approximately 150 nm thick and on the order of 100's of nm wide separated by regions of lower Bi concentration. This observation

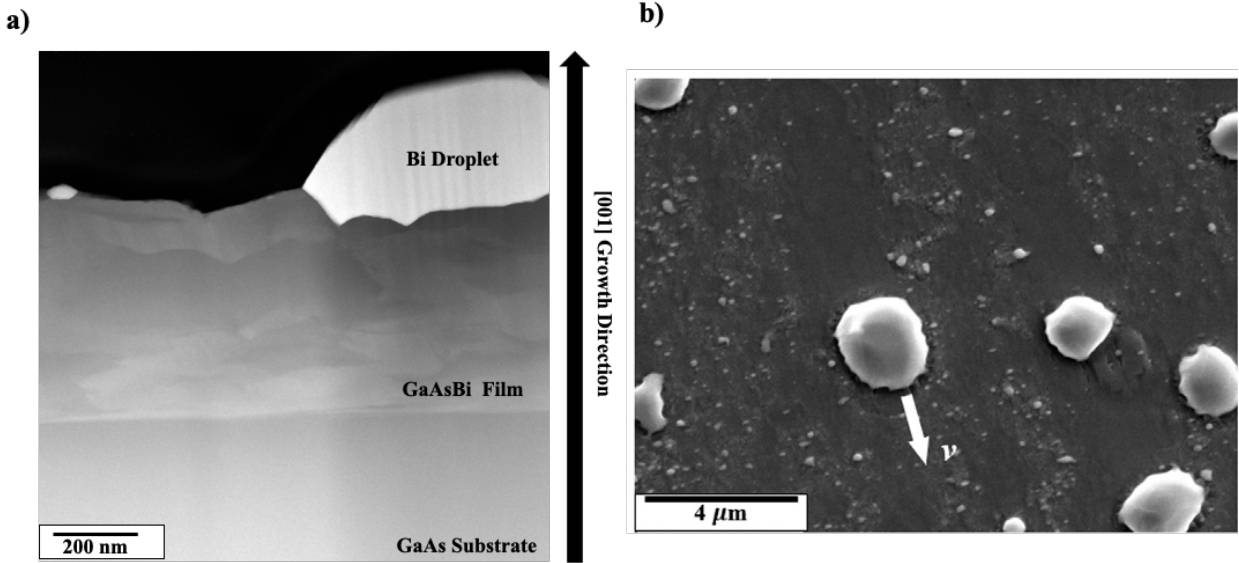


Figure 3.8 a) HAADF STEM of sample b grown under conditions that yield Bi droplets on the surface. Atomic number contrast shows compositional inhomogeneities in Bi incorporation. b) SEM micrograph showing how Bi droplets travel across the surface during growth, coalescing surface Bi in their path²⁴

verified that the large W_{OOM} linewidths in samples with Bi droplets were predominantly caused by localized variations in Bi concentration. Directly underneath the Bi droplet there is a region of low brightness, indicating Bi depletion, which we postulate is caused by strong thermodynamic driving forces for Bi to phase segregate into the droplet rather than incorporate into the film. This explains the slight reduction in Bi concentration as Bi/As₂ flux ratio is increased, because higher droplet coverage would increase the amount of Bi preferentially segregating into droplets.

Due to low bonding energy between Bi droplets and the growth interface, Bi droplets roll across the surface and coalesce smaller droplets in their path. SEM in Fig 3.8b shows evidence of this phenomena showing cleared paths of smaller droplets behind larger Bi droplets. We postulate that as the droplet travels across the surface, it blocks incoming Bi flux while also depleting Bi from the film beneath it. This is like the mechanism proposed by Wood et al.¹¹ for Ga rich droplets, however the thermodynamic driving forces for Bi to phase segregate into the droplet likely enhance this effect. Indeed, we see W_{OOM} linewidths are on average 33%

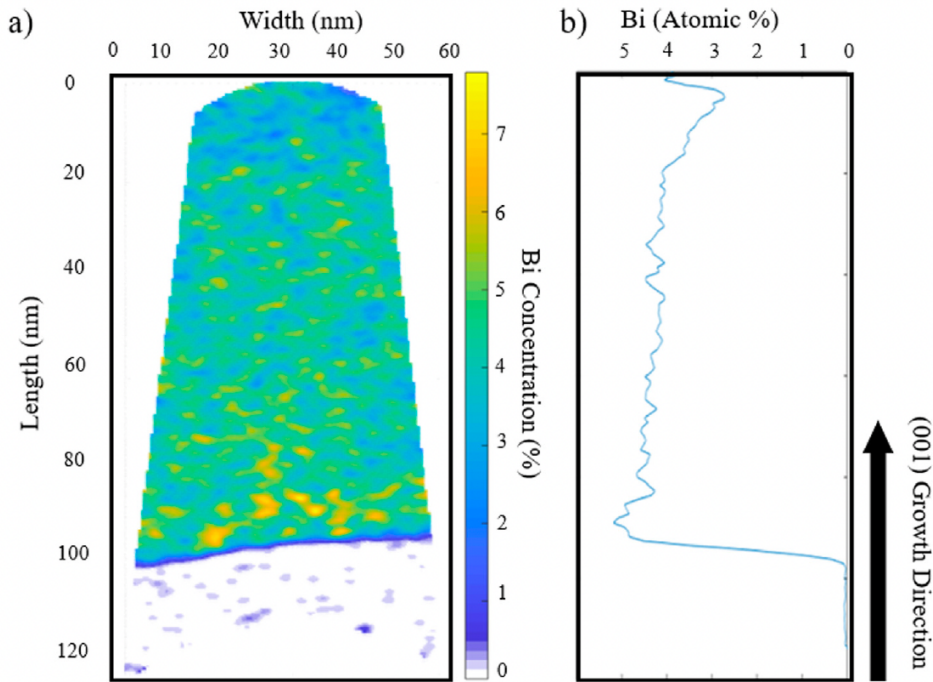


Figure 3.9 a) Bi concentration cross section of sample b with Bi droplets on the surface collected with APT. b) Average Bi concentration throughout the length of the atom probe tip²⁴

larger in films with Bi droplets compared to Ga droplets. It's also worth noting that the high levels of contrast near the film substrate interface indicate enhanced Bi incorporation before the onset of Bi droplets. As such, thin films can likely be grown in this regime without being subjected to the compositional effects caused by Bi droplets. It's also worth noting that Ptak et al. has shown that fast growth rates approaching $1 \mu\text{m hr}^{-1}$ can delay the onset of Bi droplets at high Bi/As flux ratios by trapping it in the crystal lattice before it can accumulate on the surface²⁸

Atomic Probe Tomography (APT) of sample b, given in Fig. 3.9, also corroborates the presence of inhomogeneities in Bi concentration. The Bi concentration profile in Fig 3.9b shows that Bi incorporation peaks at approximately 5% near the interface between regions of high and

low incorporation but drops off to approximately 3% in the Bi rich region as growth progresses.

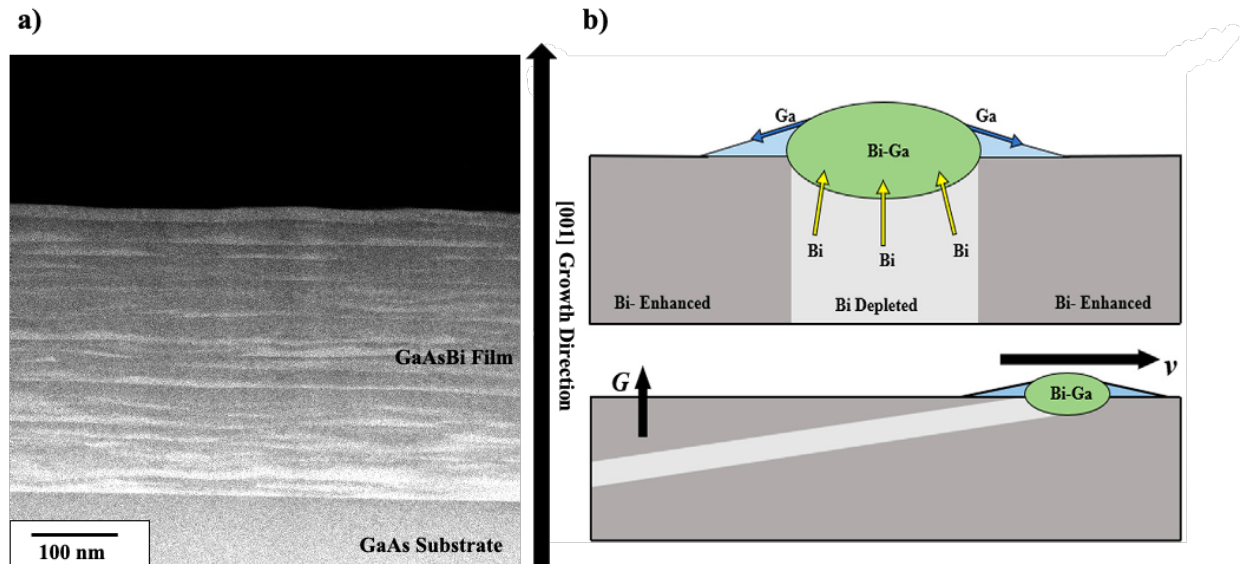


Figure 3.10 a) HAADF STEM showing streaky composition inhomogeneities in sample d with biphasic droplets. b) model for the cause of the compositional inhomogeneities showing the droplet wicking Ga and traveling across the surface²⁴

This is consistent with the XRD of Bi droplet samples that indicated linearly graded compositions. The APT indicates a mild degree of Bi clustering in the bi-deficient region with a Pearson coefficient $\mu=0.21$ and a p-value of less than 0.0001. However, the Bi appears to be randomly distributed in the Bi rich regions with a Pearson coefficient of $\mu=0.04$ and p value of 0.2058.

3.7.2 Bi-Phasic Droplets

Naturally, films with biphasic droplets exhibit compositional effects that appear to be a combination of the effects caused by Ga droplets and Bi droplets. HAADF STEM in Fig. 3.10a shows streaky high contrast bands of elevated Bi incorporation ranging between 10 to 150nm thick and hundreds of nm wide. Figure 3.10b proposes a model to explain the cause of these inhomogeneities. Like Bi droplets, we predict that biphasic droplets roll across the surface due to their high Bi content and weak interaction with the crystal termination layer. Furthermore, like

what Tait observed in films with Ga droplets,¹⁰ we predict that biphasic droplets wick Ga onto the surface and create regions of high Ga availability near the droplets that promote high levels of Bi incorporation. As the droplet travels across the surface this results in regions of enhanced Bi incorporation adjacent to biphasic droplets and depleted Bi incorporation underneath where Bi preferentially segregates into the droplets. Depending on the speed (v) at which the droplet travels relative to the growth rate (G), the resulting bands of increased and decreased Bi incorporation will be inclined at different angles relative to the growth surface. When $v \sim G$ the orientation of these bands will be observed at an angle to the surface, like the Bi deficient GaAs nanowires reported on by Wood et al.¹¹ When $v \gg G$ the orientation will be nearly parallel to the growth surface, and finally when $v \ll G$ these features will be roughly perpendicular to the growth surface.

3.8 Conclusions:

The main research goals of this chapter were to identify the growth parameters that maximize Bi incorporation and to characterize the compositional effects of Bi containing droplets. The compositional effects of Bi rich droplets had yet to be explored in literature and it was unclear if such films could be used to obtain high quality growth. Through experiment it was found that maximum incorporation was achieved when Bi droplets formed on the surface, however TEM, APT, and XRD showed that films with Bi-rich droplets exhibit high degrees of compositional inhomogeneities. TEM indicated that Bi droplets served to act as a kinetic sink for previously incorporated Bi, resulting in regions of diminished Bi incorporation as droplets traveled across the surface. A similar effect was also observed in films with biphasic droplets except Ga wicking also serves to enhance Bi incorporation next to the droplet as it travels across the surface, resulting in streaky bands of elevated Bi incorporation. Unless these compositional

effects can be harnessed in a productive way, such as in the self-assembly of quantum dots or nanostructures, the compositional effects caused by droplets of any composition greatly complicate the growth of uniformly alloyed high quality Bismide films. As such growth conditions that yield droplets, even though they maximize Bi incorporation should be avoided. Furthermore, we identified a small growth window in droplet free films that yielded Bi incorporations up to 13.6%.

3.9 References:

1. Elayech, N., Fitouri, H., Essouda, Y., Rebey, A. & el Jani, B. Thermodynamic study of the ternary system gallium-arsenic-bismuth. *Physica Status Solidi (C) Current Topics in Solid State Physics* 12, 138–141 (2015).
2. Elayech, N., Fitouri, H., Boussaha, R., Rebey, A. & Jani, B. el. Calculation of InAsBi ternary phase diagram. *Vaccum* 131, 147–155 (2016).
3. Lu, X., Beaton, D. A., Lewis, R. B., Tiedje, T. & Whitwick, M. B. Effect of molecular beam epitaxy growth conditions on the Bi content of GaAs_{1-x}Bi_x. *Appl Phys Lett* 92, (2008).
4. Lewis, R. B., Masnadi-Shirazi, M. & Tiedje, T. Growth of high Bi concentration GaAs_{1-x}Bi_x by molecular beam epitaxy. *Appl Phys Lett* 101, (2012).
5. Tait, C. R. & Millunchick, J. M. Kinetics of droplet formation and Bi incorporation in GaSbBi alloys. *J Appl Phys* 119, (2016).
6. Tait, C. R., Yan, L. & Millunchick, J. M. Spontaneous nanostructure formation in GaAsBi alloys. *J Cryst Growth* 493, 20–24 (2018).
7. Liu, X. et al. Native point defects in low-temperature-grown GaAs. *Appl Phys Lett* 67, 279 (1995).
8. Gebauer, J. et al. Ga vacancies in low-temperature-grown GaAs identified by slow positrons. *Appl Phys Lett* 71, 638–640 (1997).

9. Rodriguez, G. v. & Millunchick, J. M. Predictive modeling of low solubility semiconductor alloys. *J Appl Phys* 120, (2016).
10. Tait, C. R., Yan, L. & Millunchick, J. M. Droplet induced compositional inhomogeneities in GaAsBi. *Appl Phys Lett* 111, 1–5 (2017).
11. Wood, A. W., Collar, K., Li, J., Brown, A. S. & Babcock, S. E. Droplet-mediated formation of embedded GaAs nanowires in MBE GaAs $1-x$ Bi x films. *Nanotechnology* 27, (2016).
12. Mazzucato, S. et al. Low-temperature photoluminescence study of exciton recombination in bulk GaAsBi. *Nanoscale Res Lett* 9, 2–6 (2014).
13. Fitouri, H., Essouda, Y., Zaied, I., Rebey, A. & el Jani, B. Photoreflectance and photoluminescence study of localization effects in GaAsBi alloys. *Opt Mater (Amst)* 42, 67–71 (2015).
14. Wilson, T. et al. Assessing the Nature of the Distribution of Localised States in Bulk GaAsBi. *Sci Rep* 8, 1–10 (2018).
15. Kopaczek, J. et al. Optical properties of GaAsBi/GaAs quantum wells: Photoreflectance, photoluminescence and time-resolved photoluminescence study. *Semicond Sci Technol* 30, (2015).
16. Wu, M. et al. Detecting lateral composition modulation in dilute Ga(As,Bi) epilayers. *Nanotechnology* 26, (2015).
17. Wu, M., Luna, E., Puustinen, J., Guina, M. & Trampert, A. Formation and phase transformation of Bi- containing QD-like clusters in annealed GaAsBi. *Nanotechnology* 25, (2014).
18. Puustinen, J. et al. Variation of lattice constant and cluster formation in GaAsBi. *J Appl Phys* 114, (2013).
19. Baladés, N. et al. Analysis of Bi Distribution in Epitaxial GaAsBi by Aberration-Corrected HAADF-STEM. *Nanoscale Res Lett* 13, 0–7 (2018).
20. Norman, A. G. et al. Atomic ordering and phase separation in Atomic ordering and phase separation in MBE GaAs $1 - x$ Bi x . 121, 3–8 (2012).

21. Wu, M., Luna, E., Puustinen, J., Guina, M. & Trampert, A. Observation of atomic ordering of triple-period-A and -B type in GaAsBi. *Appl Phys Lett* 105, (2014).
22. Spencer, B. J., Voorhees, P. W. & Tersoff, J. Stabilization of strained alloy film growth by a difference in atomic mobilities. *Appl Phys Lett* 76, 3022–3024 (2000).
23. Darowski, N., Pietsch, U., Zeimer, U., Smirnitzki, V. & Bugge, F. X-ray study of lateral strain and composition modulation in an AlGaAs overlayer induced by a GaAs lateral surface grating. *J Appl Phys* 84, 1366–1370 (1998).
24. Carter, B. A., Caro, V., Yue, L., Tait, C. R. & Millunchick, J. M. The effect of III:V ratio on compositional and microstructural properties of GaAs_{1-x}Bi_x (0 0 1). *J Cryst Growth* 548, (2020).
25. Althowibi, F. A., Rago, P. B. & Ayers, J. E. X-ray diffraction analysis for step and linearly graded In_xGa_{1-x}As/GaAs (001) heterostructures using various hkl reflections. *Journal of Vacuum Science & Technology B, Nanotechnology and Microelectronics: Materials, Processing, Measurement, and Phenomena* 34, 041209 (2016).
26. Mooney, P. M. et al. Deep level defects in n-type GaAsBi and GaAs grown at low temperatures. in *Journal of Applied Physics* vol. 113 (2013).
27. Wixom, R. R., Rieth, L. W. & Stringfellow, G. B. Sb and Bi surfactant effects on homo-epitaxy of GaAs on (0 0 1) patterned substrates. *J Cryst Growth* 265, 367–374 (2004).
28. Ptak, A. J. et al. Kinetically limited growth of GaAsBi by molecular-beam epitaxy. *J Cryst Growth* 338, 107–110 (2012).
29. Schaefer, S. T., Kosireddy, R. R., Webster, P. T. & Johnson, S. R. Molecular beam epitaxy growth and optical properties of InAsSbBi. *J Appl Phys* 126, (2019).
30. Ohring, M. *The Materials Science of Thin Films*. (San Diego: Academic Press, 1992).
31. Grossklaus, K. A. *Examination of the Ion Beam Response of III-V Semiconductor Substrates*. (2012).
32. Martin, A. *Manipulating Quantum Dot Nanostructures for Photonic and Photovoltaic Applications*. (2013).

Chapter 4 Comparing Bi Incorporation on the (110) and (001) Surfaces

In Chp. 3 we discussed the effect of beam flux ratio on Bi incorporation to identify growth parameters that yield maximum incorporation. In this chapter we ask the same research question, namely: what growth conditions maximize Bi incorporation in III-Vs? However, instead of investigating the effects of variables such as material flux and growth temperature, we investigate how growing on different crystalline orientations influences Bi incorporation in InAs:Bi superlattices. We discuss differences in Bi incorporation between the (001) and (110) InAs surfaces, and characterize the effect that Bi has on surface morphology.

4.1 Introduction: Orientation Dependent Bi Incorporation

Only thinking of Bi incorporation as a function of growth temperature and beam flux ratio oversimplifies Bi incorporation mechanisms in the crystal termination layer. It neglects the fact that if Bi incorporation is not energetically favorable it will simply desorb from the surface and not incorporate¹⁻³. In Chp 3 we discussed how low V/III flux ratios encourage Bi incorporation by stabilizing group III terminated surfaces and lowering the competition between As and Bi for bonding sites.²⁻⁴ However, this model belies the thermodynamic/kinetic nature of Bi interactions on the growth surface and does not account for effects such as surface reconstructions, which can have a large effect on Bi incorporation. At low V/III beam flux ratios, the most energetically stable surface configuration in GaAsBi(001) is the Bi-rich (2x1) reconstruction which promotes {111}B CuPt type ordering, and high levels of Bi incorporation.⁵⁻⁶ In contrast, higher V/III beam flux ratios stabilize (4x3) surface reconstructions which support lower levels of Bi incorporation and stabilize

both $\{111\}$ A and $\{111\}$ B triple periodic ordering.⁷ These findings elucidate a relationship between surface structure, surface energy and Bi incorporation.

As such, we look to crystalline orientation as a method to manipulate surface energy and the interaction of Bi at the growth surface to maximize Bi incorporation. Indeed, it has been reported in literature that different growth orientations promote different levels of Bi incorporation. For example, Zaied et al. showed that Bi incorporation on the GaAs(115)A surface was higher than the (001), (111)A and (114)A, however growth proceeded at a much slower rate on the (115)A surface.⁸ Similarly, Henini et al. showed that incorporation in GaAs (311)B was larger than on the (001) surface.⁹ Moreover, Guan et al. reported that the rate of Bi incorporation is higher at (111)A step edges compared to (111)B step edges in vicinal GaAs(001) substrates.¹⁰ These findings demonstrate that surface orientation can have a meaningful effect on Bi incorporation.

4.2 Background: Growth of (110) III-V Films, and Bi Terminated Surfaces

As a result of the findings above we decided to investigate how growth on the non-polar InAs(110) surface influences Bi incorporation. The remainder of this section discusses our motivation for choosing the (110) surface. Before we begin this section; we must acknowledge that we primarily discuss literature on GaAs(110) as a proxy for the InAs(110) surface. This approach is needed as there is little literature on homoepitaxial InAs(110).

4.2.1 Applications: Why the (110) Orientation?

Studies investigating the homoepitaxial growth of (110) oriented III-Vs are motivated by numerous factors. They are particularly of interest for use in applications in 2-D electron gas structures and spintronic devices, due to their long spin relaxation times.¹¹⁻¹⁵ The (110) surface is also the sidewall facet of III-V zinc-blende nanowires.¹⁶⁻²¹ Therefore, a better understanding of

growth and Bi incorporation on the (110) surface may provide insight into future growth of Bismide core-shell nanowires.

4.2.2 Epitaxial Growth on the (110) Surface

High quality growth on non-polar III-V surfaces, such as GaAs(110), is challenging due to different incorporation and diffusion rates between group III and group V elements that introduce instabilities during growth.²² Arsenic exhibits a lower incorporation coefficient than Ga on the (110) surface due to a preferential desorption of As.^{23,24} This is thought to induce local stoichiometric disorder which ultimately results in the formation of characteristic triangular islands on the surface.²⁵⁻³³ The exact origin of these island is widely disputed, though they are often attributed to As dimerization along the side-edge direction of the triangular islands, that results in a diffusion energy barrier and the onset of 3-D growth.^{26,27} However, the tendency towards triangular growth has also been attributed to growth rate anisotropy,²² and different migration pathways and stable arriving sites for Ga and As adatoms along step edges.³⁴ For example, the (111) facet in GaAs is energetically favorable to As chemisorption resulting in it being the fastest growing facet on the (110) surface resulting in islands with the characteristic triangular shape.³⁵ Regardless, experimental studies have shown that the low As incorporation coefficient, and preferential desorption can be overcome with a high V/III ratio (> 20:1) and low growth temperature(360-420°C) resulting in smooth 2D growth.^{26,27,30,32}

Kim et al. has shown that if these conditions are not carefully optimized to achieve perfect one-to-one stoichiometry, excess As incorporation will cause compressive strain in the lattice.³⁶ Once a critical film thickness is reached the strain is relaxed via the formation of (111)B stacking fault defects. This relaxation of the film is also seen to be coincident with the re-emergence of 3D

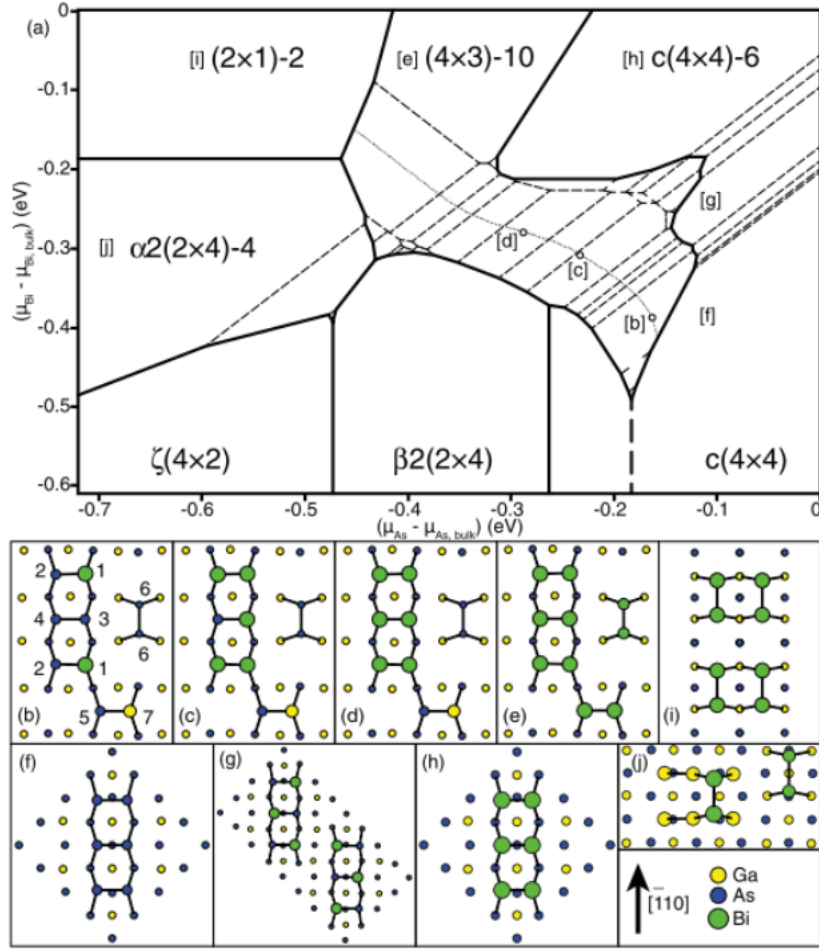


Figure 4.1a) Phase diagram of the Bi-terminated GaAs(001) surface reconstructions as a function of Bi and As chemical potentials. Thick solid lines separate the different reconstructions from one another, while dashed lines separate the individual configurations within each reconstruction. The thicker dotted line in the $c(4 \times 4)$ reconstruction region separates the $c(4 \times 4)\alpha$ reconstruction on the left of the line from the $c(4 \times 4)\beta$ configurations on the right. The entropy curves presented in Fig. 5 are plotted along the dotted line, with the open circles indicating where Monte Carlo cooling runs were performed. The letters in brackets correspond to the configurations of the region on the phase diagram. Stable configurations include the (b) $\beta(4 \times 3)$ -2, (c) $\beta(4 \times 3)$ -5, (d) $\beta(4 \times 3)$ -6, (e) $h0(4 \times 3)$ -10, (f) $c(4 \times 4)$, (g) $c(4 \times 4)$ -6/2, (h) $c(4 \times 4)$ -6, (i) (2×1) -2, and (j) $\alpha 2(2 \times 4)$ -4. The order of Bi occupation in the $\beta(4 \times 3)$ reconstruction is given in (b); sites with the same number are symmetrically degenerate.³⁹

triangular island growth, though once again the exact cause of this is not fully understood. Even so, growth in this regime should be avoided due to defect formation.

The unique nature of growth on the (110) surface piqued our interest to study Bi incorporation for several reasons. First, we postulated that the low As incorporation coefficient may reduce competition with Bi for group III bonding sites, supporting higher Bi incorporation.

Secondly, research by Wixom et al. has shown that Bi acts as a surfactant serving to lower the surface energy and increase the diffusion length of adatoms.³⁷ If the triangular islands are indeed stabilized by an energy barrier caused by As dimerization at step edges, Bi may reduce this barrier suppressing island formation. The ability to stabilize 2-D growth at lower V/III flux ratios could serve to mitigate strain related defect formation due to excess As incorporation.

4.2.3 Bi Interactions in the Crystal Termination Layer

Bi interacts with the (110) and (001) III-V crystal termination layers in very distinct ways further suggesting crystalline orientation may provide a pathway to influence bulk Bi incorporation. First, as discussed in section 4.1, Bi incorporation is directly related to the surface

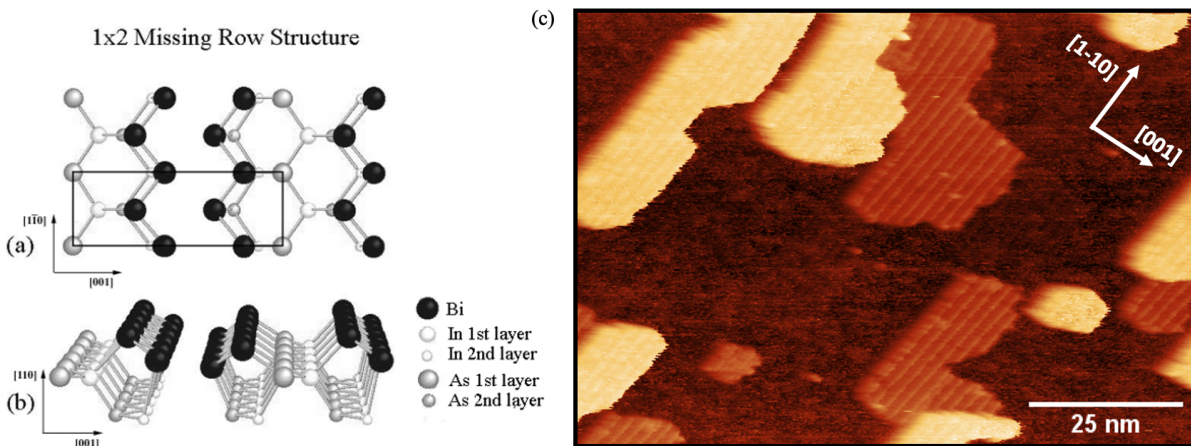


Figure 4.2 (a) Top view of the (110) plane of the (1x2) missing row structure (b) Perspective view of the (1x2) missing-row structure.³⁸(c) STM of the (1x2) missing row reconstruction showing the rows of Bi incorporation along the [1-10]

reconstruction on the (001) surface. Depending on the growth conditions, different surface reconstructions are stabilized, resulting in differences in net Bi incorporation and the compositional ordering of films. Figure 4.1 shows DFT simulations of several Bi-terminated GaAs (001) surface reconstructions as a function of chemical potential, elucidating how different surface reconstructions support varying amounts of Bi incorporation.³⁹ Bi incorporation behaves quite differently on non-polar (110) surfaces. Bi interacts with the non-reconstructed (110) surface to

induce a (1x2) missing row reconstruction shown in Fig 4.2a.^{38,40-45} This reconstruction is characterized by two zigzag chains of Bi along the [1-10] direction that are bonded to In and As respectively. It is observed that the Bi atoms in these chains are strongly vertically displaced and tilted towards the substrate. This buckling of the Bi chains is enabled through the presence of missing alternate InAs dimer rows. Figure 4.2b gives STM showing sub-monolayer Bi coverage with a (2x1) missing-row reconstruction on the InAs(110) surface with the chains of Bi atoms along the [1-10] clearly visible. Ultimately, the potential to achieve full Bi coverage in the crystal termination layer on the InAs(110) surface, opposed to partial coverage on the (001) prompted us to investigate if higher incorporation could be achieved in (110) oriented films.

The remainder of this chapter discusses the growth of a series of InAs:Bi superlattices (SLs) to compare Bi incorporation between the (001) and (110) crystal orientations. We observed that higher Bi incorporation is achievable on the (110) surface compared to the (001) surface. Furthermore, we found that the (001) surface saturates with Bi sooner than the (110) surface, marked by the onset of Bi droplets on the surface. We also observed large changes in surface morphology, depending on the amount of Bi deposited, which was attributed to the behavior of Bi as a surfactant, and structural disorder caused by Bi incorporation.

4.3 Experimental Procedures:

The InAs: Bi superlattices reported on in this chapter were prepared for growth following a standardized procedure. First, the samples were heated to 510°C under As₄ overpressure of approximately 1×10^{-6} torr to desorb the native oxide. After five minutes the RHEED was checked for a streaky (1x1) or (2x4) diffraction pattern on the (110) and (001) surfaces respectively to verify oxide desorption. Next, the temperature was lowered to 460°C, and a 400 nm buffer layer of InAs was grown using an As₄/In beam flux ratio of approximately 6 and a growth rate of

approximately 0.6 ML/s. It should be noted that we used growth rates obtained from the (001) surface to approximate the growth rate of the (110) surface. This was necessitated because we observed a sharp drop in RHEED specular beam intensity at the onset of growth on the InAs(110) surface, presumably due to 3-D roughening. The buffer layer was annealed at 460°C for 5 minutes before lowering the temperature to 290°C.

The superlattices were grown by depositing 30nm of InAs with an As₄/In beam flux ratio of approximately 6 and In rate of approximately 0.65ML/s. This was followed by Bi deposition at with beam flux of approximately 5.4 x10⁻⁸ torr for either 0, 15, 30, or 45s under As₄ deficient conditions to encourage Bi incorporation. This was repeated for 20 periods. Immediately after growth the samples were quenched to 200°C and removed from the growth chamber. A summary of the growth conditions for each sample are given in table 4.1.

Table 4.1: Growth Conditions for Superlattice Growths

| Sample | Orientation | Bi Deposition (s) | Bi Beam Flux (torr) | As ₄ :In Beam Flux Ratio (BEP) | Growth Rate (ML/s) |
|--------|-------------|-------------------|------------------------|---|--------------------|
| a | (110) | 0 | 0 | 5.02 | 0.65 |
| b | (110) | 15 | 5.1 X 10 ⁻⁸ | 5.97 | 0.69 |
| c | (110) | 30 | 5.1 X 10 ⁻⁸ | 5.97 | 0.69 |
| d | (110) | 45 | 5.1 X 10 ⁻⁸ | 5.97 | 0.69 |
| e | (100) | 15 | 5.0 X 10 ⁻⁸ | 6.67 | 0.60 |
| g | (100) | 30 | 5.7 X 10 ⁻⁸ | 6.13 | 0.64 |
| h | (100) | 45 | 5.7 X 10 ⁻⁸ | 6.13 | 0.64 |

4.4 XRD Shows Differences in Bi Incorporation Between the (001) and (110) Surfaces

XRD showed that the (001) and (110) superlattices exhibited notable differences in Bi incorporation, that will be discussed in the following sections.

4.4.1 (001) Oriented Superlattice Bi Incorporation

Figure 4.3a gives the (004) ω -2 θ XRD diffraction curves for the samples grown on the (001) surface. The diffraction curves show well defined SL peaks with an angular spacing corresponding to a period of 28.3 ± 0.6 nm for all (001) oriented samples. This was irrespective of the amount of Bi deposited, and slightly below the intended 30 nm period. The average composition of the SLs was calculated with Vegards Law⁴⁶ from the 0th order SL peak and

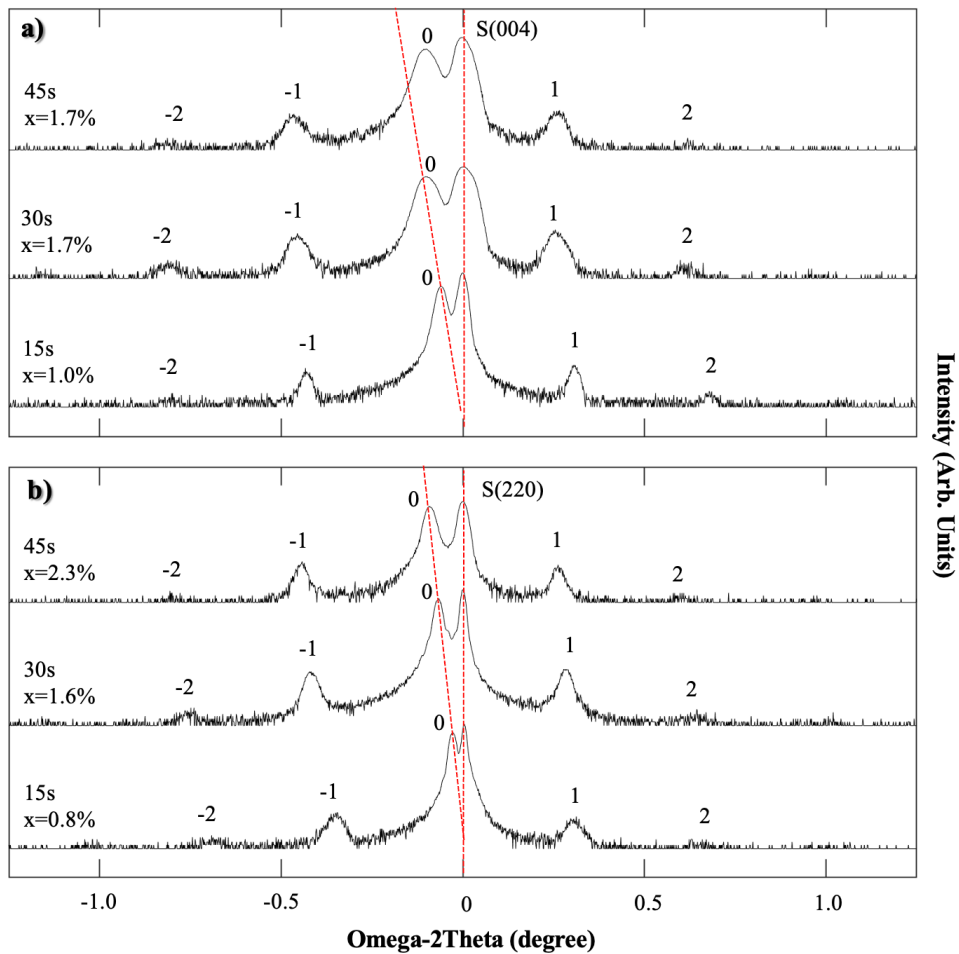


Figure 4.3 XRD line-scans showing the leftward shift corresponding to the increase in Bi incorporation for the samples grown in this study. The vertical dotted line shows the substrate peak, and the canted line tracks the leftward shift. Each curve is labeled with the Bi deposition time and corresponding incorporation calculated using Vegards law. (a) (004) ω -2 θ scans on the (001) surface show that Bi incorporation stalls at 1.7% Bi at Bi deposition times equal to or greater than 30 sec. (b) (220) ω -2 θ scans on the (110) surface show that the incorporation increases monotonically as the Bi deposition time increases, up to 2.3% Bi for the growth conditions used in this study.⁵⁸

assuming an InBi lattice parameter of 6.61\AA ⁴⁷. At 15s of Bi deposition, the bulk Bi incorporation was 1.0% Bi. Doubling the amount of Bi deposited to 30s increased the incorporation to 1.7% Bi. Further increasing the Bi deposition to 45s led to no further increase in Bi incorporation suggesting that the surface was saturated with Bi between 15 and 30s.

AFM of sample g (t=30s) given in Figs. 4.4d-f shows that saturation in Bi incorporation was marked by the appearance of Bi droplets on the surface with an average diameter of approximately 55nm and a density of $8 \times 10^8 \text{ cm}^{-2}$. This explains the saturation of Bi incorporation as additional Bi flux will be adsorbed by growing droplets rather than incorporating in the crystal termination layer. Similarly, Figs. 4.4g-i gives AFM of sample h (t=45s), showing 20 nm diameter pits on the surface. This suggested that Bi droplets formed during growth but desorbed prior to characterization. In both instances the droplets and holes have '*tails*' extending behind them suggesting the droplets promoted vapor liquid solid growth as they rolled across the surface.^{48,49}

4.4.2 (110) Oriented Superlattice Bi incorporation

Unlike the (001) surface, Bi incorporation on the (110) surface increased approximately linearly with increasing Bi deposition time, over the range tested. Figure 4.3b shows ω - 2θ (220) XRD diffraction curves corresponding to samples a-d for the superlattice growths on the InAs (110) surface. The superlattice peaks spacing corresponds to a period of 27.5 ± 0.7 nm across all samples, even as Bi incorporation increased. This may indicate that some error was introduced

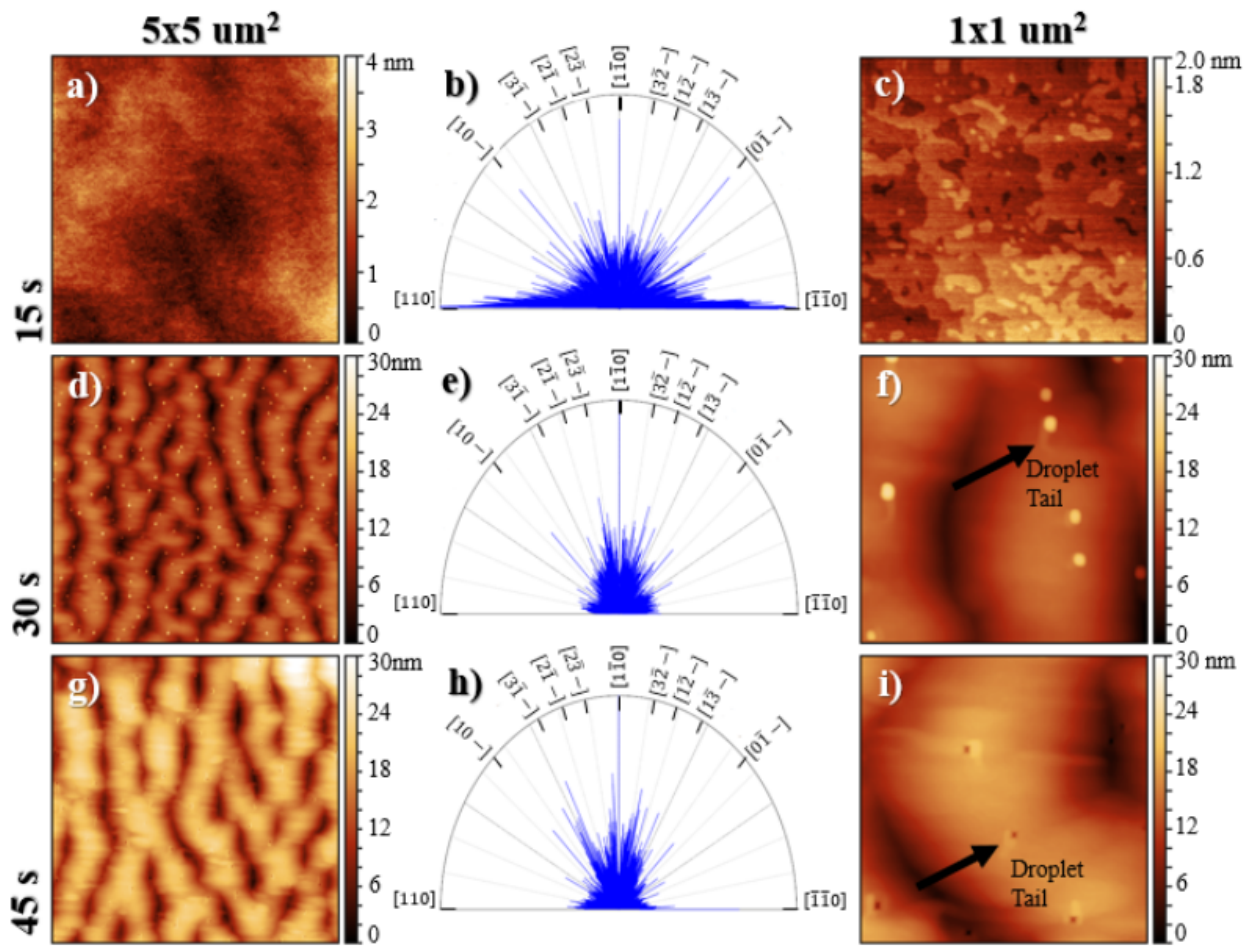


Figure 4.4 AFM micrographs and directional texture analysis maps of the (001) InAs superlattices with (a-c) 15 s of Bi deposition. (d-f) 30 s of Bi deposition and (g-i) 45s of Bi deposition.

when measuring growth rate. At 15s the Bi incorporation is 0.8% Bi, which is notably lower than what was observed on the (001) oriented sample. However, doubling the amount of Bi deposited to 30s served to double the Bi incorporation to 1.6% Bi, closing the gap between the (001) and

(110) surfaces. Tripling the deposited Bi to 45s roughly tripled the incorporation to 2.3% Bi, beyond the maximum incorporation that was observed on the (001) surface. AFM given in Fig 4.5 shows that Bi droplets did not form on the surface of these samples, suggesting that Bi saturation was not reached, and that Bi solubility is indeed higher on the (110) surface compared to the (001). Figure 4.6 shows HAADF STEM and geometric phase analysis (GPA) of sample b ($t=15s$), to quantify strain due to Bi incorporation. As expected, the GPA showed compressive strain in the $[110]$ direction due to Bi incorporation in the SL layers. It also revealed strain fluctuations in the

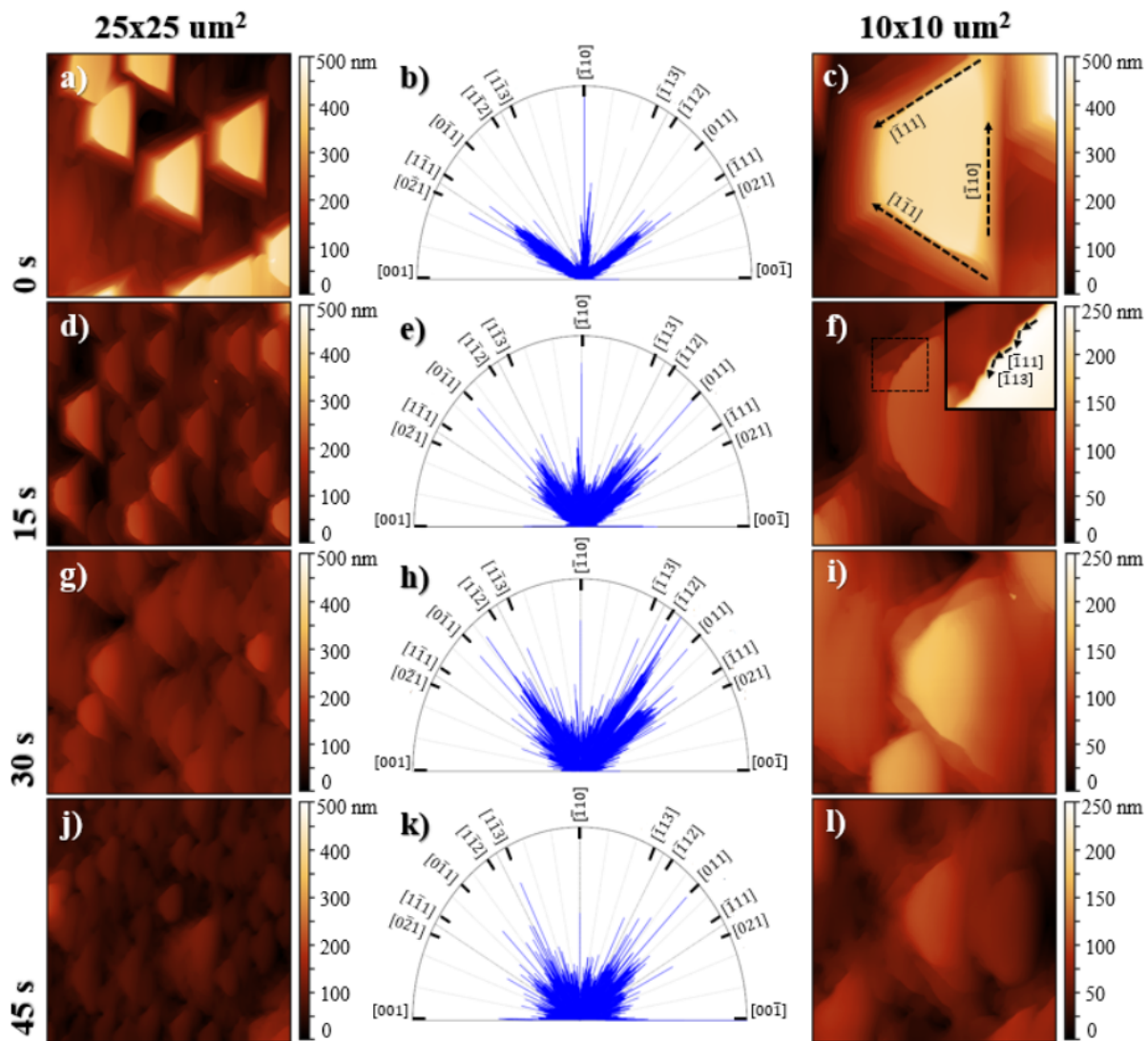


Figure 4.5 . AFM micrographs and directional texture analysis maps of the (110) InAs superlattices with (a-c) 0 s of Bi deposition. (d-f) 15 s of Bi deposition and (g-i) 30 s of Bi deposition and (j-l) 45 s of Bi deposition

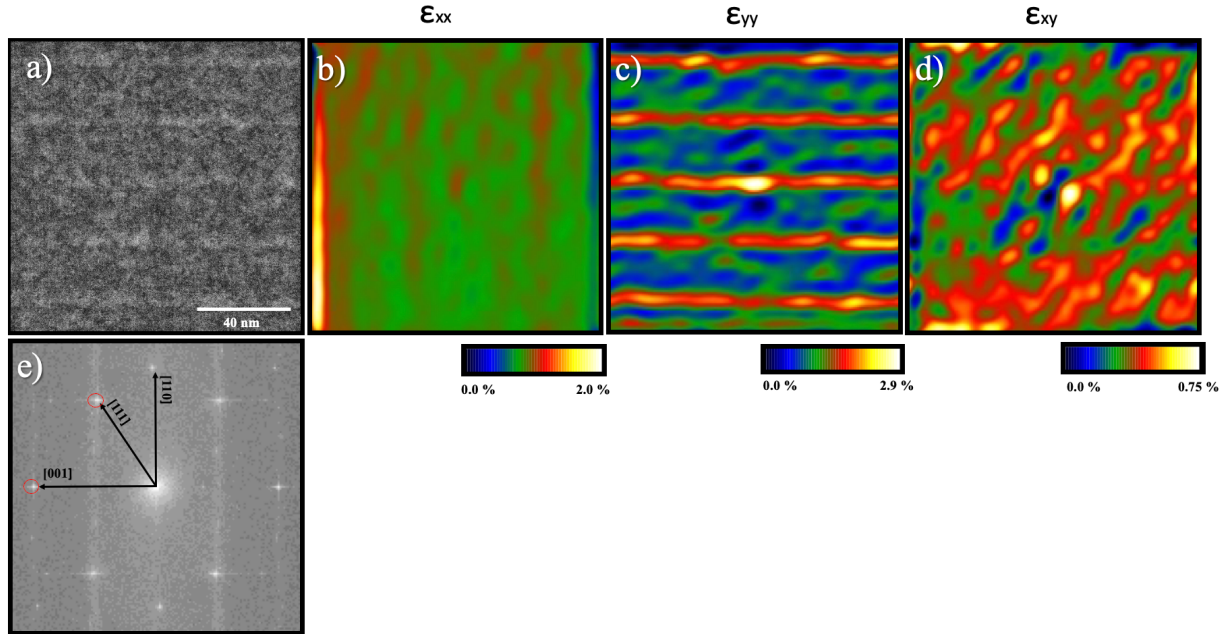


Figure 4.6 a) HAADF STEM of sample b($t=15s$) on the InAs(110) surface.(b-d) Heat maps of strain in the HAAD STEM.(e)FFT of (a) showing the reference vectors used for strain calculations.

Bi layers along the [001] and [111] directions, which indicated non-uniform Bi incorporation and suggested phase segregation and Bi clustering occurred during growth. Furthermore, GPA in Fig 4.6c also shows regions of increased compressive strain at intermediate distances between the superlattice layers indicative of Bi clustering. We postulate that this must be enabled by transport of Bi through point defects, like observations by Tait et al. in GaAsBi (001).^{50,51}

4.5 The Effect of Bi on Surface Morphology

It is also observed that Bi has a different effect on the surface morphology of samples grown on each orientation. In this section we discuss the effect that Bi deposition has on the surface morphology of the SLs grown on each crystal orientation.

4.5.1 (001) Surface Morphology Evolution

Growth of high quality homoepitaxial InAs (001) is well documented, therefore we omit discussion of the Bi free (001) sample. However, the introduction of Bi quickly changes the surface

morphology of these superlattices. AFM micrographs of sample e ($t=15s$) are given in Figs. 4.4a and 4.4c. It is observed that at 15s of Bi deposition the surface is planar with an RMS roughness of less than 2nm. The $1 \times 1 \mu m^2$ micrograph in Fig 4.4c shows a randomized and isotropic distribution of step edges. This is corroborated by a texture map given in Fig 4.4b which shows the step edges are oriented along randomized directions. The texture map also identifies strong features oriented along the $[110]$ and $[-1-10]$, however, this is attributed to remaining line noise that persisted after the image was filtered. The surface morphology transforms dramatically as additional Bi is deposited. Figures 4.4d and 4.4f show AFM micrographs from sample g when the amount of Bi was increased to 30s. The additional Bi caused the surface to transform from a planar morphology to an undulated morphology with average amplitude of approximately 3.9 nm and period of approximately 600nm. Puustinnen et al. showed that the strain introduced by Bi incorporation causes a Grinfeld instability leading to these observed undulation.⁵² However, Bi also induces a strong anisotropy in the diffusion length of group III adatoms; approximately 300 times larger in the $[1-10]$ than in the $[110]$, causing the islands to grow preferentially along the $[1-10]$, leading to the elongated undulations.³⁷ Indeed, the texture map in Fig 4.4e shows that the undulations are predominantly oriented along the $[1-10]$ direction, but they also meander exhibiting limited directionality along the $[3-10]/[1-30]$, $[2-10]/[1-20]$ and $[3-20]/[2-30]$. A similar morphology is observed in sample h ($t=45s$) shown in Figs. 4.4g-i, except the amplitude of the undulations was increased to approximately 6.4 nm and the period of undulation increased to 800 nm. It should be noted that slight variations in V/III ratio have also been reported to cause differences in undulations amplitude and period.⁵²

4.5.2 (110) Surface Morphology Evolution

This section describes the effect that Bi has on the surface morphology of InAs(110). AFM in Figs. 4.5a and 4.5c show that the pure InAs(110) surface is characterized by 291 ± 45 nm tall trapezoidal prisms with a density of $5.0 \times 10^5 \pm 1.0 \times 10^5 \text{ cm}^{-2}$. The prisms have parallel edges of lengths of $7.7 \pm 0.4 \text{ }\mu\text{m}$ and $3.1 \pm 0.2 \text{ }\mu\text{m}$ and a width of $3.6 \pm 0.3 \text{ }\mu\text{m}$. The large prisms resulted in an elevated RMS roughness of $103 \pm 9.5 \text{ nm}$. The texture analysis mapping in Fig 4.5b shows that the diagonal edges of the prisms are strongly oriented in the $[-111]$ and $[1-11]$ directions. Though similar, this is distinct from reports of homoepitaxial GaAs(110) which are shown to exhibit triangular islands with their diagonal legs along the $[1-1-3]/[-11-3]$ or $[1-1-5]/[-11-5]$.³¹ Its worth noting that one study showed the triangular shape is sensitive to annealing and can cause the islands

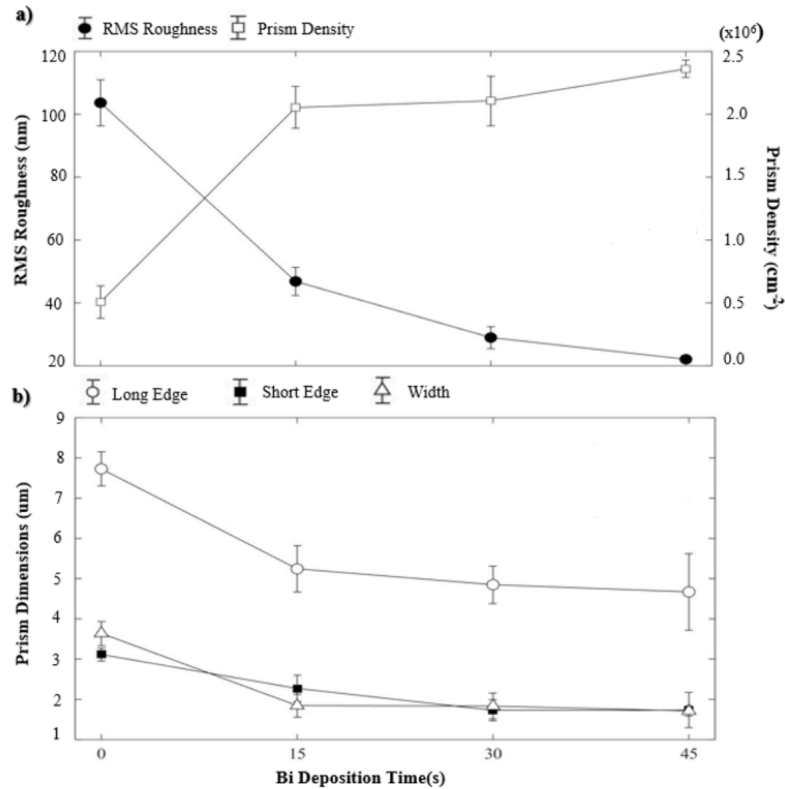


Figure 4.7 Shows the reduction in height and lateral dimensions of the prisms as more Bi is deposited on the surface, as well as the increase in island density.

to round, suggesting that the formation of prisms rather than triangles might be a temperature related effect.²⁶

Depositing Bi alters the surface in multiple ways. The first is that the prisms shrink in size and their density on the surface increases, causing a rapid decrease in the RMS roughness. Second, the islands change shape as different step edge directions are stabilized. Calculations of RMS roughness, given in Fig 4.7a, show that even small amounts of Bi (t=15s) in sample b decreased the RMS roughness by a factor of 2, to approximately 50nm. Figures 4.7a and 4.7b shows this coincided with a shrinking of the prisms' lateral dimensions and an increase in the density of prisms on the surface, which can also be seen in the AFM micrographs in Fig 4.5. These changes in surface morphology continued as additional Bi was deposited culminating in a highly reduced RMS surface roughness of approximately 22nm for the 45s Bi deposition. This was surprising as Bi incorporation introduces compressive strain into the InAs lattice which is generally associated with an increase in surface roughness⁵². Indeed, Kim et al. showed that compressive strain caused by excess As incorporation is relaxed at a critical film thickness through the formation of stacking faults which corresponded to the onset of triangular islands on GaAs(110).³⁶ As such, as Bi incorporation increased, we expected a commensurate increase in surface roughening, but instead observed the opposite.

We postulate that the trapezoidal prisms nucleate due defects related to atomic disorder in As incorporation. This is analogous to the GaAs(110) system where this disorder results from differences in the diffusion rates of Ga and As, and the preferential desorption of As on (110) surfaces^{23,29,32}. Therefore, we suggest that Bi is providing a pathway to reduce this disorder. Wixom et al. showed that Bi can have an outsized effect on the diffusion rates of adatoms, by reducing the [110] diffusion barrier on the GaAs(001) surface.³⁷ An increase in the diffusion length

of As on the InAs (110) surface could serve to mitigate disorder in As incorporation and suppress prism formation, explaining the decrease in RMS roughness. Furthermore, the added group V Bi flux may accommodate for some As desorption from the surface.

We also observed a reduction in step-bunching on the surface. AFM in Fig. 4.8 shows that the pure InAs surface exhibited the highest degree of bunching with an average step height of approximately 19nm in the [001] direction. Researchers have shown that step-bunching is caused by an asymmetric rate of adatom incorporation at upper and lower step edges: preferential incorporation of adatoms at lower step edges has been shown to induce step-bunching while preferential attachment to upper step edges prevents step-bunching.⁵³

As more Bi was deposited the steps rapidly de-bunched to an average height of approximately 3nm in sample d (t=45s), suggesting that Bi has a profound effect on adatom attachment mechanisms at step edges. Indeed, it has been shown in literature that Bi lowers the Ehrlich Schwoebel energy barriers at crystal steps which likely also modifies adatom incorporation mechanics.^{54,55} A lower energy barrier at step edges also enables more adatoms to step down into lower crystal layers reducing the total number of steps. For example, Hao et al. showed that group V decorated step edges lower the Ehrlich-Schwoebel energy barrier in Cu(111) epitaxial growth and promotes 2D growth modes.⁵⁶ A similar effect was shown in the homoepitaxial growth of Fe(100) where it was observed that a Bi surfactant increased interlayer transport and promoted 2D growth.⁵⁷

The average height of step bunching was calculated by first flattening the AFM image by removing a linear background, removing line noise, and finally drawing a line profile to measure the average step edge height in Gwydion scanning probe analysis software.

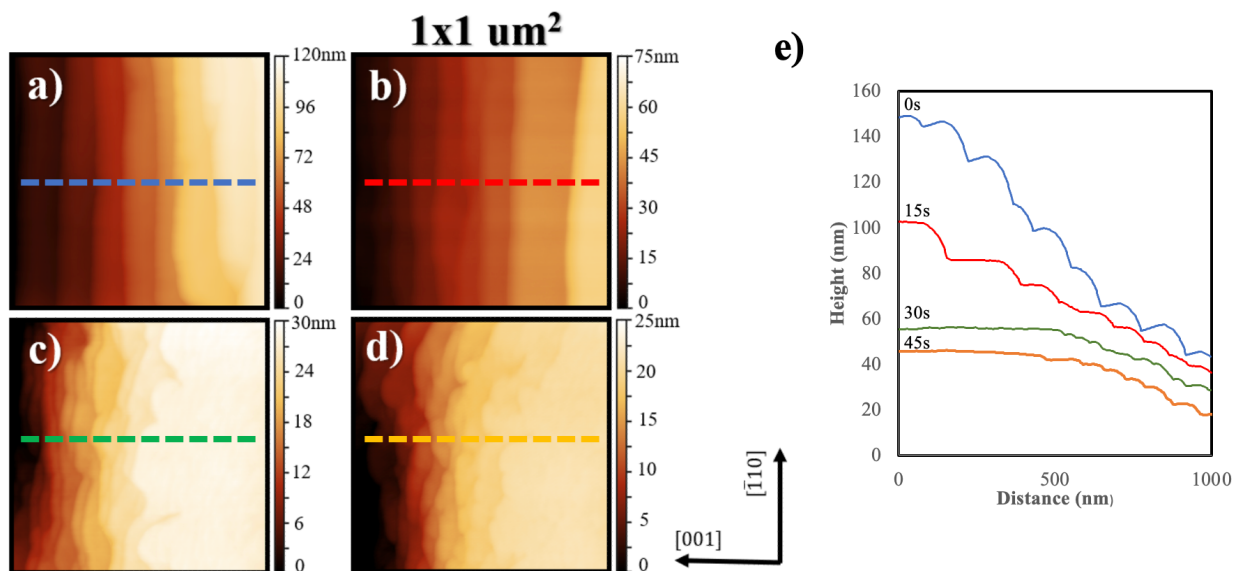


Figure 4.8 AFM micrographs show the transition of the step edges from straight to meandering as a result of Bi induced disorder in surface. (a) 0 sec Bi deposition (b) 15s Bi deposition, (c) 30 sec Bi deposition, (d) 45 s Bi deposition. (e) line profiles showing the reduction in step bunching.⁵⁸

4.5.3 Bi Induced Disorder

In addition to de-bunching, Fig 4.8 shows the prisms' (001) step edges transition from straight and highly faceted in sample b ($t=15\text{s}$) to a disordered meandering behavior first observed on sample d ($t=30\text{ s}$). We postulate that the transition from straight to meandering edges is related to the high entropy of Bi terminated III-V surfaces. While III-Vs generally exhibit a well-defined atomic order, Bismuth terminated III-V alloys are known to exhibit a wide range of surface reconstructions that are similar in energy but distinct in atomic configuration.³⁹ This entropy very likely manifests itself in variations in Bi incorporation at exposed step edges. As such we expect a localized variation in Ehrlich-Schwoebel energy barrier along step edges that correspondingly induce localized variations in adatom incorporation at upper and lower step edges. The Bales-Zangwill instability predicts that a transition from straight to wavy or meandering terraces results from anisotropic energy barriers to adatom attachment, further supporting this hypothesis⁵⁹.

Bi induced disorder also manifests itself on a larger scale as it causes the prisms to change shape. As shown in Fig 4.5, the pure InAs surface is characterized by large prisms with diagonal edges oriented along the $[-111]$ and $[1-11]$. As Bi is deposited, Figs. 4.5d and 4.5f shows that the diagonal facets in sample b ($t=15s$) appear to round. Texture mapping analysis shows that the rounding is caused by an angular spread of the diagonal edges. Indeed, the inset in Fig. 4.5f shows that this apparent rounding is actually a decomposition of the diagonal edges into a combination of both $[-111]/[1-11]$ and $[-113]/[1-13]$. This decomposition continues as more Bi is deposited. Texture maps in Fig 4.5h show that the higher index diagonal edges become more prominent in sample c ($t=30s$) as more Bi is deposited. Finally, texture maps given in Fig 4.5k show sample d ($t=45s$) appears to become more isotropic as the directionality of the peaks begin to fade into a more uniform distribution, however the higher index directions are still favored. The mechanism behind the island shape change is not well understood and can be the focus of future research, however we suggest it is also due to disorder in Bi incorporation at step edges.

4.6 Conclusions

We observed that it requires larger amounts of Bi to saturate the InAs(110) surface compared to the InAs(001) surface, as demonstrated by the onset of droplets. This is likely attributed to the Bi rich (1×2) missing row reconstruction on the InAs(110) surface supporting more Bi per unit area than the (2×4) reconstruction on the InAs(001) surface. As a result, we observed that higher incorporation is achievable in the (110) orientation compared to the (001) orientation. However, equally surprising was the effect that Bi induced on the (001) and (110) surface morphologies. The surface morphology on the (001) was seen to transition from planar to an undulated geometry as more Bi was deposited. Previous literature suggested that this was due to compressive strain inducing a 3D growth mode and Bi behaving as a surfactant increasing

adatom diffusion in the [-110] leading to an elongation of 3D islands. While the (001) surface transitioned from planar to roughened, the (110) surface became smoother as more Bi was deposited. Without Bi, the surface was characterized by large trapezoidal prisms on the surface. However, Bi incorporation was seen to shrink the size of these prisms causing up to a 5-fold reduction in RMS roughness. We postulated that disorder in Bi incorporation creates localized variations in energy barriers at step edges that destabilize the step structure serving to reduce step-bunching and change the characteristic shape of these islands. Our findings not only establish using the (110) orientation as a means for increasing Bi incorporation in III-V alloys but also open the door to the growth of high quality (110) oriented planar films.

4.7 References

1. Lu, X., Beaton, D. A., Lewis, R. B., Tiedje, T. & Whitwick, M. B. Effect of molecular beam epitaxy growth conditions on the Bi content of GaAs_{1-x}Bi_x. *Appl Phys Lett* 92, (2008).
2. Lewis, R. B., Masnadi-Shirazi, M. & Tiedje, T. Growth of high Bi concentration GaAs_{1-x}Bi_x by molecular beam epitaxy. *Appl Phys Lett* 101, 1–5 (2012).
3. Tait, C. R. & Millunchick, J. M. Kinetics of droplet formation and Bi incorporation in GaSbBi alloys. *J Appl Phys* 119, (2016).
4. Masnadi-shirazi, M., Beaton, D. A., Lewis, R. B., Lu, X. & Tiedje, T. Surface reconstructions during growth of GaAs_{1-x}Bi_x alloys by molecular beam epitaxy. *J Cryst Growth* 338, 80–84 (2012).
5. Norman, A. G., France, R. & Ptak, A. J. Atomic ordering and phase separation in MBE GaAs_{1-x}Bi_x. *Journal of Vacuum Science & Technology B, Nanotechnology and Microelectronics: Materials, Processing, Measurement, and Phenomena* 29, 03C121 (2011).
6. Reyes, D. F. et al. Bismuth incorporation and the role of ordering in GaAsBi/GaAs structures. *Nanoscale Res Lett* 9, 1–8 (2014).

7. Wu, M., Luna, E., Puustinen, J., Guina, M. & Trampert, A. Observation of atomic ordering of triple-period-A and -B type in GaAsBi. *Appl Phys Lett* 105, (2014).
8. Zaied, I., Fitouri, H., Chine, Z., Rebey, A. & el Jani, B. Atmospheric-pressure metal-organic vapor-phase epitaxy of GaAsBi alloys on high-index GaAs substrates. *Journal of Physics and Chemistry of Solids* 75, 244–251 (2014).
9. M. Henini, J. Ibanez, M. Schmidbauer, et al. Molecular beam epitaxy of GaBiAs on (311)B GaAs substrates. *Appl Phys Lett* 91, (2007).
10. Guan, Y. et al. Surface kinetics study of metal-organic vapor phase epitaxy of GaAs $1 - y$ Bi y on off cut and mesa-patterned GaAs substrates. *J Cryst Growth* 464, 39–48 (2017).
11. Hernández-Mínguez, A., Biermann, K., Hey, R. & Santos, P. v. Spin transport and spin manipulation in GaAs (110) and (111) quantum wells. *Phys Status Solidi B Basic Res* 251, 1736–1752 (2014).
12. Wegscheider, W., Schedelbeck, G., Neumann, R. & Bichler, M. (1 1 0) oriented quantum wells and modulation-doped heterostructures for cleaved edge overgrowth. *Physica E vol. 2* (1998).
13. Couto, O. D. D., Iikawa, F., Rudolph, J., Hey, R. & Santos, P. v. Anisotropic spin transport in (110) GaAs Quantum wells. *Phys Rev Lett* 98, (2007).
14. Ohno, Y., Terauchi, R., Adachi, T., Matsukura, F. & Ohno, H. Spin Relaxation in GaAs(110) Quantum Wells. (1999).
15. Schmolt, S., Gerl, C., Wurstbauer, U., Mitzkus, C. & Wegscheider, W. Carbon-doped high-mobility two-dimensional hole gases on (110) faced GaAs. *Appl Phys Lett* 86, 1–3 (2005).
16. Oliva, M., Gao, G., Luna, E. & Geelhaar, L. Axial GaAs / Ga (As,Bi) nanowire heterostructures. *Nanotechnology* (2019).
17. Ishikawa, F. & Buyanova, I. A. Self-assembled nanodisks in coaxial GaAs/GaAsBi/GaAs core–multishell nanowires. *Nanoscale* 20849–20858 (2020) doi:10.1039/d0nr05488g.
18. Matsuda, T., Takada, K., Yano, K. & Al., E. Strain deformation in GaAs / GaAsBi core-shell nanowire heterostructures. *J Appl Phys* 125, (2019).

19. Matsuda, T., Takada, K., Yano, K. & Al., E. Twin defect-triggered deformations and Bi segregation in GaAs / GaAsBi core – multishell nanowires Twin defect-triggered deformations and Bi segregation in GaAs / GaAsBi core – multishell nanowires. *Appl Phys Lett* 113105, (2020).
20. Matsuda, T., Takada, K., Yano, K., Tsutsumi, R. & Yoshikawa, K. Controlling Bi-
Provoked Nanostructure Formation in GaAs/GaAsBi Core – Shell Nanowires. *Nano Lett* (2019) doi:10.1021/acs.nanolett.9b02932.
21. Takada, K. et al. Statistical Investigations on the Development of GaAs / GaAsBi Core-
Multi. 2016 Compound Semiconductor Week (CSW) 1 (2016)
doi:10.1109/ICIPRM.2016.7528567.
22. Ishii, A., Aisaka, T., Oh, J. W., Yoshita, M. & Akiyama, H. Low and anisotropic barrier
energy for adatom migration on a GaAs (110) surface studied by first-principles
calculations. *Appl Phys Lett* 83, 4187–4189 (2003).
23. Hudait, M. K., Zhu, Y., Jain, N. & Hunter, J. L. Structural, morphological, and band
alignment properties of GaAs/Ge/GaAs heterostructures on (100), (110), and (111)A
GaAs substrates. *Journal of Vacuum Science & Technology B, Nanotechnology and
Microelectronics: Materials, Processing, Measurement, and Phenomena* 31, 011206
(2013).
24. Joyce, H. J., Wong-Leung, J., Gao, Q., Hoe Tan, H. & Jagadish, C. Phase perfection in
zinc blende and wurtzite III- V nanowires using basic growth parameters. *Nano Lett* 10,
908–915 (2010).
25. Holmes, D. M. et al. Differences between As₂ and As₄ in the homoepitaxial growth of
GaAs(110) by molecular beam epitaxy. *Appl Phys Lett* 67, 2848 (1995).
26. Holmes, D. M., Tok, E. S., Sudijono, J. L., Jones, T. S. & Joyce, B. A. Surface evolution
in GaAs(1 1 0) homoepitaxy; from microscopic to macroscopic morphology. *Journal of
Crystal Growth* vol. 192 (1998).
27. Tok, E. S., Neave, J. H., Ashwin, M. J., Joyce, B. A. & Jones, T. S. Growth of Si-doped
GaAs(110) thin films by molecular beam epitaxy; Si site occupation and the role of
arsenic. *J Appl Phys* 83, 4160–4167 (1998).

28. Tok ab, E., Neave, J., Allegretti, F., Jones, T. & Joyce, B. Incorporation kinetics of As 2 and As 4 on GaAs(110). *Surface Science* vol. 371 (1997).
29. Tok, E. S., Jones, T. S., Neave, J. H., Zhang, J. & Joyce, B. A. Is the arsenic incorporation kinetics important when growing GaAs(001), (110), and (111)A films? *Appl Phys Lett* 71, 3278–3280 (1997).
30. Tejedor, P., Allegretti, F. E., Smilauer, P. & Joyce, B. A. Temperature-dependent unstable homoepitaxy on vicinal GaAs(110) surfaces. *Surface Science* vol. 407 (1998).
31. Holmes, D. M. et al. The nature of island formation in the homoepitaxial growth of GaAs(110). *Surface Science* vol. 341 (1995).
32. Roberts, C. & Joyce, B. A. Surface-morphology evolution during unstable homoepitaxial growth of GaAs(110). *Phys Rev B Condens Matter Mater Phys* 59, 2341–2345 (1999).
33. Holmes, D. M. et al. Different growth modes in GaAs(110) homoepitaxy. *Journal of Vacuum Science & Technology A: Vacuum, Surfaces, and Films* 14, 849–853 (2002).
34. Yoshita, M., Akiyama, H., Pfeiffer, L. N. & West, K. W. Surface-morphology evolution during growth-interrupt in situ annealing on GaAs(110) epitaxial layers. *J Appl Phys* 101, (2007).
35. Allen, L. T. P., Weber, E. R., Washburn, J., Pao, Y. C. & Elliot, A. G. CHARACTERIZATION OF SURFACE FACETING ON (110)GaAs/GaAs GROWN BY MOLECULAR BEAM EPITAXY. *Journal of Crystal Growth* vol. 87 (1988).
36. Kim, H. et al. Surface morphology evolution and underlying defects in homoepitaxial growth of GaAs (110). *J Alloys Compd* 874, (2021).
37. Wixom, R. R., Rieth, L. W. & Stringfellow, G. B. Sb and Bi surfactant effects on homoepitaxy of GaAs on (0 0 1) patterned substrates. *J Cryst Growth* 265, 367–374 (2004).
38. de Renzi, V. et al. A high-resolution spectroscopy study on bidimensional ordered structures: The (1 × 1) and (1 × 2) phases of Bi/InAs(110). *Journal of Physics Condensed Matter* 11, 7447–7461 (1999).

39. Duzik, A., Thomas, J. C., van der Ven, A. & Millunchick, J. M. Surface reconstruction stability and configurational disorder on Bi-terminated GaAs(001). *Phys Rev B Condens Matter Mater Phys* 87, 1–9 (2013).
40. Betti, M. G. et al. Gap-state formation in two-dimensional ordered Bi layers on InAs(110). *Phys Rev B* 58, 115401 (1998).
41. Miwa, R. H. & Takahashi, E. K. Bi-covered InAs(110) surfaces: An ab initio study. *Surf Sci* 566–568, 949–955 (2004).
42. Miwa, R. H. & Takahashi, E. K. Occupied surface-state bands of the (1×2) ordered phase of Bi / InAs (110). *Phys Rev B* 62, 041401 (2000).
43. Nakamura, T. et al. Giant Rashba splitting of quasi-one-dimensional surface states on Bi/InAs(110)- (2×1) . *Phys Rev B* 98, 1–7 (2018).
44. Fritsch, J., Dvořák, A., Arnold, M. & Schröder, U. Dynamical properties of Sb- and Bi-covered (110) surfaces of III-V compounds. *Journal of Physics Condensed Matter* 14, 5865–5879 (2002).
45. Betti, M. G. et al. (1×2) Bi chain reconstruction on the InAs(110) surface. *Phys Rev B Condens Matter Mater Phys* 59, 760–765 (1999).
46. Denton, A. R. & Ashcroft, N. W. Vegard's law. *Phys Rev A (Coll Park)* 43, 3161–3164 (1991).
47. Shalindar, A. J., Webster, P. T., Wilkens, B. J., Alford, T. L. & Johnson, S. R. Measurement of InAsBi mole fraction and InBi lattice constant using Rutherford backscattering spectrometry and X-ray diffraction Measurement of InAsBi mole fraction and InBi lattice constant using. *arXiv preprint 145704*, (2019).
48. Steele, J. A. et al. Surface effects of vapour-liquid-solid driven Bi surface droplets formed during molecular-beam-epitaxy of GaAsBi. *Sci Rep* 28860, 1–17 (2016).
49. Kanjanachuchai, S. & Euaruksakul, C. Directions and breakup of self-running in droplets on low-index InP surfaces. *Cryst Growth Des* 14, 830–834 (2014).
50. Tait, C. R., Yan, L. & Millunchick, J. M. Spontaneous nanostructure formation in GaAsBi alloys. *J Cryst Growth* 493, 20–24 (2018).

51. Imhof, S. et al. Clustering effects in Ga(AsBi). *Appl Phys Lett* 96, 3–6 (2010).
52. Puustinen, J., Hilska, J. & Guina, M. Analysis of GaAsBi growth regimes in high resolution with respect to As / Ga ratio using stationary MBE growth. *J Cryst Growth* 511, 33–41 (2019).
53. Schwoebel, R. L. & Shipsey, E. J. Step motion on crystal surfaces. *J Appl Phys* 37, 3682–3686 (1966).
54. Webster, P. T. et al. Molecular beam epitaxy using bismuth as a constituent in InAs and a surfactant in InAs/InAsSb superlattices. *Journal of Vacuum Science & Technology B, Nanotechnology and Microelectronics: Materials, Processing, Measurement, and Phenomena* 32, 02C120 (2014).
55. Webster, P. T. et al. Molecular beam epitaxy using bismuth as a constituent in InAs and a surfactant in InAs / InAsSb superlattices and a surfactant in InAs / InAsSb superlattices. *Journal of Vacuum Science and Technology B B* 32, (2014).
56. Hao, J. & Zhang, L. Strongly reduced Ehrlich–Schwoebel barriers at the Cu (111) stepped surface with In and Pb surfactants. *Surf Sci* 667, 13–16 (2018).
57. Kamiko, M., Mizuno, H., Xu, J. H., Kojima, I. & Yamamoto, R. Bi induced layer-by-layer growth in the homoepitaxial growth of Fe on Fe (1 0 0)-c(2 × 2)O reconstruction surface. *J Cryst Growth* 263, 363–371 (2004).
58. Carter, B. A. & Millunchick, J. M. Bismuth incorporation and its influence on surface morphology of InAs (1 1 0). *J Cryst Growth* 586, (2022).
59. Bales, G. S. & Zangwill, A. Morphological instability of a terrace edge during step-flow growth. *PHYSICAL REVIEW* vol. 8.

Chapter 5 Future Work

Over the course of this dissertation, it was shown that material flux ratio and surface orientation have a large influence on Bi incorporation and the surface morphology of Bismide films. The purpose of this chapter is to suggest paths for future research to expand upon the findings presented in this dissertation.

5.1 Temperature Series Growth Maps

In Chp. 3 we mapped out a small range of beam flux ratios that yield elevated Bi incorporation in droplet-free films. We chose to perform these experiments at a fixed growth temperature of 325°C because Tait et al.¹ showed most of the lateral composition modulation and cluster formation phenomena was suppressed at temperatures at and above this threshold. Even so, growth at higher temperatures may provide a mechanism to further increase the crystallinity of films and reduce defect formation resulting from low temperature III-V growth. However higher growth temperatures are seen to reduce Bi incorporation and will likely result in a shift of the growth conditions that yield droplet-free growth. As such, we propose a similar growth mapping experiments at temperatures of 335°C and 345°C to identify the droplet-free growth conditions at higher temperature, and the effect of temperature on the maximum attainable Bi incorporation in droplet free films. Mapping across both temperature and material flux parameter space will ensure that the optimum growth conditions are identified for the growth of Bismide films.

5.2 Kinetic Bi Incorporation in (110) oriented Bismide films

The studies presented in Chp. 4 showed that Bi has a higher miscibility on the (110) surface compared to the (001) surface. However, this was demonstrated by exposing static InAs surfaces to Bi flux for varying amounts of time. It must also be determined if this finding holds true during the kinetic growth of InAsBi(110) when the surface is exposed simultaneously to In, As and Bi fluxes. To study this, we suggest keeping temperature at 290°C and growth rate at approximately 0.6 ML/s in line with growth conditions used in Chp. 4. However instead of growing superlattices, we suggest growing bulk InAsBi films on the InAs(110) and InAs(001) surfaces at increasing Bi fluxes until the onset of Bi droplets. Furthermore, this would also allow for further study of the influence of Bi on the surface morphology of (110) InAs.

5.3 STM Study of Bi Incorporation on (110) Surfaces

It is shown in Chp.4 that increasing the amount of Bi deposited served to alter the shape of 3-D prism growth on InAs(110) surface . In particular, it was observed that Bi destabilized the step edge directions on the (110) surface as they transitioned from straight to meandering. This was hypothesized to be caused by disorder in Bi incorporation at step edges, which created localized variations in Ehrlich-Schwoebel energy barriers. This in-turn induces localized variations in adatom incorporation at step edges. STM provides a technique to image Bi incorporation at step edges to understand the evolution of the surface as Bi is deposited and determine if our hypothesis is correct. This could be coupled with simulation work to identify preferential Bi incorporation sites and see how Bi incorporation effects adatom attachment at step edges.

5.4 Growth of Core-Shell Bismide Nanowires

Finally, we suggest studying the growth of (111) oriented InAs/InAsBi core shell nanowires, as their sidewalls exhibit {110} faceting. The above studies should lend insight into the incorporation mechanisms of Bi on the (110) surface and the optimum growth conditions to yield highly crystalline 2-D growth on these sidewall facets. Indeed, this has proved challenging as recent studies have shown that III-V core-shell nanowires are susceptible to the formation of Bi nanoclusters at the vertices of the nanowires, stacking faults, and rough corrugated surfaces.²⁻⁸ This study will enable the growth of reduced-dimensional Bismides that take advantage of enhanced electronic and transport properties of low dimensional nanostructures.⁹⁻¹³

5.5 References

1. Tait, C. R., Yan, L. & Millunchick, J. M. Spontaneous nanostructure formation in GaAsBi alloys. *J Cryst Growth* 493, 20–24 (2018).
2. Ishikawa, F. & Buyanova, I. A. Self-assembled nanodisks in coaxial GaAs/GaAsBi/GaAs core–multishell nanowires. *Nanoscale* 20849–20858 (2020) doi:10.1039/d0nr05488g.
3. Takada, K. et al. Statistical Investigations on the Development of GaAs / GaAsBi Core-Multi. 2016 Compound Semiconductor Week (CSW) 1 (2016) doi:10.1109/ICIPRM.2016.7528567.
4. Matsuda, T., Takada, K., Yano, K., Tsutsumi, R. & Yoshikawa, K. Controlling Bi-Provoked Nanostructure Formation in GaAs/GaAsBi Core – Shell Nanowires. *Nano Lett* (2019) doi:10.1021/acs.nanolett.9b02932.
5. Matsuda, T., Takada, K., Yano, K. & Al., E. Twin defect-triggered deformations and Bi segregation in GaAs / GaAsBi core – multishell nanowires Twin defect-triggered deformations and Bi segregation in GaAs / GaAsBi core – multishell nanowires. *Appl Phys Lett* 113105, (2020).

6. Ishikawa, F. et al. Metamorphic GaAs/GaAsBi Heterostructured Nanowires. *Nano Lett* (2015) doi:10.1021/acs.nanolett.5b02316.
7. Matsuda, T., Takada, K., Yano, K. & Al., E. Strain deformation in GaAs / GaAsBi core-shell nanowire heterostructures. *J Appl Phys* 125, (2019).
8. Oliva, M., Gao, G., Luna, E. & Geelhaar, L. Axial GaAs / Ga (As,Bi) nanowire heterostructures. *Nanotechnology* (2019).
9. Balaghi, L. et al. High electron mobility in strained GaAs nanowires. *Nat Commun* 12, 1–11 (2021).
10. Anyebe, E. A. & Kesaria, M. Photoluminescence Characteristics of Zinc Blende InAs Nanowires. *Sci Rep* 9, 177666 (2019).
11. Blel, S. & Bilel, C. Modeling of the Growth Mechanisms of GaAsBi and GaAs Nanowires. *J Electron Mater* 50, 3380–3384 (2021).
12. Zelewski, S., Kopaczek, J., Linhart, W. M. & Al., E. Photoacoustic spectroscopy of absorption edge for GaAsBi / GaAs nanowires grown on Si substrate. *Appl Phys Lett* 182106, (2019).
13. Roy, D., Prakash, D. & Biswas, A. Photovoltaic performance improvement of GaAs 1-x Bi x nanowire solar cells in terms of light trapping capability and efficiency. *Solar Energy* 221, 468–475 (2021).

Chapter 6 Promoting Effective Educational Research in MSE

In this chapter I discuss the procedures and findings of a systematic review of educational research conducted by Materials Science and Engineering (MSE) faculty over the past decade. We find that while this research is diverse and broad in scope, it is unlikely to result in meaningful changes to the educational system or in the teaching practices of instructors. I analyze the reasons behind this shortcoming and discuss possible solutions.

6.1 Introduction

In recent decades there has been increased concern that the United States is falling behind other countries in STEM education.^{1,2} This has led to an emphasis on shifting undergraduate education from more traditional teacher-centered instruction methods to a more efficacious student-centered approach to teaching and learning.³ In pursuit of this goal, between 2000 and 2020, NSF has awarded more than one billion dollars in funding devoted to researching student-centered learning (SCL).⁴ However, these efforts have been largely unsuccessful at encouraging instructors to adopt student-centered teaching approaches in their classrooms.^{5,6,7,8} In 2011, Henderson et al. conducted a literature review on scholarship about how to promote change in the instructional practices used in STEM classrooms.⁹ Their findings provided insight as to why previous efforts were ineffective at promoting changes in instructional practices and encouraging SCL.

First, Henderson found that there were several different research communities, each with a unique approach to promote and encourage changes in instructional practices. Furthermore, these research communities were largely isolated from each other preventing the exchange of

ideas and findings. As a result, new work often didn't build upon existing theoretical or empirical findings, leading to less effective approaches to changing instruction practices in STEM.

Henderson also categorized papers based on how they approached promoting change in instructional practices by asking two questions. The first question asks: what is the desired change target, or in other words, what aspect of the educational system does the paper seek to change? They determined that papers either seek to change the beliefs and teaching behaviors of individual instructors or educational environments and structures as a whole. The second question asks: What is the desired change outcome of the study and if it was known in advance (prescribed) or not (emergent).

Henderson found that the majority of papers attempted to change the teaching behavior of instructors in a prescribed fashion by developing and encouraging the use of "best practice" curricular materials. Papers describing "top-down" policy implementation that seek to change the educational environment in a pre-prescribed manner were also common. However, Henderson showed that these papers, despite making up most of the literature didn't provide strong evidence of their efficacy at promoting changes in instructional practices. Instead, they found that papers describing emergent change outcomes that described long-term interventions and treated the university setting/educational environment as a complex system, provided strong evidence of their ability to promote changes. As a result, it was determined that interventions with emergent change outcomes, although less common, are more effective than prescribed change outcomes at promoting change in instructional practices.

In this work, we utilize Henderson's approach of determining change target and change outcome as a framework to interpret the results of a systematic literature review to determine

how materials science faculty approach change in their instructional practices. This resulted in a quadrant like classification system, shown in Fig 6.1. We analyze our results and the state of MSE educational research by asking the following three research questions.

- (1) What types of change targets and change outcomes are used in education articles published by authors in Materials Science between 2010 and 2022?
- (2) What are the common themes in the approaches used to promote change?
- (3) What relationships exist between author affiliation, identified theoretical framework, and journal type?

We use these findings to understand if research conducted by MSE faculty is effective at encouraging changes in the teaching practices used in MSE. Furthermore, we suggest methods to

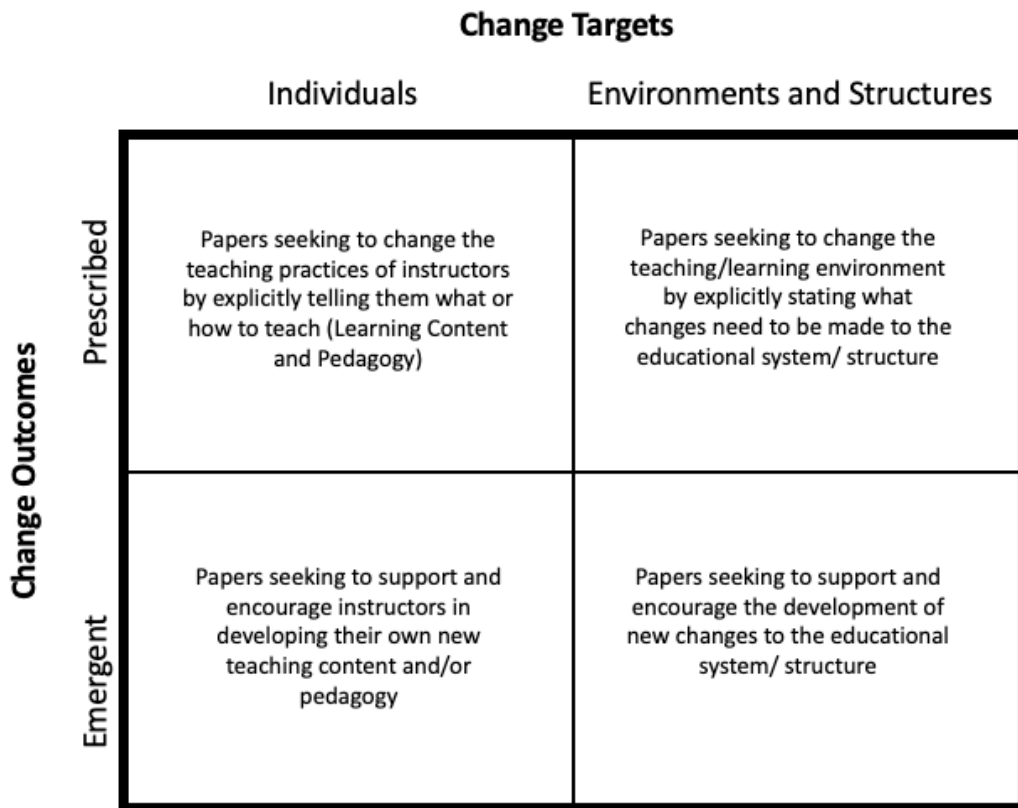


Figure.6.1: Quadrant based classification of papers based on the change target and change outcome adapted from ⁹. Within each quadrant a brief description of the types of papers that fall within it are included.

improve the state of MSE educational research with the intent of promoting the use of more student-centered learning methodologies in classroom settings.

6.2 Methodology

In this section, the methods used to conduct the literature review, coding procedures and analysis procedures are presented and explained.

6.2.1 Search and. Refinement Criteria

To conduct this literature review we utilized a multi-stage process. Detailed descriptions of our inclusion/ exclusion criteria are given in Fig. 6.2 and Table 6.1. The literature search was conducted on May 24th, 2022, in the Web of Science database using the search string "education" (Topic) AND "mat sci" (Address). This search yielded n=856 results which were refined using the following procedures. First, to ensure the literature reflected recent educational work, the results were filtered in Web of Science to exclude papers published outside of the years between 2010 and May 2022. After this step n=708 articles remained. Second, we used the Web of Science filters to exclude all article types except peer-reviewed journal articles. After this step n=355 articles remained. Next, we excluded all papers not published in the USA, resulting in n=141 articles to be reviewed for content.

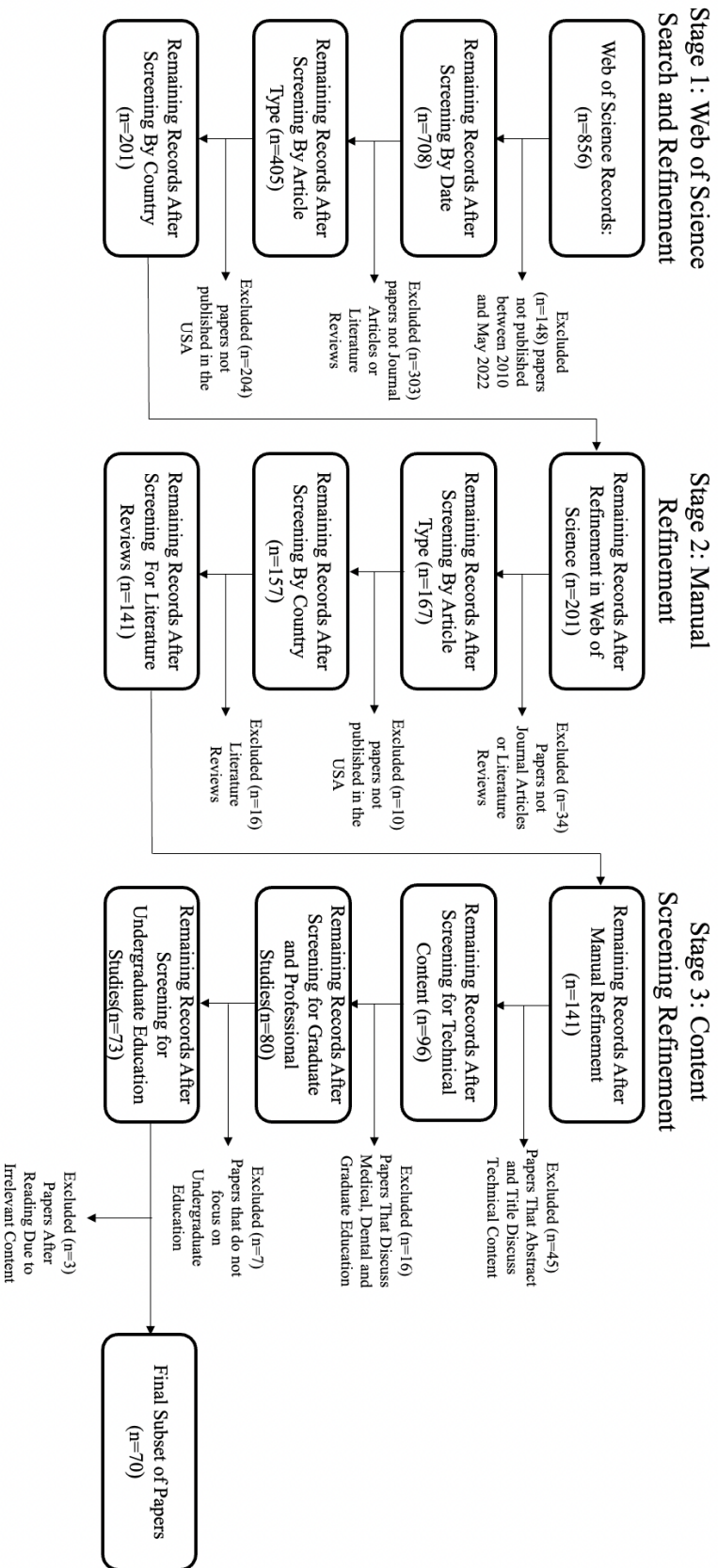


Figure 6.2 Flow Chart of the refinement procedures used in this review

Table 6.1 Inclusion and exclusion criteria for article refinement procedures

| Criteria | Inclusion | Exclusion |
|-------------------|--|---|
| Time Frame | Published between 2010 and May 2022 | Published outside 2010 and May 2022 |
| Literature Type | Peer-reviewed journal articles | Conference proceedings, literature reviews, symposiums, book chapters, bulletin articles, etc. |
| Country | Conducted in the USA | Conducted outside the USA |
| Educational Level | Undergraduate | K-12, general public, graduate, professional studies (medical, dental, law) |
| Topic | Concerned with or related to the education of STEM undergraduates, and/or the educational practices of instructors | Not concerned with or related to the education of STEM undergraduates, and/or the educational practices of instructors (technical research) |

From this point forward the refinement was performed manually, and the exclusion criteria dealt with the topical content of the papers. The titles and abstracts of the remaining papers were reviewed to separate those pertaining to educational research from those that exclusively report technical results, which were removed. This yielded n= 96 papers. Papers related to dental and medical education were also excluded because we were interested in physical sciences and engineering educational studies as opposed to health and professional education studies. This exclusion criteria yielded n=80 papers. Finally, we limited the literature review to educational studies and publications that influence undergraduate education. Note that topics such as faculty development, were not necessarily excluded if there was a discussion on how it influences education for undergraduate students. At the end of this refinement step n=73 papers remained. If we were unsure about any of these exclusion criteria from the titles or abstracts, the papers were left in analysis for the third and final stage of refinement. In the final refinement step, we read the remaining 73 papers to ensure that they met all our criteria. Three

papers were removed as they were found to deal with graduate education, technical results, and medical education. This left n=70 papers for analysis.

6.2.2 Coding Procedures and Analysis

The 70 papers were coded based on the Henderson framework by classifying the intended outcome: prescribed or emergent, and the aspect of the system to be changed: individuals or environments and structures. While Henderson's review only included papers that explicitly advocated for change, this review was more inclusive. We included papers describing new teaching ideas, learning activities, and learning tool development even if they did not have an explicit emphasis on promoting change in instructional practices. We justify the inclusion of these papers by arguing that the act of publishing implies that the author intended to change education in some way by disseminating new knowledge. These broader inclusion criteria were needed to obtain a large enough body of literature, because we limited this review to education research published by authors situated in materials science departments.

Multiple coders were used to classify the papers according to the change outcome and change target. To ensure consistency between coders, ten random papers were coded independently, followed by a joint discussion to resolve discrepancies in our interpretations and to arrive at a common understanding of how to apply the framework. Other features of the studies, including whether the authors used any kind of theoretical framework, the journal in which the articles were published, and the listed departments of the authors were also recorded. Papers were identified to use a theoretical framework if it was explicitly stated in the text, or if there was a background section that outlined a specific idea or theory within which the article and/or analysis was situated. There were instances when an article would briefly invoke an idea or theory, such as active learning, but give little or no citation to the corresponding theory or

description of how it pertained to the paper. These papers were not considered as using a theoretical framework.

We also identified interdisciplinary collaboration between materials science faculty and researchers from other disciplines. We classified five categories of researchers: STEM researchers, social science researchers (SSR), engineering education researchers (EER), industry researchers (I), and others(O). We define STEM researchers as individuals whose departmental affiliation is in a STEM discipline. All papers had at least one author in MSE per the search query used in the literature review. We define social science researchers as individuals with departmental affiliation in the social sciences including psychology and education. We define engineering education researchers as individuals with departmental affiliations in engineering education. It should be noted that this identification schema can overlook engineering education researchers that are housed within other STEM departments. We defined industry researchers as individuals who are affiliated with companies or government laboratories as opposed to academic institutions. The other category was created as a catch-all for researchers who did not fit into the previous four categories. An example of an author who would fall into this category is a university employee that is not affiliated with a specific department such as a writing center employee. In the instance that an author fit into more than one of the five categories, fractional authorship was assigned. For example, if an author had listed appointments in both MSE and engineering education they were assigned 0.5 authorship for each.

We also classified the papers based on the types of journals that they were published in; disciplinary journals, disciplinary education journals, engineering education journals, education journals and learning science journals. Disciplinary journals generally publish technical research articles in STEM, but also publish some educational research related to STEM. An example of a

disciplinary journal is MRS Advances. Disciplinary education journals publish educational studies in a specific discipline of engineering. An example is the Journal of Chemical Education. Engineering education journals focus on education in field of engineering and emphasize rigor and grounding studies in educational theories and theoretical frameworks. An example of an engineering education journal is the Journal of Engineering Education. Education journals focus on education research, without a specific emphasis on engineering education. An example of an educational journal is the International Journal of Inclusive Education. The final journal type was learning science journals. These journals publish articles on human inquiry and learning processes. As example is Cognition and Instruction.

6.3 Results

The purpose of this section is to present the results of our analysis as it pertains to the research questions: what are the change targets and change outcomes used in the articles? What themes emerge in change strategy? And, what relationships exist between author affiliation, identified theoretical framework, and journal type?

6.3.1 Henderson Framework: Change Targets and Change Outcomes

In this section we present the results of using the Henderson Framework to classify the papers according to change outcomes and change targets. Figure 6.3 presents the results of this analysis. Furthermore, table 6.2 provides a comprehensive list of the change outcomes, change targets, journal type, author collaboration and framework usage for the papers in this review.

A large majority (n=57) of the articles discuss studies with prescribed change outcomes. Of these articles, n=40 described individuals as change targets, and n=17 described educational environments and structures as change targets. Articles that discuss studies with emergent

change outcomes(n=13) were less common. Of these articles, n=9 articles described individuals as change targets, and n=4 articles described environments and structures as change targets. In the remainder of this section, we discuss the specific approaches/themes that are used to promote change in the instructional practices of STEM faculty. The frequencies of these themes are graphically represented in Fig 6.3.

The n=40 papers in the Individual/Prescribed quadrant of the Henderson framework attempt to change instructional practices with three different approaches or themes. The first and most common theme (n=23) is pedagogical practices.¹⁰⁻³² These articles are characterized by an emphasis on disseminating and encouraging the use of specific pedagogical teaching techniques. They discuss a broad array of pedagogical techniques including writing to learn^{11,20} active inquiry,¹² course-based undergraduate research,³⁰ culturally relevant pedagogy,¹⁷ collaborative team peer review,¹⁸ module-based learning,^{25,27} process oriented guided inquiry learning,²⁹ and open-ended problem solving.³² An example of a paper that falls within this theme is Colina and

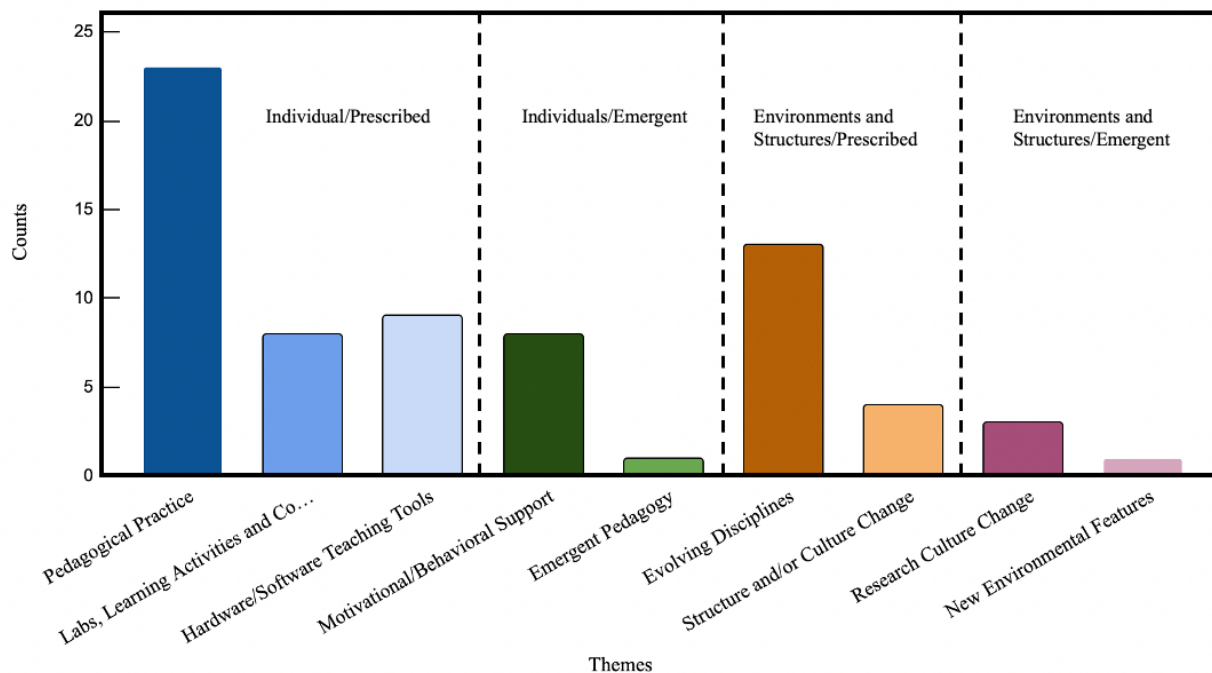


Figure 6.3 Bar graph showing the number of papers that fall into each quadrant of the Henderson Framework and the themes of the papers

Goethe¹⁷ which encourages instructors and educators to engage in culturally relevant pedagogy by incorporating students' interest, culture and lived experiences into the classroom. They provided examples of culturally relevant lessons such as a chemistry instructor discussing chemical reactions driven by sunlight, and its relation to urban smog in predominantly lower-class neighborhoods. Another example was a course called Chemistry en la Cocina Latina at the University of Florida where students analyzed chemical reactions that occur in Hispanic cooking. The second theme that we identified was labs, learning activities and course curriculum (n=8).³³⁻⁴⁰ These articles are characterized by their dissemination of a specific learning activity, lab, or course. They included learning activities and labs designed to teach hydrogen storage,³⁹ graphene synthesis,³⁸ and polymer chemistry,³³ as well as courses such as the BASIL CURE,^{35,36} a biochemistry focused course-based undergraduate research experience. An example of an article with this theme is found in Arnold et al.³⁸ in which a lab describing the synthesis of multilayer graphene films using chemical vapor deposition is presented. This paper outlined laboratory procedures and learning objectives but did not give an analysis on its implementation or effectiveness at promoting student learning. The lack of testing and reporting on learning outcomes is a recurring trend in papers that fell within this theme. The third theme that we identified was hardware and software teaching tools(n=9).⁴¹⁻⁴⁹ These articles are characterized by the dissemination of teaching tools and/or experimental equipment for use in classroom settings, such as a 3D printed mesoreactor,⁴⁸ a stretching device for uniaxial strain of cells,⁴⁷ and a small-scale rotational fiber collection device.⁴² They also include software-based tools such as virtual labs,⁴³ and a spreadsheet-based program for simulating atomic emission spectra.⁴⁹ An example of an article with this theme is found in Love et al.⁴² They elaborate on the need for an affordable device that can produce high quality spun fibers in an educational setting that mimics industry.

This paper focuses on the development process of this device and its technical specifications and performance. They encourage the adoption of their device by educational instructors as a prescribed outcome, however, do not demonstrate its use in an educational setting or show its effectiveness at promoting learning. While its promising that a large majority of the papers in these themes discuss elements of SCL, it should be noted that they didn't discuss any procedures to directly influence the adoption of the described teaching innovations.

The n=17 papers in the Environment & Structures/Prescribed quadrant of the Henderson framework approached change utilizing one of two different themes. The first and most common theme is adapting to evolving disciplines (n=13).⁵⁰⁻⁶² These articles are characterized by their understanding that advancements in technology and research are driving the rapid evolution of engineering disciplines. As such they argue that the educational environment for these disciplines must correspondingly evolve by adapting the material and content that is taught to students and provide suggestions for how to drive this change. Papers in this theme discussed the need for an increased focus on sustainability^{51,55,59,61} and computational materials design^{52,53,57,58} in chemical and materials engineering. An example of an article with this theme is McDowell and Liu⁵⁸ in which the development of the Penn State-Georgia Tech Center for Computational Materials Design is discussed. The center was developed in response to the increased emphasis of computation in materials engineering, and served to couple industry, government, and academia with the purpose of advancing the state of computational materials science and mechanics. A priority of this center was the focus on education and training of the future workforce in computational materials design. The second theme in this quadrant is structural and/or cultural change(n=4).⁶³⁻⁶⁶ The articles in this theme are characterized by understanding an aspect of the educational environment and making or suggesting changes to the academic

environment or departmental culture to support student learning. An example is given in Belchier and Callahan⁶⁵ where the role of STEM students' first grade in english and mathematics is analyzed to predict retention. They find that the grades students earn in their first college level mathematics and english courses are directly correlated to retention. They argue their findings should inform university-wide resource allocation, to ensure proper course placement of incoming students as well as robust student support systems. They suggest a wide range of strategies to accomplish this, including devoting adequate resources for tutoring, learning assistance, supplemental instruction, and evidence-based professional development for instructors. Another example of an article with this theme is found in Kennedy et al.⁶⁶ In this article they analyze the aspects of research experience for undergraduates (REU's) that make students more likely or unlikely to participate. They find that that the topical focus of the REU, stipend amount and the date of acceptance play a large factor as to whether a student will accept an REU. They use their findings to suggest potential changes and actions that research administrators can take to recruit a diverse set of students. These changes to the REU include, ensuring the research mentor elucidates the intellectual merit of their research project and allows for feedback to ensure the student is a good fit. They also discuss the importance of competitive stipends and implementation of a rolling deadline to ensure recruited students can make an informed decision about what REU to accept. Interestingly, these papers generally do not discuss the implementation of their approaches to improving the educational environment and therefore give weak, if any, evidence of their effectiveness at accomplishing their desired changes.

The n=9 papers in the Individual/Emergent quadrant of the Henderson framework approached change utilizing two different themes. The most common theme, motivational/behavioral support,⁶⁷⁻⁷⁴ is characterized by understanding student and instructor

motivation and self-efficacy to guide development of new teaching practices (n=8). An example of an article with this theme is Stolk et al,⁷⁰ in which they presented their Intrinsic Motivation Course Design Method to make motivation theory more accessible to instructors. They use self-determination theory to boost instructors' sense of competence in applying motivation theory in their classrooms. Their method provides instructors with general guidelines; however, they retain a great deal of autonomy in the exact design of their courses. In this sense, the design method is a tool that helps instructors develop their own individualized courses leading to the emergent change outcome classification. Another example of a paper in this theme is Kennedy et al.⁷¹ where they developed two instruments designed to measure students' self-efficacy. Their surveys found that general engineering self-efficacy predicted academic achievement, and that students' intrinsic value in engineering predicted their intention to persist in engineering as a career choice. They suggest their instruments should be used as a tool to assess students' self-efficacy when designing new interventions to improve students' academic performance, which led to the emergent classification. The second theme in this quadrant was emergent pedagogy practices. The lone paper in this theme is categorized by encouraging instructors to incorporate systems thinking into their curricula to link and improve traditionally separate aspects of STEM education.⁷⁵ The author explains this approach is necessary to teach students about how their chemistry education is intertwined with the world around them. This paper gave the example of community college chemistry students engaging younger (K-12) students in interdisciplinary research-based outreach activities. This outreach not only served as a learning experience for the community college chemistry students, but also helped to encourage younger underrepresented groups to engage in STEM. This systems-based approach links two usually separate portions of the STEM pipeline to teach underrepresented youth their importance to the future of STEM. This

paper was presented in a way that encouraged individual instructors to change their teaching practices. As such we classified the change target as individuals. The change outcome of this article was difficult to classify. While they gave specific examples of activities, the primary purpose was to encourage instructors to develop and implement their own new system-based learning by using this case-study as a framework, leading to the emergent classification. Once again, the papers in these themes do not discuss any mechanisms to promote the adoption of their approaches to changing the teaching practices of instructors. As such there is little evidence of their ability to successfully encourage changes in the teaching practices of instructors.

Only n=4 papers were classified in the environments and structures/ emergent quadrant of the Henderson framework. Again, we were able to classify two distinct themes. The first theme was research culture change(n=3).⁷⁶⁻⁷⁸ The articles in this theme are defined by acknowledging and identifying areas to improve in the behaviors and practices of engineering education and physics education research communities. By acknowledging these challenges and addressing them they attempt to create a new culture in their respective research disciplines that will undoubtedly influence the creation of new teaching conceptions. An example of this is Borrego et al⁷⁸ in which they make a case for advancing the culture and practices of engineering education through the promotion of epistemological diversity. They advocate for the increased use of qualitative research. Borrego acknowledges that while this may lead to increased personal and professional conflicts resulting in reduced consensus in EER, it also has the potential to improve dialogue between EER researchers. They contend that this would lead to a more fruitful and supportive research environment which can have a profound effect on the development of new teaching conceptions and practices in the future. This led us to the emergent classification. The second theme in this quadrant is new environmental features (n=1). In this paper Ruzycki et

al.⁷⁹ investigates the implementation of a community of practice as a response to challenges brought upon by the COVID-19 pandemic. Instructor participation in the community of practice was shown to support faculty resilience, life-long learning, and curriculum development. The educational outcomes of the CoP are not prescribed, instead they support faculty to collectively develop teaching strategies that work best for them in a given educational context. This led to the emergent classification. Unlike the rest of the papers included in this review, this article discusses a method to develop new teaching conceptions and environmental features while also ensuring that these teaching conceptions are implemented in classroom settings. As such it is the lone paper in this review that provides strong if any evidence of its ability to change the teaching practices of instructors.

6.3.2 Trends in Framework Usage, Author Affiliations and Publication Type

In this section we present the result of our literature review in the context of research question 3; what relationships exist between author affiliation, identified theoretical framework, and journal types? As discussed previously, table 6.2 gives a comprehensive list of the author types that collaborated on each paper, whether they utilized a theoretical framework, and what type of journal the paper was published in.

Table 6.2 List of paper titles, journal types, collaboration author types, whether a paper utilized a theoretical framework, change targets, and change outcomes

| Citation No. | Title | Journal Type | Collaboration | Framework | Change Target | Change Outcome |
|--------------|--|--------------|---------------|-----------|---------------|----------------|
| 79 | Leveraging a Community of Practice to Build Faculty Resilience and Support Innovations in Teaching during a Time of Crisis | Disc. | O | Y | Environments | Emergent |
| 77 | Exploring tensions of using interpretative phenomenological analysis in a domain with conflicting cultural practices | Disc. | EER | Y | Environments | Emergent |

| | | | | | | |
|----|--|-------|--------|---|--------------|------------|
| 73 | The hidden gender effect in online collaboration: An experimental study of team performance under anonymity | Disc. | SSR | Y | Individual | Emergent |
| 15 | Smaller Classes Promote Equitable Student Participation in STEM | Disc. | SSR | Y | Individual | Prescribed |
| 50 | Achieving a quantum smart workforce | Disc. | I, O | | Environments | Prescribed |
| 55 | Green Engineering Education in Chemical Engineering Curricula: A Quarter Century of Progress and Prospects for Future Transformations | Disc. | O | | Environments | Prescribed |
| 56 | Nanotechnology Education for the Global World: Training the Leaders of Tomorrow | Disc. | SSR, O | | Environments | Prescribed |
| 59 | Sustainable practices: Solar hydrogen fuel and education program on sustainable energy systems | Disc. | I, O | | Environments | Prescribed |
| 60 | Future Outlook for materials Technology Education | Disc. | O | | Environments | Prescribed |
| 43 | The proliferation of virtual laboratories in educational fields | Disc. | O | | Individual | Prescribed |
| 23 | Teaching advanced science concepts through Freshman Research Immersion | Disc. | O | | Individual | Prescribed |
| 51 | Reinvigorating electrochemistry education | Disc. | | | Environments | Prescribed |
| 52 | Gaps and Barriers to Successful Integration and Adoption of Practical Materials Informatics Tools and Workflows | Disc. | | | Environments | Prescribed |
| 64 | Impact of a pilot laboratory safety team workshop | Disc. | | | Environments | Prescribed |
| 57 | Integrated computational materials design for high-performance alloys | Disc. | | | Environments | Prescribed |
| 58 | The Penn State-Georgia Tech CCMD: ushering in the ICME Era | Disc. | | | Environments | Prescribed |
| 61 | Teaching sustainable development in materials science and engineering | Disc. | | | Environments | Prescribed |
| 53 | Computational Materials Science and Engineering Education: An Updated Survey of Trends and Needs | Disc. | | | Environments | Prescribed |
| 41 | Free and open-source software for computational chemistry education | Disc. | | | Individual | Prescribed |
| 11 | Writing-to-learn in introductory materials science and engineering | Disc. | | | Individual | Prescribed |
| 34 | Team-Based Learning of Sustainability: Incorporation of Sustainability Concept and Assessment into Chemical Engineering Senior Design Course | Disc. | | | Individual | Prescribed |

| | | | | | | |
|----|--|-----------|----------|---|--------------|------------|
| 45 | Learnings from developing an applied data science curricula for undergraduate and graduate students | Disc. | | | Individual | Prescribed |
| 47 | A Low-Cost Mechanical Stretching Device for Uniaxial Strain of Cells: A Platform for Pedagogy in Mechanobiology | Disc. | | | Individual | Prescribed |
| 46 | Online simulation powered learning modules for materials science | Disc. | | | Individual | Prescribed |
| 19 | Life Cycle Inventory Assessment as a Sustainable Chemistry and Engineering Education Tool | Disc. | | | Individual | Prescribed |
| 44 | Harnessing Legacy Data to Educate Data-Enabled Structural Materials Engineers | Disc. | | | Individuals | Prescribed |
| 69 | Measuring Engineering Faculty Views about Benefits and Costs of Using Student-Centered Strategies | Disc. Ed. | SSR, EER | Y | Individual | Emergent |
| 20 | Investigation of the Influence of a Writing-to-Learn Assignment on Student Understanding of Polymer Properties | Disc. Ed. | O | Y | Individual | Prescribed |
| 31 | Introducing Discipline-Based Computing in Undergraduate Engineering Education | Disc. Ed. | O | Y | Individual | Prescribed |
| 54 | History of Polymer Education in the United States through the Efforts of the Committee on Polymer Education and the Intersociety Polymer Education Council | Disc. Ed. | | | Environments | Prescribed |
| 22 | Affordances and Challenges of Computational Tools for Supporting Modeling and Simulation Practices | Disc. Ed. | O | | Individual | Prescribed |
| 38 | Simple Graphene Synthesis via Chemical Vapor Deposition | Disc. Ed. | SSR | | Individual | Prescribed |
| 48 | Development and Application of 3D Printed Mesoreactors in Chemical Engineering Education | Disc. Ed. | O | | Individual | Prescribed |
| 27 | REFORMING AN UNDERGRADUATE MATERIALS SCIENCE CURRICULUM WITH COMPUTATIONAL MODULES | Disc. Ed. | EER | | Individuals | Prescribed |
| 76 | Anti-Deficit Framing of Sociological Physics Education Research | Disc. Ed. | | Y | Environments | Emergent |
| 75 | Systems Thinking in Science Education and Outreach toward a Sustainable Future | Disc. Ed. | | Y | Individual | Emergent |
| 17 | Taking Advantage of Diversity within the Classroom | Disc. Ed. | | Y | Individual | Prescribed |

| | | | | | |
|----|--|-----------|---|--------------|------------|
| 26 | Blending Education and Polymer Science: Semiautomated Creation of a Thermodynamic Property Database | Disc. Ed. | Y | Individual | Prescribed |
| 28 | Increasing the Use of Student-Centered Pedagogies from Moderate to High Improves Student Learning and Attitudes about Biology | Disc. Ed. | Y | Individual | Prescribed |
| 21 | Writing In-Code Comments to Self-Explain in Computational Science and Engineering Education | Disc. Ed. | Y | Individual | Prescribed |
| 62 | Chemistry of Carbon Nanotubes for Everyone | Disc. Ed. | | Environments | Prescribed |
| 10 | Sign Language Incorporation in Chemistry Education (SLICE): Building a Lexicon to Support the Understanding of Organic Chemistry | Disc. Ed. | | Individual | Prescribed |
| 42 | Development of a Microcontroller-Based, Small-Scale Rotational Fiber Collection Device | Disc. Ed. | | Individual | Prescribed |
| 13 | Developing and applying computational resources for biochemistry education | Disc. Ed. | | Individual | Prescribed |
| 14 | Translatable Research Group-Based Undergraduate Research Program for Lower-Division Students | Disc. Ed. | | Individual | Prescribed |
| 39 | Hydrogen Storage Experiments for an Undergraduate Laboratory Course-Clean Energy: Hydrogen/Fuel Cells | Disc. Ed. | | Individual | Prescribed |
| 49 | Spreadsheet-Based Program for Simulating Atomic Emission Spectra | Disc. Ed. | | Individual | Prescribed |
| 40 | Simulation of two dimensional electrophoresis and tandem mass spectrometry for teaching proteomics | Disc. Ed. | | Individual | Prescribed |
| 35 | Responses to the COVID-19 Pandemic by the Biochemistry Authentic Scientific Inquiry Lab (BASIL) CURE Consortium: Reflections and a Case Study on the Switch to Remote Learning | Disc. Ed. | | Individual | Prescribed |
| 36 | Flexible Implementation of the BASIL CURE | Disc. Ed. | | Individual | Prescribed |
| 33 | Zooming in on Polymer Chemistry and Designing Synthesis of High Sulfur-Content Polymers for Virtual Undergraduate Laboratory Experiment | Disc. Ed. | | Individuals | Prescribed |
| 12 | Something old, something new: Teaching the BMB lab | Disc. Ed. | | Individuals | Prescribed |
| 37 | Application of virtual laboratories and molecular simulations in teaching nanoengineering to undergraduate students | Disc. Ed. | | Individuals | Prescribed |

| | | | | | | |
|----|--|-----------|----------|---|--------------|------------|
| 25 | Using module-based learning methods to introduce sustainable manufacturing in engineering curriculum | Disc. Ed. | | | Individuals | Prescribed |
| 67 | Instructional Supports for Motivation Trajectories in Introductory College Engineering | Ed. | SSR | Y | Individual | Emergent |
| 68 | Experiential education of deaf and hard of hearing students in the lab with non-signing advisors | Ed. | O | Y | Individual | Emergent |
| 74 | Tinkering and Technical Self-Efficacy of Engineering Students at the Community College | Ed. | SSR, O | Y | Individuals | Emergent |
| 65 | Testing Our Assumptions: The Role of First Course Grade and Course Level in Mathematics and English | Ed. | | Y | Environments | Prescribed |
| 78 | Challenges and promises of overcoming epistemological and methodological partiality: Advancing engineering education through acceptance of diverse ways of knowing | Eng. Ed. | SSR, EER | Y | Environments | Emergent |
| 18 | Impact of Collaborative Team Peer Review on the Quality of Feedback in Engineering Design Projects | Eng. Ed. | SSR, O | Y | Individual | Prescribed |
| 30 | Incorporating Research Experiences into an Introductory Materials Science Course | Eng. Ed. | SSR | Y | Individual | Prescribed |
| 70 | The Intrinsic-Motivation Course Design Method | Eng. Ed. | EER, O | Y | Individuals | Emergent |
| 71 | Measuring Undergraduate Students' Engineering Self-Efficacy: A Validation Study | Eng. Ed. | SSR, O | Y | Individuals | Emergent |
| 72 | Mathematics Identity and Student Persistence in Engineering | Eng. Ed. | SSR | Y | Individuals | Emergent |
| 32 | Moving beyond formulas and fixations: solving open-ended engineering problems | Eng. Ed. | SSR | Y | Individuals | Prescribed |
| 63 | Moving Forward in Engineering Education with the COVID-19 Challenges | Eng. Ed. | EER | | Environments | Prescribed |
| 65 | Factors Associated With Student Decision-Making for Participation in the Research Experiences for Undergraduates Program | Eng. Ed. | EER | | Environments | Prescribed |
| 24 | Slow and Steady: The Effects of Teaching a One-Semester Introductory Mechanics Class Over a Year | Eng. Ed. | | Y | Individual | Prescribed |
| 29 | Student Construction of Knowledge in an Active Learning Classroom | Eng. Ed. | | Y | Individual | Prescribed |

6.3.3 Author Collaboration Journal Types and Framework Usage

Figure 6.4 shows our analysis of the frequency of collaboration between authors of different disciplinary backgrounds, the types of journals that articles were published in, and whether papers used theoretical frameworks. The abscissa shows whether there was collaboration between different author types, and the ordinate shows the type of journal an article was published in. The size of the data points is proportional to the number of papers that fall into each combination of collaboration and journal types, and the fraction of papers that use a framework is represented by the pie charts.

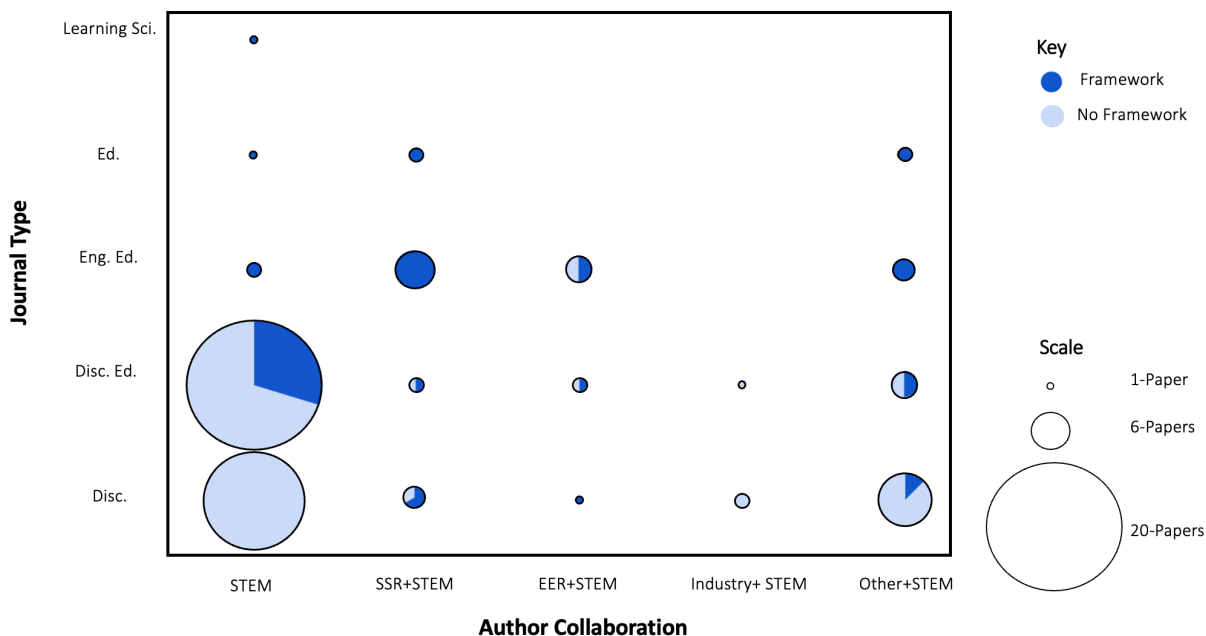


Figure 6.4 Frequency of an article being published in a type of journal versus the types of authors that published it. The size of the data points is proportional to the number of papers and the pie charts show the fraction of papers that utilize a theoretical framework

It was found that of the 360 authors, 283.5 (78.8%) were listed in STEM departments, 34 (9.4%) in social science departments, 9 (2.5%) in EER departments, 9 (2.5%) from industry and 24.5 (6.8%) fell into the other classification.

The stark difference in the size of the data points in Fig 6.4 shows that it was more common for STEM researchers to work individually or only with other STEM researchers $n=39$ than it was for them to collaborate with members of other disciplines $n=31$. It also shows that the majority of papers were published in disciplinary ($n=26$) and disciplinary education ($n=28$) journals.

This showed that STEM authors overwhelmingly publish in disciplinary and disciplinary education journals when they do not collaborate. Furthermore, it also showed that STEM authors are very likely to eschew the use of theoretical frameworks when they do not collaborate. In contrast, it is seen that papers published by interdisciplinary teams of authors from STEM, SSR, and EER and other affiliations, are more frequently published in engineering education and education journals and are more likely to employ the use of a theoretical framework. Interestingly, it was observed that the only paper published in a learning science journal was written by STEM authors without collaboration.

We also observed notable trends in framework usage based on the change outcomes of articles. Articles that described prescribed change outcomes were unlikely to situate their work in theory. Specifically, of the $n=57$ papers describing prescribed change outcomes, only $n=14$ utilized frameworks. Given the low usage of frameworks it followed that a majority of the papers with prescribed change outcomes were published in disciplinary ($n=23$) and disciplinary education ($n=25$) journals, and that the majority ($n=37$) of these papers were published by STEM

authors without collaboration. On the other hand, all n=13 of the papers that described emergent change outcomes situated their work within a framework. Given the high usage of theoretical frameworks it followed that a majority of these papers were published in education (n=3) and engineering education journals (n=4), and that a majority (n=11) were published by an interdisciplinary team of researchers in STEM, EER,SSR and Other.

6.4 Discussion:

Through our analysis it's clear that there are strong relationships between the change targets, change outcomes, framework utilization, interdisciplinary collaboration, and journal type. In this section we discuss how these trends elucidate two main areas of improvement in the way MSE faculty approach educational research.

6.4.1 Areas For Improvement: It's Unclear if the Themes and Approaches Utilized by MSE Authors are Effective at Promoting Change

A decade ago, Henderson showed that engineering education literature that describes interventions with prescribed change outcomes, generally also provide weak evidence of their ability to change the instructional practices of faculty. They observed that that dissemination of pedagogical/ curricular materials was a particularly ineffective ways to encourage change. We observed that this trend is also true in educational literature published by MSE faculty over the past decade. Like Henderson, the majority of the papers in this review described prescribed interventions focused on disseminating pedagogical/ curricular materials. This is demonstrated by the high frequency of the themes; pedagogical practices, labs/learning activities and course curriculum, and hardware/software teaching tools. Furthermore, articles in these themes provided little if any evidence that their studies prompted the adoption of their respective

teaching practices. We are careful to acknowledge that this doesn't imply that these studies are not educationally sound. Instead, it suggests that there is a need for researchers to place an additional emphasis on investigating and publishing strategies that ensure their new teaching practices are adopted.

. In contrast, Henderson showed that articles describing emergent change strategies are more likely to provide strong evidence of their ability to change the instructional practices of faculty. In particular, they showed that long-term interventions that seek to change the beliefs of individuals and treat the university as a complex system were the most effective approaches to promoting change. We identified 13 interventions that describe emergent change outcomes however, only Ruzycki et al⁷⁹, provided strong evidence that their intervention changed the teaching practices of the faculty involved . Indeed, we determine that this study treated the university as complex system by acknowledging the challenges introduced by COVID on the teaching strategies and resiliency of instructors. They described the implementation of a community of practice to support instructors in generating new engineering entrepreneurship curricula that was compatible with COVID protocol. This process was conducted over a semester, and the new curriculum was used by members of the community of practice demonstrating its ability to promote changes in the teaching practices of instructors.

Taken as a whole, it's clear that educational research in MSE is not generally performed in ways that promote changes in the educational practices of faculty, mimicking findings by Henderson et al. a decade ago. Indeed, only 1 out of 70 papers gave compelling evidence that it promoted change in instructional practices. This elucidates the need for a paradigm shift in education research published by MSE faculty. Rather than simply disseminating a new pedagogy, lab, learning activity or other teaching technique they must also understand the

complex dynamics of the university system in order to promote the adoption of their findings. Otherwise, it is unclear if their findings and teaching tools are implemented in educational settings or if they simply languish in a journal. We think that this may be partially explain the slow adoption of SCL in STEM curricula, despite the prevalence of research describing new pedagogies, and learning activities.

6.4.2 Areas For Improvement: MSE Educational Research Needs To Be Situated in Theory

The finding that STEM researchers are unlikely to situate their studies in existing literature and theoretical frameworks represents another area for improvement in educational research conducted by MSE faculty. In order to validate a learning activity, pedagogy or more generally any learning conception, its efficacy at promoting learning must be evaluated. This stands as a necessary step, yet as this systematic review shows, it is often overlooked. As such, we postulate that these unvalidated learning tools and conceptions are at least partially responsible for their lack of adoption and the slow progress of educational literature at changing the teaching practices of STEM instructors. This is understandable as we believe faculty generally want to ensure any given teaching approach works before implementing it in their classrooms. This points for a need to design future educational studies and interventions through the lens of theoretical frameworks. Approaching educational research in a more systematic way, dictated by the framework chosen, allows researchers to better design their studies in ways that they can evaluate their findings and deduce how and why their learning intervention promotes student learning. As such these studies can be iterated on more easily and have the potential to lead to highly efficacious approaches to student learning, and higher levels of adoption.

Furthermore it shows that an effort needs to be made to familiarize STEM researchers with rigorous educational literature. Further familiarizing STEM researchers with educational

theory could serve to provide a pathway to improve research approaches and promote the adoption of their findings in educational settings. One way this can be addressed is by encouraging STEM authors to collaborate with SSR and EER researchers that are more familiar with educational theory. However, addressing the underlying cause of this unfamiliarity may represent a more sustainable approach. We find that papers that use theoretical frameworks are more likely to be published in engineering education and education journals. Meanwhile, STEM researchers, when they don't collaborate, are overwhelmingly likely to publish in disciplinary and disciplinary education journals. This could indicate that STEM researchers' unfamiliarity with educational literature arises from an unfamiliarity with educationally oriented journals. One way this barrier can be overcome is for EER and SSR researchers to publish in disciplinary and disciplinary education journals where STEM researchers are more likely to see it. However, for this approach to be effective, editors of disciplinary and disciplinary education journals will have to raise the bar on the standard of educational studies that they publish and ensure that work published by STEM researchers is both rigorous and situated in theory. We suggest that they have EER or SSR researchers review the work prior to publication to accomplish this. Without an increased emphasis on rigor and overall quality of research it is unlikely that SSR and EER authors will forgo publishing in more prestigious and high impact engineering education and education journals.

6.5 Conclusions

MSE faculty approach educational research to improve undergraduate education in a variety of ways. This is shown by the 9 themes or approaches that MSE authors used to promote change in instructional practices. While it is encouraging to see an emphasis being placed on improving the state of MSE education, there is evidence that suggests the predominant

approaches are not effective at promoting changes in the educational practices of faculty. Highly prescribed approaches are observed to provide little evidence of their effectiveness at promoting changes in the educational practices of faculty yet make up most of the literature. Overall, it was observed that only one paper provided evidence of its ability to promote changes in the teaching practices of instructors. As a result, we conclude that MSE education research is unlikely to promote changes in the instructional practices of faculty. As such we recommend that MSE researchers understand the complex dynamics of the university system in order to design studies that simultaneously promote the adoption of their findings. Furthermore, we postulate that the prevalence of ineffective research is exacerbated by the finding that STEM authors rarely situating their work in educational theory or a theoretical framework, unless they collaborate with EER or SSR researchers. Therefore, to ensure effective research is being conducted it is imperative to familiarize MSE and STEM faculty with educational research. This can be accomplished in several ways including by collaborating with EER and SSR researchers, or by encouraging journal editors in disciplinary and disciplinary education to increase the standards of the educational literature that they publish.

6.6 References

1. Labov, J. B., Devino, N. L., Johnston, K., Pritchard, G. E. & Holmer, T. K. Transforming undergraduate education in science, mathematics, engineering, and technology. (National Academy Press, 1999).
2. President Obama Launches 'Educate to Innovate' Campaign for Excellence in Science, Technology, Engineering and Math (STEM) Education.
<https://obamawhitehouse.archives.gov/the-press-office/president-obama-launches-educate-innovate-campaign-excellence-science-technology-en> (2009).

3. Barr, R. B. & Tagg, J. From Teaching to Learning: A New Paradigm for Undergraduate Education. 27, 12–25.
4. National Science Foundation. NSF.gov
<https://www.nsf.gov/awardsearch/advancedSearchResult?PIId=&PIFirstName=&PILastName=&PIOrganization=&PIState=&PIZip=&PICountry=&ProgOrganization=11000000&ProgEleCode=&BooleanElement=All&ProgRefCode=&BooleanRef=All&Program=&ProgOfficer=&Keyword=Student+Centered&AwardNumberOperator=&AwardAmount=&AwardInstrument=&ExpiredAwards=true&OriginalAwardDateOperator=Range&OriginalAwardDateFrom=01%2F01%2F2000&OriginalAwardDateTo=12%2F31%2F2010&StartDateOperator=&ExpDateOperator=>.
5. Bok, D. C. Our Underachieving Colleges: A candid look at how much students learn and why they should be learning more. (Princeton University Press, 2006).
6. Handelsman, J. et al. Scientific Teaching. New Series vol. 304 (2004).
7. Kezar, A. J. Understanding and Facilitating Organizational Change in the 21st Century: Recent Research and Conceptualizations. (ERIC- Clearing House on Higher Education, 2001).
8. Strum, K. et al. The Boyer Commission on Educating Undergraduates in the Research University Reinvigorating Undergraduate Education: A Blueprint of Americas Research Universities. (1998).
9. Henderson, C., Beach, A. & Finkelstein, N. Facilitating change in undergraduate STEM instructional practices: An analytic review of the literature. J Res Sci Teach 48, 952–984 (2011).
10. Clark, K. et al. Sign Language Incorporation in Chemistry Education (SLICE): Building a Lexicon to Support the Understanding of Organic Chemistry. J Chem Educ 99, 122–128 (2022).
11. Marks, L., Lu, H., Chambers, T., Finkenstaedt-Quinn, S. & Goldman, R. S. Writing-to-learn in introductory materials science and engineering. MRS Communications vol. 12 Preprint at <https://doi.org/10.1557/s43579-021-00114-z> (2022).

12. Craig, P. A. Something old, something new: Teaching the BMB lab. *Biochemistry and Molecular Biology Education* 48, 640–642 (2020).
13. Craig, P. A. Developing and applying computational resources for biochemistry education. *Biochemistry and Molecular Biology Education* 48, 579–584 (2020).
14. Hauwiller, M. R., Ondry, J. C., Calvin, J. J., Baranger, A. M. & Alivisatos, A. P. Translatable Research Group-Based Undergraduate Research Program for Lower-Division Students. *J Chem Educ* (2019) doi:10.1021/acs.jchemed.9b00159.
15. Ballen, C. J. et al. Smaller classes promote equitable student participation in STEM. *Bioscience* 69, 669–680 (2019).
16. Vieira, C., Magana, A. J., Roy, A. & Falk, M. L. Student Explanations in the Context of Computational Science and Engineering Education. *Cogn Instr* 37, 201–231 (2019).
17. Goethe, E. v. & Colina, C. M. Taking Advantage of Diversity within the Classroom. *Journal of Chemical Education* vol. 95 189–192 Preprint at <https://doi.org/10.1021/acs.jchemed.7b00510> (2018).
18. Mandala, M. et al. Impact of Collaborative Team Peer Review on the Quality of Feedback in Engineering Design Projects*.
19. Reichmanis, E. & Sabahi, M. Life Cycle Inventory Assessment as a Sustainable Chemistry and Engineering Education Tool. *ACS Sustain Chem Eng* 5, 9603–9613 (2017).
20. Finkenstaedt-Quinn, S. A. et al. Investigation of the Influence of a Writing-To-Learn Assignment on Student Understanding of Polymer Properties. *J Chem Educ* 94, 1610–1617 (2017).
21. Vieira, C., Magana, A. J., Falk, M. L. & Garcia, R. E. Writing in-code comments to self-explain in computational science and engineering education. *ACM Transactions on Computing Education* 17, (2017).
22. Magana, A. J. et al. Affordances and challenges of computational tools for supporting modeling and simulation practices. *Computer Applications in Engineering Education* 25, 352–375 (2017).

23. Wahila, M. J., Amey-Propert, J., Jones, W. E., Stamp, N. & Piper, L. F. J. Teaching advanced science concepts through freshman research immersion. *Eur J Phys* 38, (2017).
24. Thouless, M. D. Slow and Steady: The Effects of Teaching a One-Semester Introductory Mechanics Class Over a Year*.
25. Sengupta, D. et al. Using module-based learning methods to introduce sustainable manufacturing in engineering curriculum. *International Journal of Sustainability in Higher Education* 18, 307–328 (2017).
26. Tchoua, R. B. et al. Blending Education and Polymer Science: Semiautomated Creation of a Thermodynamic Property Database. *J Chem Educ* 93, 1561–1568 (2016).
27. Mansbach, R. et al. REFORMING AN UNDERGRADUATE MATERIALS SCIENCE CURRICULUM WITH COMPUTATIONAL MODULES. *Journal of Materials Education* vol. 38 <http://bit.ly/25OzbzG> (2016).
28. Connell, G. L., Donovan, D. A. & Chambers, T. G. Increasing the use of student-centered pedagogies from moderate to high improves student learning and attitudes about biology. *CBE Life Sci Educ* 15, (2016).
29. Douglas, E. P., Vargas, J. & Sotomayor, C. Student Construction of Knowledge in an Active Learning Classroom*.
30. Zhou, Y. et al. Incorporating Research Experiences into an Introductory Materials Science Course*.
31. Magana, A. J., Falk, M. L. & Reese, M. J. Introducing discipline-based computing in undergraduate engineering education. *ACM Transactions on Computing Education* 13, (2013).
32. Douglas, E. P., Koro-Ljungberg, M., McNeill, N. J., Malcolm, Z. T. & Therriault, D. J. Moving beyond formulas and fixations: Solving open-ended engineering problems. *European Journal of Engineering Education* 37, 627–651 (2012).
33. Karayilan, M., Vakil, J., Fowler, D., Becker, M. L. & Cox, C. T. Zooming in on polymer chemistry and designing synthesis of high sulfur-content polymers for virtual undergraduate laboratory experiment. *J Chem Educ* 98, 2062–2073 (2021).

34. Amini-Rankouhi, A. & Huang, Y. Team-based learning of sustainability: Incorporation of sustainability concept and assessment into chemical engineering senior design course. *Smart Sustain Manuf Syst* 5, (2020).
35. Sikora, A. et al. Responses to the covid-19 pandemic by the biochemistry authentic scientific inquiry lab (basil) cure consortium: Reflections and a case study on the switch to remote learning. *J Chem Educ* 97, 3455–3462 (2020).
36. Roberts, R. et al. Flexible Implementation of the BASIL CURE. *Biochemistry and Molecular Biology Education* 47, 498–505 (2019).
37. Kilani, M., Torabi, K. & Mao, G. Application of virtual laboratories and molecular simulations in teaching nanoengineering to undergraduate students. *Computer Applications in Engineering Education* 26, 1527–1538 (2018).
38. Jacobberger, R. M. et al. Simple Graphene Synthesis via Chemical Vapor Deposition. *J Chem Educ* 92, 1903–1907 (2015).
39. Bailey, A. et al. Hydrogen storage experiments for an undergraduate laboratory course—clean energy: Hydrogen/fuel cells. *J Chem Educ* 92, 688–692 (2015).
40. Fisher, A., Sekera, E., Payne, J. & Craig, P. Simulation of two dimensional electrophoresis and tandem mass spectrometry for teaching proteomics. *Biochemistry and Molecular Biology Education* 40, 393–399 (2012).
41. Lehtola, S. & Karttunen, A. J. Free and open source software for computational chemistry education. *Wiley Interdisciplinary Reviews: Computational Molecular Science* vol. 12 Preprint at <https://doi.org/10.1002/wcms.1610> (2022).
42. Dean, J., Rieland, J. M. & Love, B. J. Development of a Microcontroller-Based, Small-Scale Rotational Fiber Collection Device. *J Chem Educ* 98, 4061–4066 (2021).
43. Vergara, D., Extremera, J., Rubio, M. P. & Dávila, L. P. The proliferation of virtual laboratories in educational fields. *ADCAIJ: Advances in Distributed Computing and Artificial Intelligence Journal* 9, 85–97 (2020).
44. Carter, J. L. W., Cerma, A. K. & Senanayake, N. M. Harnessing Legacy Data to Educate Data-Enabled Structural Materials Engineers. *MRS Adv* 5, 319–327 (2020).

45. French, R. H. & Bruckman, L. S. Learnings from developing an applied data science curricula for undergraduate and graduate students. *MRS Adv* 5, 347–353 (2020).
46. Online simulation powered learning modules for materials science.
47. Atcha, H. et al. A Low-Cost Mechanical Stretching Device for Uniaxial Strain of Cells: A Platform for Pedagogy in Mechanobiology. *J Biomech Eng* 140, (2018).
48. Tabassum, T. et al. Development and Application of 3D Printed Mesoreactors in Chemical Engineering Education. *J Chem Educ* 95, 783–790 (2018).
49. Flannigan, D. J. Spreadsheet-Based Program for Simulating Atomic Emission Spectra. *J Chem Educ* 91, 1736–1738 (2014).
50. Aiello, C. D. et al. Achieving a quantum smart workforce. *Quantum Science and Technology* vol. 6 Preprint at <https://doi.org/10.1088/2058-9565/abfa64> (2021).
51. Kempler, P. A., Boettcher, S. W. & Ardo, S. iScience Reinvigorating electrochemistry education. doi:10.1016/j.isci.
52. McDowell, D. L. Gaps and Barriers to Successful Integration and Adoption of Practical Materials Informatics Tools and Workflows. *JOM* 73, 138–148 (2021).
53. Enrique, R. A., Asta, M. & Thornton, K. Computational Materials Science and Engineering Education: An Updated Survey of Trends and Needs. *JOM* 70, 1644–1651 (2018).
54. Carraher, C. E. et al. History of Polymer Education in the United States through the Efforts of the Committee on Polymer Education and the Intersociety Polymer Education Council. *J Chem Educ* 94, 1607–1609 (2017).
55. Allen, D. T., Shonnard, D. R., Huang, Y. & Schuster, D. Green engineering education in chemical engineering curricula: A quarter century of progress and prospects for future transformations. *ACS Sustain Chem Eng* 4, 5850–5854 (2016).
56. Jackman, J. A. et al. Nanotechnology Education for the Global World: Training the Leaders of Tomorrow. *ACS Nano* 10, 5595–5599 (2016).
57. Xiong, W. & Olson, G. B. Integrated computational materials design for high-performance alloys. *MRS Bull* 40, 1035–1043 (2015).

58. Liu, Z. K. & McDowell, D. L. The Penn State-Georgia Tech CCMD: ushering in the ICME Era. *Integr Mater Manuf Innov* 3, 409–428 (2014).
59. Nowotny, J. et al. Sustainable practices: Solar hydrogen fuel and education program on sustainable energy systems. *Int J Hydrogen Energy* 39, 4151–4157 (2014).
60. Future Outlook for materials Technology Education.
61. Lesar, R., Chen, K. C. & Apelian, D. Teaching sustainable development in materials science and engineering. *MRS Bull* 37, 449–454 (2012).
62. Basu-Dutt, S., Minus, M. L., Jain, R., Nepal, D. & Kumar, S. Chemistry of carbon nanotubes for everyone. *J Chem Educ* 89, 221–229 (2012).
63. Yunus Khan, T. M. et al. Moving Forward in Engineering Education with the COVID-19 Challenges*.
64. Miller, K. A. & Tyler, K. I. Impact of a pilot laboratory safety team workshop. *J Chem Health Saf* 26, 20–26 (2019).
65. Callahan, J. & Belcheir, M. Testing Our Assumptions: The Role of First Course Grade and Course Level in Mathematics and English. *J Coll Stud Ret* 19, 161–175 (2017).
66. Economy, D. R., Sharp, J. L., Martin, J. P. & Kennedy, M. S. Factors Associated With Student Decision-Making for Participation in the Research Experiences for Undergraduates Program*.
67. Robinson, K. A., Lira, A. K., Walton, S. P., Briedis, D. & Linnenbrink-Garcia, L. Instructional Supports for Motivation Trajectories in Introductory College Engineering. *AERA Open* 8, (2022).
68. Gehret, A. U., Michel, L. v. & Trussell, J. W. Experiential education of deaf and hard of hearing students in the lab with non-signing advisors. *International Journal of Inclusive Education* (2021) doi:10.1080/13603116.2021.1879948.
69. Judson, E., Ross, L., Middleton, J. & Krause, S. Measuring Engineering Faculty Views about Benefits and Costs of Using Student-Centered Strategies. *International Journal of Engineering Pedagogy (iJEP)* 7, 65 (2017).

70. Herman, G. L., Goldberg, D. E., Trenshaw, K. F., Somerville, M. & Stolk, J. The Intrinsic-Motivation Course Design Method*.
71. Mamaril, N. A., Usher, E. L., Li, C. R., Economy, D. R. & Kennedy, M. S. Measuring Undergraduate Students' Engineering Self-Efficacy: A Validation Study. *Journal of Engineering Education* 105, 366–395 (2016).
72. Cribbs, J. D., Cass, C., Hazari, Z., Sadler, P. M. & Sonnert, G. Mathematics Identity and Student Persistence in Engineering*.
73. Song, H. G. et al. The hidden gender effect in online collaboration: An experimental study of team performance under anonymity. *Comput Human Behav* 50, 274–282 (2015).
74. Baker, D. R., Wood, L., Corkins, J. & Krause, S. Tinkering and Technical Self-Efficacy of Engineering Students at the Community College. *Community Coll J Res Pract* 39, 555–567 (2015).
75. Blatti, J. L. et al. Systems Thinking in Science Education and Outreach toward a Sustainable Future. *J Chem Educ* 96, 2852–2862 (2019).
76. Exarhos, S. Anti-Deficit Framing of Sociological Physics Education Research. *Phys Teach* 58, 461–464 (2020).
77. Kirn, A., Huff, J. L., Godwin, A., Ross, M. & Cass, C. Exploring tensions of using interpretative phenomenological analysis in a domain with conflicting cultural practices. *Qual Res Psychol* 16, 305–324 (2019).
78. Douglas, E. P., Koro-Ljungberg, M. & Borrego, M. Challenges and promises of overcoming epistemological and methodological partiality: Advancing engineering education through acceptance of diverse ways of knowing. *European Journal of Engineering Education* 35, 247–257 (2010).
79. Mead, T. et al. Leveraging a community of practice to build faculty resilience and support innovations in teaching during a time of crisis. *Sustainability (Switzerland)* 13, (2021).

Chapter 7 Reflecting on Using VR to Teach Crystal Structures

The purpose of this chapter is to present a critical analysis of three studies that we conducted to determine if Virtual Reality (VR) can improve student learning of 3D concepts in Materials Science and Engineering (MSE); specifically crystal structures. We were motivated by the goal of encouraging the increased adoption of VR teaching tools by instructors.

We begin this chapter by discussing our motivation for studying VR as a teaching tool. Specifically, we discuss the importance of spatial reasoning skills in STEM, and present VR as an opportunity to improve these skills in students. This is followed by a short review of studies that used VR in educational settings. Next, the bulk of this chapter discusses the implementation and findings of three studies that we conducted to test the efficacy of using VR to teach crystal

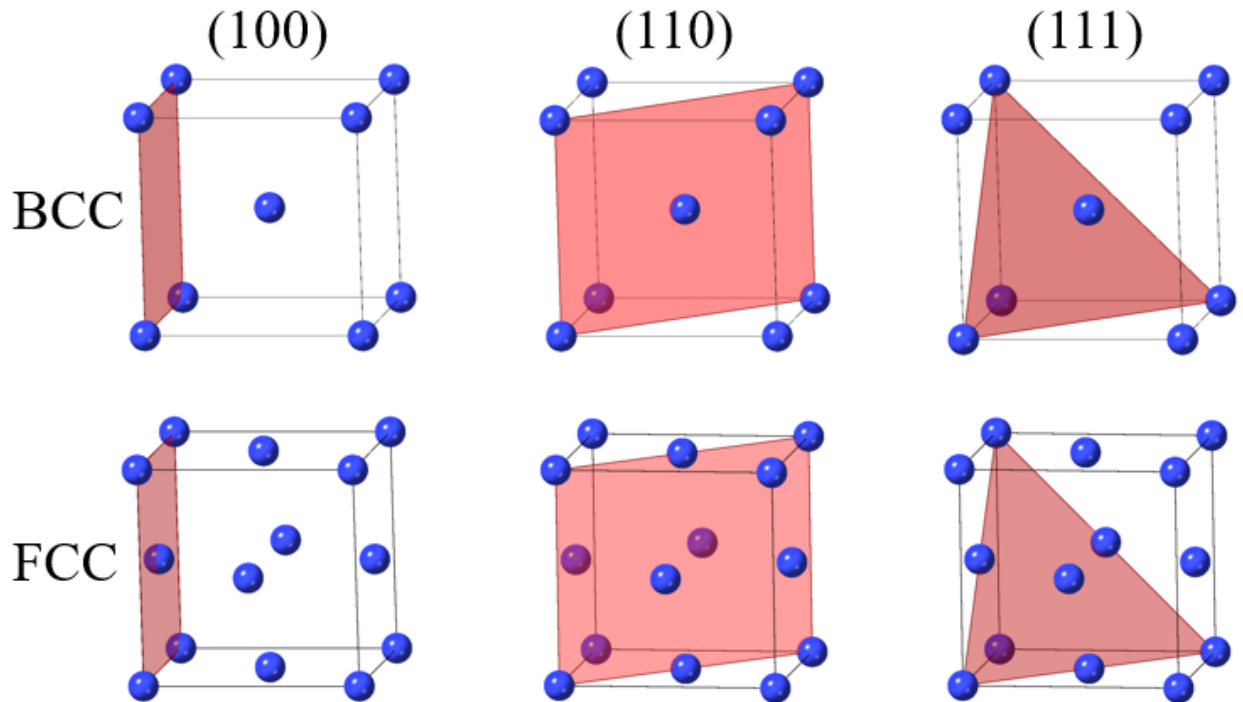


Figure 7.1 Reduced sphere representations of commonly taught crystal structures in introductory level MSE classes; Body Centered Cubic (BCC) and Face Centered Cubic (FCC) with different crystal planes superimposed

structures. We discuss the positive and negative aspects of our experimental design and place an emphasis on whether our study is tailored to our goal of convincing more instructors to use VR in their classrooms. We conclude this chapter by suggesting changes to future research to increase the likelihood that instructors adopt VR.

7.1 Introduction: Motivation for Studying VR to Teach Crystal Structure

Spatial reasoning skills are particularly important in MSE where students need a solid understanding of the 3-D crystal structures of materials. Figure 7.1 shows examples of common crystal structures and crystal planes that students typically encounter in introductory level MSE courses. However, literature has shown that students commonly exhibit misconceptions related to the atomic arrangement and atomic packing of atoms¹⁻⁴ suggesting that these representations don't convey 3-D information well and don't support high levels of spatial reasoning.

Advancements in virtual and augmented reality, collectively referred to as XR, provide a unique opportunity to improve the teaching of crystal structures by improving the spatial reasoning skills of students and correcting these misconceptions.

XR headsets enable users to interact with their environments and manipulate 3-D figures such as crystal structures. Literature has shown that this leads to an increased level of interaction with learning content compared to traditional paper-based representations and is shown to benefit student learning.^{6,7} For example, educational literature has shown that VR based learning leads to, increased memory, increased motivation, increased engagement with learning content, the ability to better conceptualize ideas, and increased problem-solving ability.⁸⁻¹³ Despite this, using XR to teach STEM concepts is still relatively novel. However, its use has been increasing in recent years, especially in the fields of chemistry⁸ and mathematics.¹⁴

7.2 Background: Crystal Structure Visualization in Educational Literature

Gentry et al.⁵ showed that computer-based crystal structure visualization software can aid in correcting student misconceptions related to the atomic arrangement and the atomic packing of atoms. In their work, the authors designed and tested an activity using a crystal visualization software called Ovito that allowed students to interact with various crystal structures. They found that by using Ovito, students were able to correct previously held misconceptions related to atomic packing and crystalline planes of atoms. We hypothesized that the highly immersive VR environment can diminish these misconceptions to a larger degree, by allowing students to view, interact and annotate 3-D content in an inherently 3-D setting. Specifically, we asked the research question: How do XR learning tools enhance student learning of multidimensional concepts, specifically crystal structures?

Table 7.1 Demographic data for each iteration cohort

| | Cohort 1: Fall 2018 (%) | Cohort 2: Fall 2019 (%) |
|--------------------------------|--------------------------------|--------------------------------|
| Sex | | |
| Female | 42 (29.37) | 47 (33.10) |
| Majors | | |
| Aerospace Eng. | 50 (34.96) | 36 (25.35) |
| Chemical Eng. | 40 (27.97) | 40 (28.17) |
| Industrial and Operations Eng. | 27 (18.88) | 30 (21.13) |
| Materials Science and Eng. | 15 (10.49) | 11 (7.75) |
| Other | 11 (7.69) | 25 (17.61) |
| Standing | | |
| 1 st year | 0 (0) | 0 (0) |
| 2 nd year | 20 (13.99) | 14 (9.86) |
| 3 rd year | 54 (37.76) | 58 (40.85) |
| 4 th year | 68 (47.55) | 70 (49.30) |

7.3 Design and Implementation of VR Learning Activities

In this chapter we discuss the development and implementation of three learning activities that we designed to test the efficacy of using VR to teach crystal structures.

7.3.1 Context and Participants

We developed a series of learning activities for an introductory course in Materials Science and Engineering; MSE220 Introduction to Materials and Manufacturing. This course teaches students about the relationships between the structure of materials and their engineering properties. It consisted of three one-hour lectures (~145 students) per week and smaller (~30 students) discussion sections once a week that were led by a graduate student instructor (GSI). The demographic data, including sex, major and class standing for the students that participated in the study are given in Table 7.1.

The research team consisted of subject material researchers (materials science graduate students and faculty), the course instructor, XR developers, and education researchers. All learning activities were collaboratively developed by the research team. Subject material

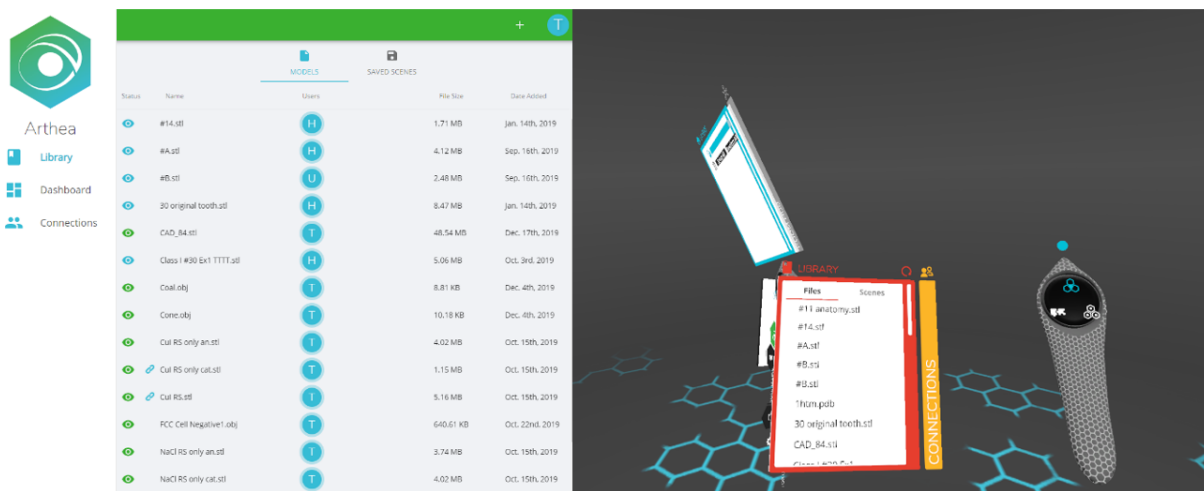


Figure 7.2 Screenshot of the Arthea web interface (left) and the virtual environment user interface (right) for importing 3D tiles

researchers administered the learning activities during the discussion sections that followed the lectures on crystal structures.

7.3.2 Arthea: The XR application

Arthea was a XR visualization and manipulation tool (<https://arthea.io>) for the Oculus Rift, Oculus Go, and HTC Vive headsets. It went through multiple iterations to improve its user interface, functionality, and usability. Since September 2018, the user interface has evolved to be more intuitive and better integrate core manipulation actions such as translational motion, 3-D model scaling and rotational motion. It supported multiple popular 3-D file formats, including FBX, OBJ, STL, WRL, PDB, DAE, and DICOM, which enabled its usage across several STEM disciplines. Finally, it was packaged with a web interface, shown in Fig. 7.2, that allowed for easy cloud-based upload and management of a user's 3-D files. Once the 3-D models were uploaded to the web interface, users could load the model into their XR headsets by clicking on

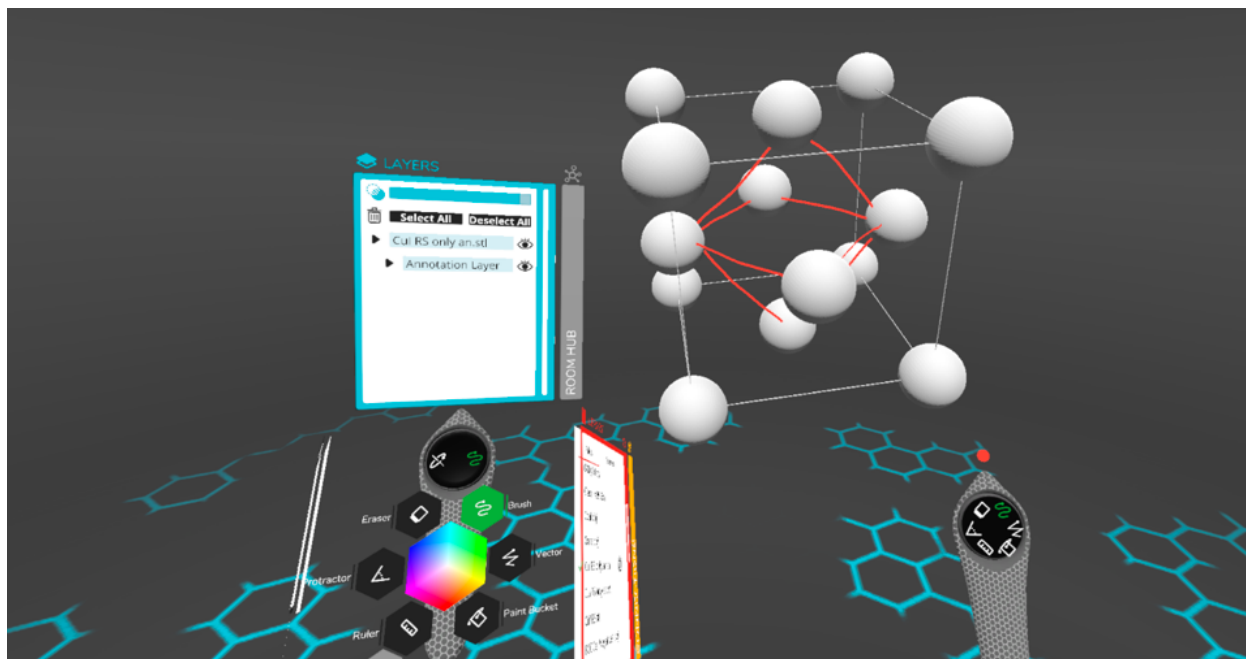


Figure 7.3 Arthea user interface and virtual environment with an FCC crystal structure unit cell loaded. This scene shows the annotation capacity of Arthea with an octahedral interstitial site drawn in red.

the model's name in the user interface. At this stage users were able to interact with, manipulate, measure, and annotate the models shown in Fig. 7.3.

7.3.3 Methods: Development of Learning Activities

We conducted a small-scale pilot study and two subsequent iterations of a larger class-wide study. After each iteration we modified the activities and added elements to help us improve the student experience. Table 7.2 shows which elements were included in each iteration.

Table 7.2 Summary of the elements included in each iteration of the study.

| Study | Term | Pre-Test | XR Training | Activity | Post-Test | Interviews |
|-------------|-------------|----------|-------------|----------|-----------|------------|
| Pilot | Spring 2018 | | | x | | x |
| Iteration 1 | Fall 2018 | a | x | b | | |
| Iteration 2 | Fall 2019 | a | x | x | a | |

In the pilot iteration of our study in Spring 2018 we wanted to better understand the viability of using VR to teach concepts related to crystal structure. We developed an activity that consisted of 4 questions related to crystal structure, typical of what could be expected in an introductory materials science course. These questions are provided in table 7.3. Question 1 required prior knowledge, asking students to name the four crystal structures: simple cubic (SC), face-centered cubic (FCC), body-centered cubic (BCC), and diamond cubic (DC). However, the remaining three questions could be answered using purely deductive and spatial reasoning skills. This was an intentional design choice given that the activities were administered to 7 student volunteers whom we did not know the academic background of in advance.

Table 7.3 Questions asked to students in the pilot iteration

| Question # | Question Text: |
|------------|--|
| 1 | Given in figures 1-4 are four crystal structures, please identify them. |
| 2 | For each structure identify and shade in the densest packed plane of atoms. |
| 3 | Explain why FCC (2) and HCP (4) have the same packing factor, i.e., density of atoms |
| 4 | Compare and contrast FCC (2) and Diamond Cubic (3) |

We created two versions of this activity to see if there were any advantages in using VR over traditional 2-D paper-based representations of crystal structure. The first version utilized paper-based representations of crystal structures. In this version, students were provided with 2-D projections of the crystal structures along three orthogonal axes and a perspective view printed on a sheet of paper. Students were encouraged to directly annotate and draw upon these figures. The second version utilized 3-D models of the same crystal structures to be viewed using Oculus Rift VR headsets. An example response to question 2 is given in Fig. 7.4, showing what the students saw in this version.

Each of the 7 participants were randomly assigned a version, which resulted in four students completing the VR version and 3 students completing the paper version. Note, that students were asked to consent to being audio recorded. These recordings were used to help

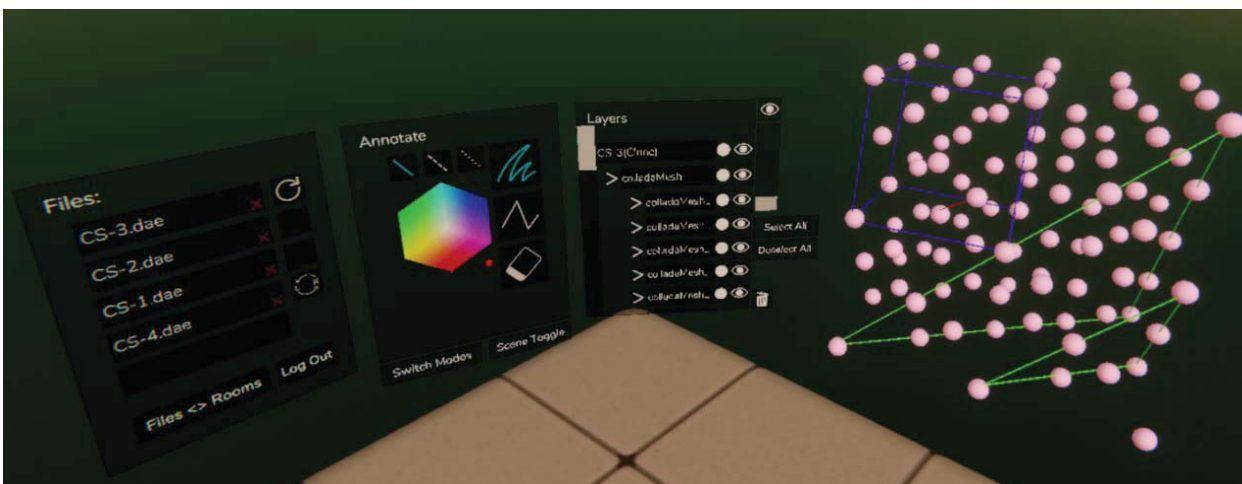


Figure 7.4 Example of a student response to question 2 in the pilot study. The densest packed plane is identified by the green triangle towards the bottom right of the image. The unit cell is also identified in blue towards the top left of the crystal structure.

understand the thought processes of students and to gather qualitative data on the student experience.

The functional limitations of the Arthea application made it impossible for the students that completed the activity in VR to view the questions and 3-D models simultaneously, without taking the headset on and off. To accommodate this, the proctors read the questions aloud to students while they completed the activity in VR. Since students could not easily write their answers in Arthea, the proctors recorded students' verbal responses to questions 1, 3 and 4. Since question 2 required drawing and the use of Arthea's annotation capability, screenshots of student responses were taken for analysis. Furthermore, the proctors were available to help students with any questions related to the controls and operation of Arthea.

In Fall 2018 we conducted a larger study over the course of hour long MSE 220 discussion sections. It is important to note that this was done in the discussion sections immediately following the lectures on the corresponding crystal structure subject matter. Prior to beginning, we passed out consent forms to the class explaining that their data may be used anonymously in an educational study. Then we administered several paper-based activities to

students in the following order. First, we administered a pre-test in the form of the multiple-choice crystal structures concept inventory¹ to gauge student understanding of crystal structures prior to completing the activity. This document is given in appendix A. After students completed the pre-test, they were given another paper-based activity to be completed individually. The focus of this activity involved drawing the atomic arrangement of atoms on different crystal planes. Specifically, students were asked to draw the (001) plane for simple cubic (SC), face centered cubic (FCC) and body centered cubic (BCC), as well as the (001), (110), and (111) planes for FCC. They were also asked to rank the atomic density of these planes and provide a brief description of how they arrived at their answer. This individual activity is provided in appendix B. Students were then paired with a partner and completed a subset of the previous activity to see if working with a partner helped them correct previous mistakes. Specifically, they were asked to identify, draw, and rank the (001), (110) and (111) planes for FCC again. This paired activity is provided in appendix C.

We were unable to perform a large-scale implementation of this iteration in VR due to time constraints and delays in setting up a VR lab . However, a subset of the students agreed to repeat the paired activity in VR outside of normal class hour for extra-credit. Prior to completing the activity in VR, students were given a short booklet tutorial that explained the controls of Arthea in a step-by-step fashion. Once students reviewed this booklet and familiarized themselves with the operation of Arthea, they were paired and completed the same paired activity. The only difference was that crystal structure figures were provided as 3D models in VR, as opposed to representations on paper. However, it must be noted that students were required to provide their answers as a 2-D drawing on paper.

Due to limitations in the number of headsets, only one student could use the Oculus Rift Headset at a time. However, the other student was able to see an approximation of the VR environment on an external monitor. Because of this, students were strongly encouraged to take turns in VR before submitting their final answers. Like the pilot study, the proctors of the activity were present to help answer questions related to the use of VR.

We revised the activities for the Fall 2019 section of MSE 220. This was done predominantly through addressing ambiguities in the wording of the questions and asking students to clearly indicate where atoms touch and do not touch in their drawings by marking where atoms touch with an 'x'. Deducing the intentions of students in their drawings was difficult during analysis of the first iteration and necessitated this additional instruction. Additionally, students participated in a dedicated discussion section to train in the controls of Arthea a week prior to completing the learning activities. In this training session, students were tasked with creating a snowman using preloaded objects in Arthea and then submitting a picture of the snowman as proof of completion. This activity ensured that each student was able to use the necessary tools required to complete the learning activity, namely opening files, manipulating and moving the objects, and annotation. We also added a post-test, identical to the pre-test, to measure if our activities led to lasting learning gains.

We assigned 3 discussion sections to use VR, and 2 discussion sections to complete the activities using paper-based representations of crystal structures. In keeping with the first iteration of the study, students completed a consent form followed by the crystal structure concept inventory pre-test. Due to time constraints the individual learning activity was removed. However, the paired learning activity was revised to also include a question that asked students to draw and rank the planar densities for the (001) plane of atoms in the SC, BCC and FCC

crystal structures. This activity is provided in appendix D. The students that completed the paired activity in VR were encouraged to take turns in VR before submitting their final responses. Again, students were required to translate their answers from VR to a 2D drawing on paper. Finally, we re-administered the concept inventory a week after the activity as a post-test to detect any changes in learning between students who completed the activities in VR and students who completed the activities on paper.

7.4 Analysis Procedures

When we analyzed the pilot study, we were cognizant of the fact that 7 student volunteers were not a large enough sample size to draw statistically significant data. However, we were able to use the audio recordings of students to qualitatively understand differences in how students interact with VR based representations compared to paper-based representations of crystal structures.

The first and second iterations were large enough to perform statistical analysis of student responses to deduce the benefits of using VR. First, we needed to grade all the pre-test, post-tests, and learning activities. The grading of the crystal structure learning inventory pre and post-tests was straightforward. It was in a multiple-choice format and therefore student responses were either marked as correct or incorrect. Grading of the learning activities was less straightforward due to the free response nature of the questions that asked students to draw different crystal planes of atoms. Through a preliminary analysis of student responses, we found several common mistakes. The most common mistakes included atoms touching where they should not touch, atoms not touching where they should touch, including additional atoms in the plane, and omitting atoms from the plane. For drawings where the intentions of students were unclear, we had multiple reviewers deduce the intention of the student and come to a consensus

answer. This led to us clarifying our instructions in the second iteration asking students to clearly mark where atoms touch with an 'x'. Ultimately, we classified all answers as either correct or incorrect. This approach allowed us to compare correct response rates between VR and paper-based visualization methods. In the first iteration, we compared the correct response rates of the subset of students who completed the individual paper-based activity, the paired-paper based activity, and the paired VR-based activity to compare the two modes of representations. In the second iteration we compared correct response rates between the population of students who completed the paired activity in VR and the population who completed the paired activity on paper. We compared these results to their performance on the pre -post tests to determine if the activities led to lasting learning gains.

7.5 Results

Each iteration of our study provided additional insight into the potential benefits of using VR to teach crystal structure. Although the pilot study was too small to provide statistically significant data, our recordings captured significant differences in the ways students go about solving problems in VR compared to on paper. For instance, students who completed the pilot activity in VR were more likely to use visual inspection of the crystal structures to answer questions, while students working on paper relied on memory for the answers. For example, students who conducted the activity in VR made statements such as:

“I can layer them on one another”, and

“The planes with closest packing are the same, ..., it's just FCC rotated.”

While one participant who conducted the activity on paper said:

“I don't think I remember enough of this to answer these questions adequately.”

This suggested that the paper-based representations didn't promote inspection of the given figures and information, but instead encouraged the reliance on previously learned information. Even with the limited number of participants it became clear that VR was promoting higher levels of student engagement with the learning content.

Table 7.4 Percent scores for the correct answers to each question when answered individually on paper, in pairs on paper, and in pairs in XR for the first iteration of the crystal structure activity ***indicates p-values<0.001

| Crystal Plane | (100) FCC | (110) FCC | (111) FCC |
|------------------------|-----------|-----------|-----------|
| Individual Score (%) | 0.58 | 0.68 | 0.00 |
| Paired Paper Score (%) | 0.63 | 0.74 | 0.11 |
| Paired XR Score (%) | 0.58 | 0.86 | 0.68 |
| F (2,54) | 0.09524 | 0.10588 | 26.460*** |

Our results from the first iteration suggest that XR promotes tangible increases in correct response rates on the learning activities. By analyzing the responses of the subset of students who completed the individual activity on paper, the paired-paper activity on paper, and the paired-VR activity we were able to find differences in correct response rate as a function of how the crystal structures were represented. However, it must be noted that this subset of students would have seen the questions two times prior to completing the activity in VR. It's possible that this repeated exposure to the content could have had an undue influence on their answers. Nevertheless, table 7.4 shows the correct response rates for the question that was included on all three activities. It also shows the results of statistical tests between the paired activities on paper and in VR. One-way between subjects ANOVA tests show a significant increase in correct response rate for the (111) FCC crystal plane ($F(2, 54) = 26.46, p < .00001$) when students completed the paired activities in VR compared to when they completed the paired activity on paper. Furthermore, post hoc Tukey HSD testing showed a significant increase in correct

response rates for the (111) plane between the individual and paired paper activities as well as the paired paper and paired XR activities. This suggested that pairing students and VR impart separate but beneficial effects on student learning.

Table 7.5 Percent scores for the correct answers to each question for two separate treatment groups of the crystal structure activity in iteration 2. ***indicates p-values<0.01.

| | N | BCC | | FCC | |
|-------|----|------|------|------|---------|
| | | 100 | 110 | 100 | 110 |
| Paper | 24 | 0.71 | 0.79 | 0.71 | 0.13 |
| XR | 36 | 0.78 | 0.86 | 0.81 | 0.31*** |

We obtained similar results in the second iteration of the crystal structure activity in which we used two separate student populations to test paper-based representations against VR-based representations. Table 7.5 shows the correct response rates for the student pairs who completed the activity on paper (N=24) and the student pairs who completed the activity in VR (N=36). The results show that students who completed the activity in VR consistently scored higher than those who completed the activity on paper. However, t-test shows that the difference in correct response rate is only statistically significant for the (111) FCC plane. This was very similar to what was observed in iteration 1. Furthermore, we observed that students who used VR in the first iteration answered the (111) FCC plane correctly more than 2 times as often as students using VR in the second iteration. This suggested that the increased exposure to the question in the first iteration may have partially caused the improvement in correct response rates.

Table 7.6 Pre and Posttest results for the second iteration of the crystal structure learning activity, understand the thought processes of students and to gather qualitative data on the student experience.

| | N | BCC | | | FCC | | |
|----------|----|-----------------|--------------|-----------------|---------------|-----------------|-----------------|
| | | 100 | 110 | 111 | 100 | 110 | 111 |
| Paper | 39 | | | | | | |
| Pretest | | 0.487 | 0.846 | 0 | 0.923 | 0.436 | 0.231 |
| Posttest | | 0.821 | 0.872 | 0.128 | 0.872 | 0.744 | 0.282 |
| Δ | | 0.333*** | 0.026 | 0.128*** | -0.051 | 0.308*** | 0.051 |
| XR | 63 | | | | | | |
| Pretest | | 0.476 | 0.746 | 0.079 | 0.905 | 0.508 | 0.317 |
| Posttest | | 0.683 | 0.825 | 0.095 | 0.889 | 0.683 | 0.19 |
| Δ | | 0.206*** | 0.079 | 0.016 | -0.016 | 0.175** | -0.127** |

We performed analysis of the crystal structure learning inventory pre and post-tests in the second iteration to determine if VR promoted long term learning gains. Table 7.6 shows the correct response rates to the six questions on the crystal structure learning inventory for the students who completed the activities on paper and VR. Also shown is the difference in correct response rates between the pre and post-test along with t-tests to indicate if the change was significant.

We observed that students who completed the study on paper showed significant increases in correct responses for BCC (100), BCC (111) and FCC (110). Students who completed the activity in VR showed statistically significant improvement for BCC (100) and FCC (110). In contrast to the learning activities themselves, students who completed the activity in VR showed a significant decline in correct response rates for FCC (111). This result was

unexpected, as VR was seen to be beneficial in helping students get the correct answer for the FCC (111) in both iterations of the learning activity.

7.6 Discussion:

Our pilot study showed that VR-based representations of crystal structures promote different problem-solving strategies⁶ compared to paper-based representations of crystal structures. This agreed with Radu's¹⁵ meta-analysis of literature, which reported that XR-based student learning can alter how students conceptualize information. For example, students learning astronomy in VR might focus on planetary movement, instead of the visual qualities of planets leading to different learning outcomes. Our findings also showed that VR improved student performance on the learning activities. This was demonstrated by the significant increases in correct answers for FCC (111) plane when students used VR compared to paper. We suggest that correctly answering the FCC (111) plane in the learning activities requires a higher degree of spatial reasoning than the (001) and (110) planes. There is more information to parse as it intersects a higher density of atoms than the (001) and (110) planes. Additionally, the (001) plane represents the face of the unit cell and is less obscured than the (110) and (111) planes that pass through the interior of the unit cell. Despite this, the benefit of using VR did not appear to last. We observed a decrease in performance when we compared the results of the pre and post-test on the FCC (111) plane. This decrease in performance is consistent with previous findings in literature¹³ that suggest VR may reduce the load on working memory, and as a result have a negative outcome on information retention. In this interpretation, VR does not promote higher levels of spatial reasoning, as it allows students to directly observe the correct answer.

7.7 Critique:

We originally stated that our research question was: how do XR learning tools enhance student learning of multidimensional concepts, specifically crystal structures? However, after performing the literature review discussed in Chp. 6 it became clear that we were short-sighted in our research question. At its core, the overall purpose of our study was to use crystal structures as a case study to showcase the learning benefits of VR and encourage its use in engineering classrooms. Indeed, there is a large body of literature that shows VR can benefit student learning in the form of increased memory, motivation, and increased problem-solving ability.^{7-10,12,15} Despite the benefits documented in literature, the use of VR is not commonly reported on in MSE. The fact that our findings show inconclusive results regarding the benefits of using VR, strongly undermines our goal of changing this. However, even if our results showed strong learning gains, Henderson¹⁶ suggests that our approach of disseminating a learning activity is generally ineffective at changing the teaching behaviors of instructors, and therefore unlikely to successfully encourage increased adoption of VR. As such, we recognize the need for a different experimental approach to both demonstrate clearer evidence of student learning and encourage the use of VR in engineering classrooms. In the remainder of this section, we discuss the positive and negative design elements of our experimental study and propose a more efficacious approach to encouraging the effective utilization and adoption of VR in classroom settings.

7.7.1 The Positive: Incorporating a Variety of Representation Types

Even though our studies and learning activities may not be successful at promoting the adoption of VR, it does not preclude us from recognizing positive design elements that can be used to inform future studies. Lesh¹⁷ suggests that developing students' representational fluency is vital in developing well trained engineers and is necessary for students to exhibit expertise in a

subject matter. In practice this means that students should understand several different types of representations, the information provided by each and how they relate to one another. Figure 7.5 gives examples of the five types of representations described by Lesh: language, symbolic, realistic, concrete, and pictorial.^{17,18} Language based representations describe concepts with words, for example a student could describe a SC crystal by saying its unit cell is the same as placing an atom on the corners of a cube. Symbolic based representations use symbols to impart information and knowledge, for example, using vector notation to describe the unit cell vectors in a crystal. Realistic representations use real-life interactions or data, for example, using XRD data to deduce the lattice parameter of a crystal. Concrete representations are tangible 3D models, for example, models of crystal structures that show bonding and the atomic arrangement of atoms. Finally pictorial representations are any representation shown in a 2-D media format, such as an image of an FCC crystal in a textbook. Each representation type has unique affordances in the information they provide to students. Therefore, instructors must be cognizant to include a variety of representation types when they teach to promote optimum learning outcomes.

Caro et al¹⁹ performed a systematic review of learning activities used to teach crystal structures and found that instructors generally used several representation types in their activities. By far the most common mode of representations used were pictorial. This is understandable because most students learn crystal structures by looking at figures in textbooks and slides during lectures. As such it is the type of representation that students are most familiar with. Instructors also frequently used language, symbolic, and realistic representations of crystal structures in their activities. Notably, the least commonly used representation type was concrete.

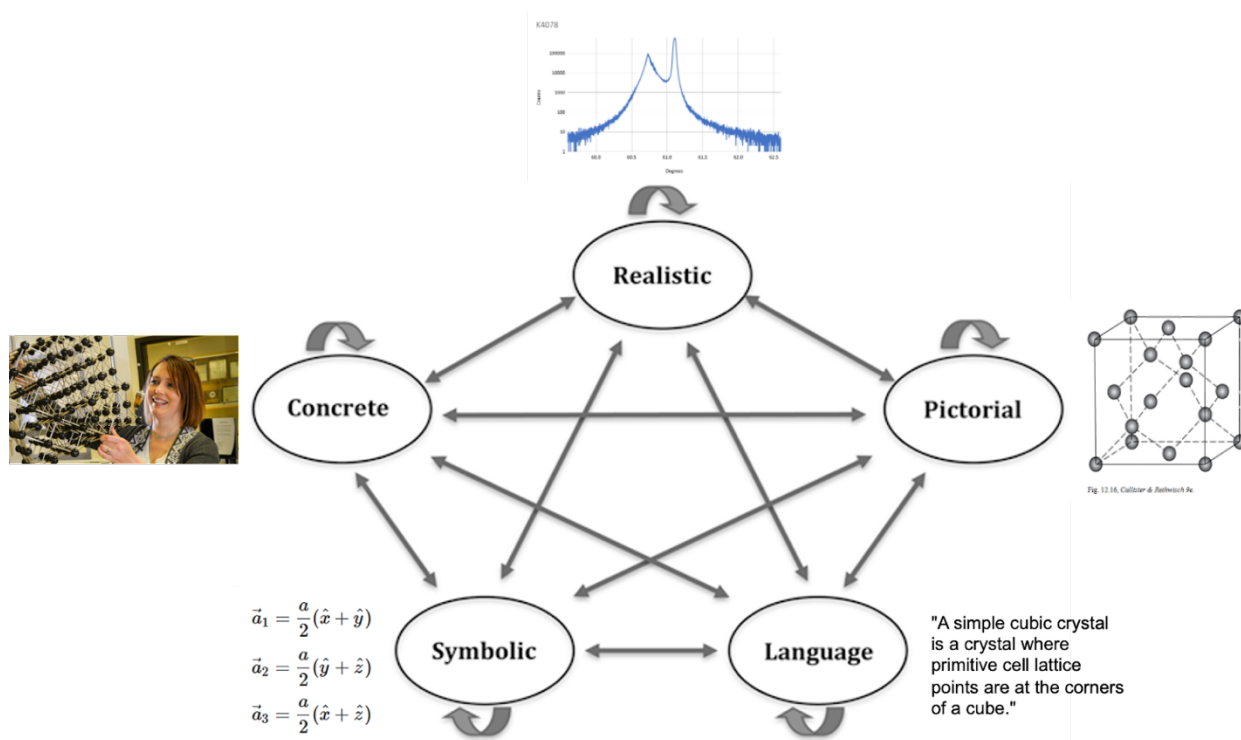


Figure 7.5 The different types of representations described by Lesh, the arrows indicate that students must be able to understand how these representations relate to one another and the information provided by each¹⁸

This may be because physical models can be expensive and cumbersome to provide to a class full of students, particularly when multiple crystal structures are being taught. Using VR to show virtual models can be used to address the low use of concrete representations, and advance students' representational fluency. Our approach of taking a well-developed VR platform (Arthea) to view 3D models of crystal structures represents a useful approach, by lowering the

amount of overhead work required by instructors to incorporate concrete representations in their classrooms.

7.7.2 The Room for Improvement: Supporting Different Learner Roles

We also critique our learning activities through the lens of the expanded four resource model; an educational model designed to describe how engaging students in a variety of ways promotes effective learning.²⁰ Serafini et al²⁰ says that students take on a subset of four different roles when they engage in learning activities: navigator, interpreter, designer and interrogator. Students engage in the navigator role any time they are expected to know and carry out a procedure such as in a laboratory setting or reading instructions and completing a question in an activity. The interpreter role describes when students are tasked with analyzing data, interpreting results and drawing conclusions. The designer role describes when students engage with activities in ways that affect their outcome. An example of this is a term-project where students have a high degree of autonomy. Finally, the interrogator role describes whenever students are asked to put their actions in the context of the topic at hand, the wider scientific community, or their education. In other words, when students are asked to explain the motivation behind their actions or understand the purpose of an activity. Instructors must design activities that support all four of these learner roles to prepare engineers for their careers. However, Caro et al¹⁹ discovered that most learning activities designed to teach crystal structures neglect the designer and interpreter roles. In Table 7.7 we classify the learner roles that our learning activities supported.

Table 7.7 Analysis of learner roles supported in the activities in this study

| Activity | Question # | Navigator | Interpreter | Designer | Interrogator |
|-----------------------------------|------------|-----------|-------------|----------|--------------|
| Pre/Post Test | 1-6 | x | | | |
| Individual Activity (Iteration 1) | 1 | x | | | |
| | 2 | x | | | |
| | 3 | x | x | | |
| | 4 | x | x | | |
| | 5 | x | | | |
| | 6 | x | | x | |
| Paired Activity (Iteration 1) | 1 | x | x | | |
| | 2 | x | | | x |
| Paired Activity (Iteration 2) | 1 | x | x | | |
| | 2 | x | x | | |

Given the requirement that students must read and comprehend the questions and instructions in the learning activities, we find that they are always engaged as a navigator. However, many of the questions in the learning activities also engage students as interpreters. Figure 7.6 shows an example of the questions in the individual and paired activities that first engaged students as navigators by providing them instructions to draw crystal planes of atoms, and then as interpreters, asking them to interpret their drawings and rank them by planar density. We found that we never engaged students as designers as the instructions of the activities were intended to be highly prescribed with little room for interpretation by students. Similarly, we rarely engaged students as interrogators; the only time being on question 2 of the paired activity

in iteration 1. Specifically, we asked students to reflect on their experience with the learning activity and if working in pairs helped them correct any misconceptions. However, at the time we conducted these studies, we were unaware of the importance of supporting different learner roles and removed these questions in the second iteration of the paired activity. Overall, we found that we generally only engaged students as navigators and interpreters and not designers or interrogators. This highlighted a shortcoming in the experimental design of our activities and suggests an area for improvement in future activities.

3. Draw the space filling representation of the atoms lying on the grayed planes shown below. Only include atoms that are bisected through the center by the plane in your drawings. Next, rank the planar density of these planes.

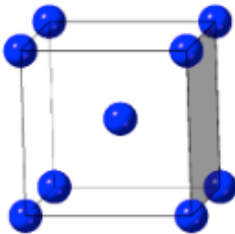
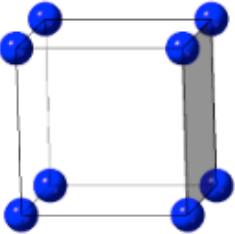
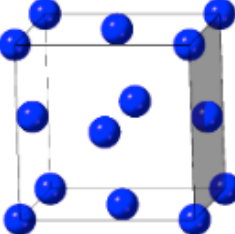

| | | | |
|---|--|--|--|
| Crystal Structure with Plane. (Reduced Sphere) |  |  |  |
| Space-filling drawing of the atoms lying on the plane shown: | | Ex.  | |
| Planar Density Rank: (1 = Highest) | | | |

Figure 7.6: Example of a question asking students to draw the planes of atoms and rank their planar density

7.7.3 The Bad: Not Likely to Encourage the Use of VR

The pre/post test results in the second iteration showed that our learning activities had an unclear effect on student learning. Admittedly, this is probably unlikely to inspire confidence in

our learning activities and may lead instructors to question the efficacy of using VR to teach crystal structures. However, even if we were able to create a perfect learning activity that showed a clear increase in student understanding, it is likely that we would not have been successful in convincing instructors to adopt it. Henderson¹⁶ conducted a literature review on approaches used to change undergraduate STEM education. They found that highly prescribed outcomes that seek to change the behaviors of instructors are largely ineffective at promoting change. Reflecting on our studies, we find that we implicitly advocate for instructors to adopt our learning activities to increase their use of VR in the classroom. Indeed, this falls under the category of prescribed outcomes and is therefore unlikely to be successful. Contrastingly, Henderson found that the most effective methods to promote change in the behaviors of instructors is to use emergent change outcomes. In other words, successfully changing the behaviors of instructors generally involves long-term interventions that encourage and support instructors to develop new teaching conceptions and teaching practices, while treating the university as a complex system. In this regard it becomes clear that if our goal is to increase the use of VR in classroom settings, particularly in MSE, we must shift our focus from developing learning activities to supporting instructors in using VR and developing VR activities. If done correctly this approach could have the added benefit of rapidly expanding VR-based teaching content.

7.8 Suggestions for Future Work

In order to simultaneously generate better teaching content while increasing the adoption of VR we suggest future work focus on emergent change outcomes and supporting instructors. One way that we can support instructors is through the creation of an XR learning center where instructors can develop classroom activities. For such an environment to be successful it would

need to be a collaborative space for engineering faculty (content experts), education researchers (activity/experimental design experts), learning scientists (VR cognition experts) and XR developers. The multidisciplinary nature of such a center would ensure that learning activities are pedagogically sound and use XR in the most effective way to promote student learning gains. Although we would have to relinquish control over the content that ultimately gets taught to students in this scenario, it has the potential to rapidly speed up the development of VR teaching content and teach us best practices for using XR in the classroom.

However, this approach could lead to an opportunity for another interesting study. Ideally the XR learning center would lead to an uptick in instructors wanting to use XR technologies in their classrooms. Due to this we propose using the XR learning center as a foundation for a community of practice (CoP) to provide faculty an environment to connect with and support (and be supported by) other individuals who share a common interest, in this case using XR as a teaching tool. The benefits of CoP's include "a sense of community, self-awareness, motivation and validation of current practices and beliefs".²¹ Research has shown that these benefits serve to prompt the exchange of innovative teaching practices.²¹⁻²⁴ In this regard a CoP could help increase the use of XR in classroom settings, while also partially addressing the lack of communication between STEM-based education researchers and education researchers that we briefly discussed in Chp 6.

In order to establish a CoP around using XR technologies in the classroom, we first need to find a critical mass of instructors interested in using XR and/or studying the effect of XR on student learning. From this stage we propose studying the organic growth of the CoP and investigating how it accelerates adoption of XR within a given department and across the university setting. The findings of such a study could have widespread implications for

overhauling departmental teaching culture in engineering, especially as many departments are trying to promote a shift towards an increase in active learning and student-centered learning.^{22,24}

7.9 Conclusions

In this work, we developed and tested several iterations of a crystal structures activity to compare how well students learned multidimensional concepts on paper versus using VR. The pilot study suggested that students may benefit from XR because they interacted with the structures in ways not possible on paper. It was also observed that students who completed the learning activity in VR performed better than students who completed the activity on paper. However, this benefit did not appear to be retained, as a post-test shows a degradation in correct responses for these students.

We find that our learning activities do some things well and some things poorly. We discuss that our VR based learning activities are a good way to familiarize students with concrete models and increase their representational literacy. However, we also find that our learning activities fail to consistently engage students in the designer and interpreter learner roles. Finally, we recognize that our learning activity is unlikely to be adopted by instructors due to its prescribed change outcomes. Therefore, our experimental approach is also unlikely to encourage more instructors to implement VR in their classrooms. To remedy this, we suggest supporting instructors through the creation of a XR learning center and starting a community of practice centered around the use of XR in educational settings.

7.10 References

1. Sorby, S. A. Educational research in developing 3-D spatial skills for engineering students. *Int J Sci Educ* **31**, 459–480 (2009).

2. Hsi, S., Linn, M. C. & Bell, J. E. Role of spatial reasoning in engineering and the design of spatial instruction. *Journal of Engineering Education* **86**, 151–158 (1997).
3. Uttal, D. H. & Cohen, C. A. *Spatial Thinking and STEM Education. When, Why, and How? Psychology of Learning and Motivation - Advances in Research and Theory* vol. 57 (Elsevier Inc., 2012).
4. Krause, S. & Waters, C. Uncovering and repairing crystal structure misconceptions in an introductory materials engineering class. *Proceedings - Frontiers in Education Conference, FIE* (2012) doi:10.1109/FIE.2012.6462296.
5. Krause, S., Kelly, J., Baker, D. & Kurpius-Robinson, S. Effect of pedagogy on conceptual change in repairing misconceptions of differing origins in an introductory materials course. *ASEE Annual Conference and Exposition, Conference Proceedings* (2010).
6. Gentry, S. P. & Faltens, T. A computer-based interactive activity for visualizing crystal structures in introductory materials science courses. *ASEE Annual Conference and Exposition, Conference Proceedings 2017-June*, (2017).
7. Caro, V., Carter, B., Dagli, S., Mark Schissler & Joanna Millunchick. Can Virtual Reality Enhance Learning: A Case Study in Materials Science. in *Frontiers in Education 2018: Fostering Innovation Through Diversity Conference Proceedings* (2018).
8. Vergara, D., Rubio, M. P. & Lorenzo, M. A virtual resource for enhancing the spatial comprehension of crystal lattices. *Educ Sci (Basel)* **8**, (2018).
9. Merchant, Z., Goetz, E. T., Cifuentes, L., Keeney-Kennicutt, W. & Davis, T. J. Effectiveness of virtual reality-based instruction on students' learning outcomes in K-12 and higher education: A meta-analysis. *Comput Educ* **70**, 29–40 (2014).
10. Akçayır, M. & Akçayır, G. Advantages and challenges associated with augmented reality for education: A systematic review of the literature. *Educ Res Rev* **20**, 1–11 (2017).
11. Ibáñez, M. B. & Delgado-Kloos, C. Augmented reality for STEM learning: A systematic review. *Comput Educ* **123**, 109–123 (2018).
12. Radu, I. Augmented reality in education: A meta-review and cross-media analysis. *Pers Ubiquitous Comput* **18**, 1533–1543 (2014).
13. Chittaro, L. & Buttussi, F. Assessing Knowledge Retention of an Immersive Serious Game vs. a Traditional Education Method in Aviation Safety; Assessing Knowledge

- Retention of an Immersive Serious Game vs. a Traditional Education Method in Aviation Safety. *IEEE Trans Vis Comput Graph* **21**, (2015).
14. Hine, K. & Tasaki, H. Active View and Passive View in Virtual Reality Have Different Impacts on Memory and Impression. *Front Psychol* **10**, (2019).
 15. Hwang, W. Y. & Hu, S. S. Analysis of peer learning behaviors using multiple representations in virtual reality and their impacts on geometry problem solving. *Comput Educ* **62**, 308–319 (2013).
 16. Judson, E., Ross, L., Middleton, J. & Krause, S. Measuring Engineering Faculty Views about Benefits and Costs of Using Student-Centered Strategies. *International Journal of Engineering Pedagogy (iJEP)* **7**, 65 (2017).
 17. Corkins, J. *et al.* Determining the factor structure of the Materials Concept Inventory. *ASEE Annual Conference and Exposition, Conference Proceedings* (2009).
 18. Radu, I. Augmented reality in education: A meta-review and cross-media analysis. *Pers Ubiquitous Comput* **18**, 1533–1543 (2014).
 19. Henderson, C., Beach, A. & Finkelstein, N. Facilitating change in undergraduate STEM instructional practices: An analytic review of the literature. *J Res Sci Teach* **48**, 952–984 (2011).
 20. Moore, T. J., Guzey, S. S., Roehrig, G. H. & Lesh, R. A. Representational Fluency: A Means for Students to Develop STEM Literacy. in vol. 11 13–30 (2018).
 21. Caro, V. Comparative III-As-Bi Surface Morphologies and Microstructure & Disciplinary Literacy in MSE. Preprint at (2022).
 22. Caro, V., Carter, B. A., Millunchick, J. M. & Reeves, S. Teaching crystal structures in undergraduate courses: a systematic review from a disciplinary literacy perspective. *The Royal Society of Chemistry* (2022).
 23. Serafini, F. Expanding the four resources model: Reading visual and multi-modal texts. *Pedagogies* **7**, 150–164 (2012).
 24. Mead, T. *et al.* Leveraging a community of practice to build faculty resilience and support innovations in teaching during a time of crisis. *Sustainability (Switzerland)* **13**, (2021).

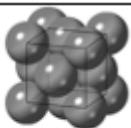



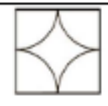

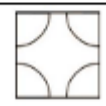

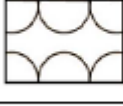
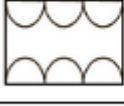
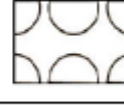
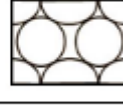
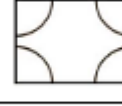
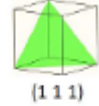
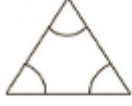


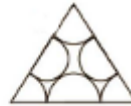
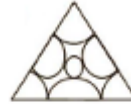
25. Gehrke, S. & Kezar, A. The Roles of STEM Faculty Communities of Practice in Institutional and Departmental Reform in Higher Education. *Am Educ Res J* **54**, 803–833 (2017).
26. Kezar, A. & Gehrke, S. Sustaining Communities of Practice Focused on STEM Reform. *Journal of Higher Education* **88**, 323–349 (2017).
27. Glaze-Crampes, A. L. Leveraging communities of practice as professional learning communities in science, technology, engineering, math (STEM) education. *Education Sciences* vol. 10 1–8 Preprint at <https://doi.org/10.3390/educsci10080190> (2020).

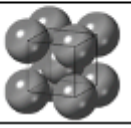




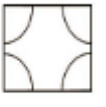
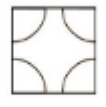
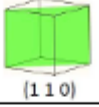
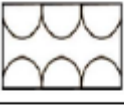

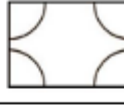

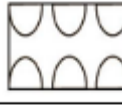



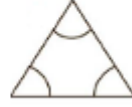

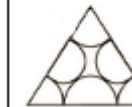
Appendix A Crystal Structure Concept Inventory Pretest/Posttest

Name: _____
 Section: _____
 Date: _____

MSE 220 Crystal Structure Prelim

Instructions: In questions 1-3 below a orthometric view of a space filling FCC (face centered cubic) unit cell. Each individual question indicates a specific plane, to which you must identify how the atoms are arranged, and clearly indicate your answer choice by circling the corresponding letter. Note: Only consider atoms whose centers lie on the plane. When finished with questions 1-3 continue to 4-6 and do the same for BCC (body centered cubic).

| | | | | | |
|--|---|---|---|---|---|
|  | To the left is a FCC unit cell, please identify the following planes of atoms. Only consider atoms that centers lie on the plane. | | | | |
| 1. | A. | B. | C. | D. | E. |
|  (1 0 0) |  |  |  |  |  |
| 2. | A. | B. | C. | D. | E. |
|  (1 1 0) |  |  |  |  |  |
| 3. | A. | B. | C. | D. | E. |
|  (1 1 1) |  |  |  |  |  |

| | | | | | |
|--|---|---|---|---|---|
|  | To the left is a BCC unit cell, please identify the following planes of atoms. Only consider atoms that centers lie on the plane. | | | | |
| 4. | A. | B. | C. | D. | E. |
|  (1 0 0) |  |  |  |  |  |
| 5. | A. | B. | C. | D. | E. |
|  (1 1 0) |  |  |  |  |  |
| 6. | A. | B. | C. | D. | E. |
|  (1 1 1) |  |  |  |  |  |

Appendix B Crystal Structure Individual Activity

Name: _____
 Class Section: _____
 Date: _____

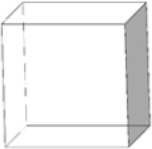
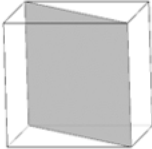
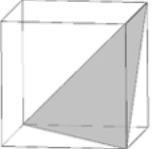
Crystal Structure Individual Activity

Instructions: Complete the activity in the order it is presented, utilizing the given figures. Please only include your final answer in the box provided, you may use blank space for scratch work.

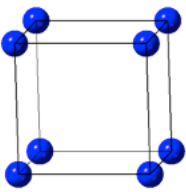
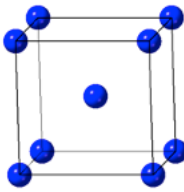
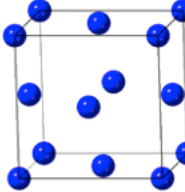
Additional Notes:

The images shown below are given in reduced sphere representation, meaning only the cores of the atoms are shown for clarity. These structures are actually space filling, meaning that nearest neighbor atoms touch.

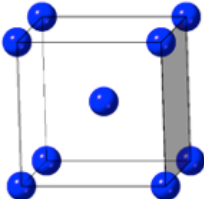
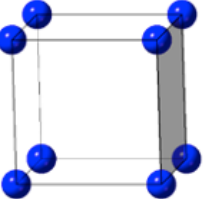
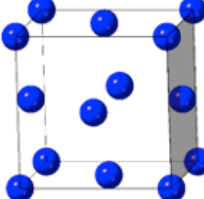

1. Record the miller indices of the grayed planes below.

| | | | |
|---------|--|---|--|
| Plane: |  |  |  |
| Answer: | | | |

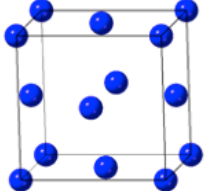
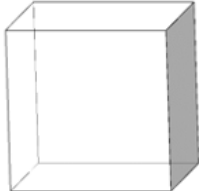
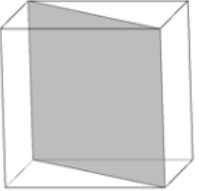
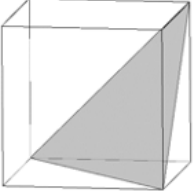
2. Identify and name the crystal structure of the unit cells below and record your answer.

| | | | |
|---------------------------------------|---|--|---|
| Crystal Structure (Reduced Sphere) |  |  |  |
| Answer: | | | |

3. Draw the space filling representation of the atoms lying on the grayed planes shown below. Only include atoms that are bisected through the center by the plane in your drawings. Next, rank the planar density of these planes.

| | | | |
|--|---|--|---|
| Crystal Structure with Plane. (Reduced Sphere) |  |  |  |
| Space-filling drawing of the atoms lying on the plane shown: | | Ex.  | |
| Planar Density Rank: (1 = Highest) | | | |

4. On each grayed plane draw the positions of the atoms that lie on it, given by the provided crystal structure. Only include atoms that are bisected through the center by the plane in your drawings. Next draw a space filling representation of the atoms lying on these planes. Finally rank the planar densities of these planes.

| | | | |
|--|---|--|---|
| Crystal Structure (Reduced Sphere) |  | | |
| Plane: |  |  |  |
| Space-filling drawing of atoms lying on the plane shown: | | | |
| Planar Density Rank (1 = Highest) | | | |

5. Describe your method for determining relative atomic planar densities.

6. Which of the 5 planes + structure combinations that you drew in questions 3 and 4 has the highest planar density of atoms? Name the structure and the plane.

Appendix C Crystal Structure Paired Activity Iteration 1

Names: _____

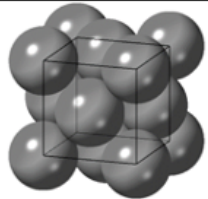
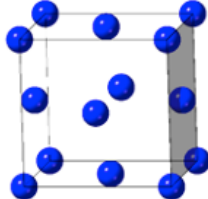
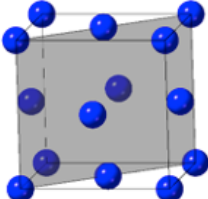
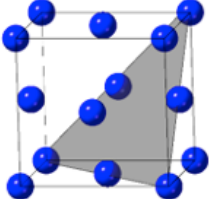
Crystal Structure Paired Activity

Class Section: _____

Date: _____

Complete the activity, with a partner in the order it is presented, utilizing the given figures. Please only include your final answers in the box provided you may use blank space for scratch work.

- For each plane indicated below, draw the corresponding cross section of atoms in FCC. Rank the planar density of these planes. **Note: The figures with the planes below are shown in reduced sphere representation, meaning only the cores of the atoms are shown for clarity. In actuality, the nearest neighbor atoms touch, as illustrated by the space filling model below. Consider this when answering the following questions. All drawings should be for the space filling model, and only include atoms that the planes bisect through the center in your drawing.**

| | | | |
|---|---|--|---|
| Space-Filling FCC: |  | | |
| Planes of FCC: (Pictures shown in reduced sphere representation) |  |  |  |
| Space-filling drawing of atoms lying on the plane shown: | | | |
| Planar Density Rank (1 = Highest) | | | |

2. Individually write your answers to the following reflection questions:

a) Did working in pairs help you catch any errors you made in individual work? If so, describe the errors

b) What did you find most interesting or eye-opening about this activity?

c) Generate at least two questions you have about structures of materials or how we visualize work with them.

Appendix D Crystal Structure Paired Activity Iteration 2

Name: _____
 Class Section: _____
 Date: _____

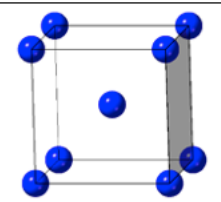
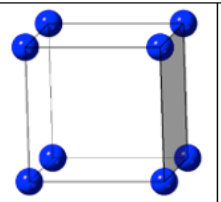
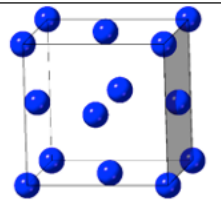

Crystal Structure Paired Activity

Instructions: Complete the activity in the order it is presented, utilizing the given figures. Please only include your final answer in the box provided, you may use blank space for scratch work. **READ THE ACTIVITY THOROUGHLY.**

Additional Notes:

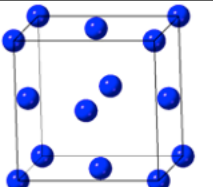
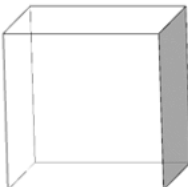
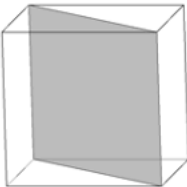
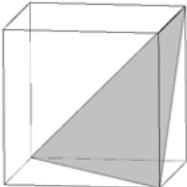
The images shown below are given in reduced sphere representation, meaning only the cores of the atoms are shown for clarity. These structures are actually space filling, meaning that nearest neighbor atoms touch.

1.a) Draw the space filling representation of the atoms lying on the greyed-out planes shown below. Indicate where the atoms touch with an X. Only include atoms **whose centers lie on the plane** in your drawings. Use the filled-out example as a guide.

| | | | |
|--|---|--|---|
| Crystal Structure with Plane. (Reduced Sphere) |  |  |  |
| Give a Space-filling drawing of the atoms lying on the plane shown: Indicate touching atoms with an X. | | Ex.  | |

1.b) Clearly indicate which plane above has the **lowest** packing density and **explain with words** how you know this.

2.a) For each grayed out plane draw a space filling picture of the atoms that lie on it, given the provided crystal structure. Only include atoms **whose centers lie on the plane** in your drawings. Consider both the location of atoms on the plane and whether or not the atoms touch in your drawings. Mark where the atoms touch with an X.

| | | | |
|--|---|--|---|
| Crystal Structure (Reduced Sphere) |  | | |
| Grayed Out Planes |  |  |  |
| Give a Space-filling drawing of atoms lying on the plane above: Mark where atoms touch with an X. | | | |

2.b) Clearly indicate which plane above has the **highest** packing density and **explain with words** how you know this.